



SMIJ

Siriraj Medical Journal

The world-leading biomedical science of Thailand

ORIGINAL ARTICLE

REVIEW ARTICLE

MONTHLY

PMAC
PRINCE MAHIDOL
AWARD CONFERENCE 2026



Navigating Global
Demographic Transition
through Innovative Policy: An Equity-Centered Approach



Indexed by



EBSCO



<https://he02.tci-thaijo.org/index.php/sirirajmedj/index>
E-mail: sjournal92@gmail.com

ORIGINAL ARTICLE

- 1** Morphologic Features and Morphometric Measurements of Human Oocytes That Failed to Cleave after Intracytoplasmic Sperm Injection (ICSI)
Ali Mohsin Alwaeli, Shatha Sadiq Almarayaty, Maan Hamad Al-Khalisy, Mohammed Hussein Assi
-
- 11** Application of Artificial Intelligence for Osteoporosis Screening Using Chest Radiographs
Polasan Santanapitkul, Lakkana Jirapong, Anchalee Chumjam, Nantika Wannasoupol, Rapeepat Narkbunnam
-
- 20** Prevalence and Factors Associated with Urologic Abnormalities in Hypospadias Patients
Donlaporn Rungwilaicharoen, Ravit Ruangtrakool
-
- 29** The Correlation between Chest X-ray and Cardiac Magnetic Resonance Imaging in the Assessment of Left Atrial Enlargement
Satchana Pumprueg, Methat Meechuen, Thananya Boonyasirinant
-
- 39** Incidence and Factors Associated with Perioperative Respiratory Adverse Events in Pediatric Patients with Upper Respiratory Tract Infection Undergoing Surgery Under General Anesthesia: A Retrospective Cohort Study
Sutida Boonkamjad, Darunee Sripadungkul, Cattleya Kasemsiri, Prathana Wittayapairoch, Panaratana Ratanasuwan
-
- 51** Comparison of Bridging and Contactless Technique for Umbilical Catheter Securement in Preterm Infants: A Pilot Randomized Controlled Trial
Sujitra Terdnueakao, Punnanee Wutthigate, Chanoknan Sriwiset, Walaiporn Bowornkitiwong
-
- 59** Hospital Mortality and Predicting Factors in Patients with Sepsis-associated Acute Kidney Injury Requiring Renal Replacement Therapy
Chairat Permpikul, Nattapat Wongtirawit, Surat Tongyoo, Methawoot Khemmongkon, Thummaporn Naorungroj
-
- 68** Diagnostic Utility of Reticulocyte Hemoglobin Equivalent for Identifying Iron Deficiency in Hospitalized Children in a Thalassemia-endemic Region: A Single-center Cross-sectional Study
Phakatip Sinlapamongkolkul, Tasama Pusongchai, Jassada Buaboonnum, Wallee Satayasai, Pacharapan Surapolchai

REVIEW ARTICLE

- 79** Dental Management in Natal and Neonatal Teeth
Narawan Chieowwit



Executive Editor:

Professor Apichat Asavamongkolkul, Mahidol University, Thailand

Editorial Director:

Professor Aasis Unnanuntana, Mahidol University, Thailand

Associate Editors

Assistant Professor Adisorn Ratanayotha, Mahidol University, Thailand

Pieter Dijkstra, University of Groningen, Netherlands

Professor Phunchai Charatcharoenwitthaya, Mahidol University, Thailand

Professor Varut Lohsiriwat, Mahidol University, Thailand



Editor-in-Chief:

Professor Thawatchai Akaraviputh,
Mahidol University, Thailand

International Editorial Board Members

Allen Finley, Delhousie University, Canada

Christopher Khor, Singapore General Hospital, Singapore

Ciro Isidoro, University of Novara, Italy

David S. Sheps, University of Florida, USA

David Wayne Ussery, University of Arkansas for Medical Sciences, USA

Dennis J. Janisse, Medical College of Wisconsin, USA

Dong-Wan Seo, University of Ulsan College of Medicine, Republic of Korea

Folker Meyer, Argonne National Laboratory, USA

Frans Laurens Moll, University Medical Center Utrecht, Netherlands

George S. Baillie, University of Glasgow, United Kingdom

Gustavo Saposnik, Unity Health Toronto, St. Michael Hospital, Canada

Harland Winter, Harvard Medical School, USA

Hidemi Goto, Nagoya University Graduate School of Medicine, Japan

Ichizo Nishino, National Institute of Neuroscience NCNP, Japan

Intawat Nookaew, University of Arkansas for Medical Sciences, USA

James P. Doland, Oregon Health & Science University, USA

John Hunter, Oregon Health & Science University, USA

Karl Thomas Moritz, Swedish University of Agricultural Sciences, Sweden

Kazuo Hara, Aichi Cancer Center Hospital, Japan

Keiichi Akita, Institute of Science Tokyo, Japan

Kyoichi Takaori, Kyoto University Hospital, Japan

Marcela Hermoso Ramello, University of Chile, Chile

Marianne Hokland, University of Aarhus, Denmark

Matthew S. Dunne, Institute of Food, Nutrition, and Health, Switzerland

Mazakayu Yamamoto, Tokyo Women's Medical University, Japan

Mitsuhiro Kida, Kitasato University & Hospital, Japan

Moses Rodriguez, Mayo Clinic, USA

Nam H. CHO, Ajou University School of Medicine and Hospital, Republic of Korea

Nima Rezaei, Tehran University of Medical Sciences, Iran

Noritaka Isogai, Kinki University, Japan

Philip A. Brunell, State University of New York At Buffalo, USA

Philip Board, Australian National University, Australia

Ramanuj Dasgupta, Genome Institution of Singapore

Richard J. Deckelbaum, Columbia University, USA

Robert W. Mann, University of Hawaii, USA

Robin CN Williamson, Royal Postgraduate Medical School, United Kingdom

Sara Schwanke Khilji, Oregon Health & Science University, USA

Seigo Kitano, Oita University, Japan

Seiji Okada, Kumamoto University

Shomei Ryozaawa, Saitama Medical University, Japan

Shuji Shimizu, Kyushu University Hospital, Japan

Stanley James Rogers, University of California, San Francisco, USA

Stephen Dalton, Chinese University of HK & Kyoto University

Tai-Soon Yong, Yonsei University, Republic of Korea

Tomohisa Uchida, Oita University, Japan

Victor Manuel Charoenrook de la Fuente, Centro de Oftalmologia Barraquer, Spain

Wikrom Karnsakul, Johns Hopkins Children's Center, USA

Yasushi Sano, Director of Gastrointestinal Center, Japan

Yik Ying Teo, National University of Singapore, Singapore

Yoshiki Hirooka, Nagoya University Hospital, Japan

Yozo Miyake, Aichi Medical University, Japan

Yuji Murata, Aizenbashi Hospital, Japan

Editorial Board Members

Vitoon Chinswangwatanakul, Mahidol University, Thailand

Jarupim Soongswang, Mahidol University, Thailand

Jaturat Kanpittaya, Khon Kaen University, Thailand

Nopphol Pausawasdi, Mahidol University, Thailand

Nopporn Sittisombut, Chiang Mai University, Thailand

Pa-thai Yenchitsomanus, Mahidol University, Thailand

Pornprom Muangman, Mahidol University, Thailand

Prasit Wattanapa, Mahidol University, Thailand

Prasert Auewarakul, Mahidol University, Thailand

Somboon Kunathikom, Mahidol University, Thailand

Supakorn Rojananin, Mahidol University, Thailand

Suttipong Wacharasindhu, Chulalongkorn University, Thailand

Vasant Sumethkul, Mahidol University, Thailand

Watchara Kasinrerak, Chiang Mai University, Thailand

Wiroon Laupattrakasem, Khon Kaen University, Thailand

Yuen Tanniradorn, Chulalongkorn University, Thailand

Editorial Assistant: Nuchpraweeapawn Saleeon, Mahidol University, Thailand

Proofreader: Amornrat Sangkaew, Mahidol University, Thailand, Nuchpraweeapawn Saleeon, Mahidol University, Thailand

Morphologic Features and Morphometric Measurements of Human Oocytes That Failed to Cleave after Intracytoplasmic Sperm Injection (ICSI)

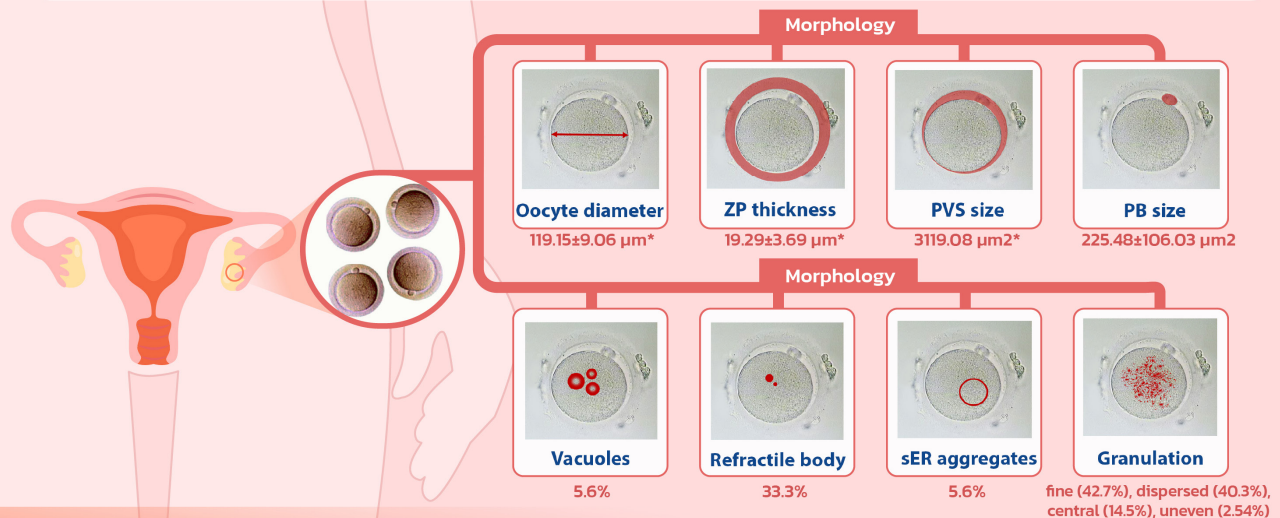
Ali Mohsin Alwaeli, MBChB, M.Sc., Ph.D.^{1*}, Shatha Sadiq Almarayaty, MBChB, M.Sc., Ph.D.², Maan Hamad Al-Khalisy, MBChB, M.Sc., Ph.D.³, Mohammed Hussein Assi, MBChB, M.Sc., Ph.D.¹

¹Department of Anatomy, College of Medicine, Al-Mustansiriyah University, Baghdad, Iraq, ²Department of Physiology, Alrafidain University College, Baghdad, Iraq, ³Department of Anatomy, College of Medicine, Baghdad University, Baghdad, Iraq.

Morphology and Morphometry of Oocytes that Fail to Cleave

Specific morphologic features of human oocytes may affect the outcome of intracytoplasmic sperm injection (ICSI). We examined the morphology of oocytes that failed to cleave after ICSI. 142 oocytes that failed to cleave were collected from women having ICSI cycles.

*** A significant inverse correlation was found between the oocyte cytoplasmic diameter and PVS size ***



OUTCOME

Failed oocytes have no significant morphologic differences from oocytes that cleaved normally after intracytoplasmic sperm injection.

SCAN FOR FULL TEXT



*Corresponding author: Ali Mohsin Alwaeli

E-mail: ali.alwaeli@uomustansiriyah.edu.iq

Received 6 August 2025 Revised 19 October 2025 Accepted 19 October 2025

ORCID ID: <http://orcid.org/0000-0001-9345-6717>

<https://doi.org/10.33192/smj.v78i1.274826>



All material is licensed under terms of the Creative Commons Attribution 4.0 International (CC-BY-NC-ND 4.0) license unless otherwise stated.

ABSTRACT

Objective: Human oocytes collected for in vitro fertilization (IVF) vary in morphologic features and measurements. This study aimed to describe the morphology of human oocytes that failed to cleave after intracytoplasmic sperm injection (ICSI).

Materials and Methods: Oocytes that failed to cleave post-ICSI were collected from IVF cycles. The oocytes were microscopically examined and the cytoplasmic diameter, zona pellucida thickness, perivitelline space (PVS) size, and first polar body (PBI) size were measured. The granularity pattern of cytoplasm; the color of cytoplasm; the presence of smooth endoplasmic reticulum (sER) aggregates, vacuoles, refractile bodies, and pronuclei; and, the status of polar bodies were all recorded.

Results: A total of 142 oocytes were analyzed. The mean cytoplasmic diameter was $119.15 \pm 9.06 \mu\text{m}$ (range: 90.66-137.79 μm). The mean zona pellucida thickness was $19.29 \pm 3.69 \mu\text{m}$ (range: 12.86-33.69 μm). The mean PVS size was $3119.08 \mu\text{m}^2$ (range: 765-6448 μm^2). The mean PBI size was $225.48 \pm 106.03 \mu\text{m}^2$ (range: 53.56-703.65 μm^2). The cytoplasm showed fine (42.7%), dispersed (40.3%), central (14.5%), and uneven (2.54%) patterns of granulation. Other cytoplasmic abnormalities included refractile bodies (33.3%), sER aggregates (5.6%), vacuoles (5.6%), and dark cytoplasm (14.5%). A significant inverse correlation was found between the oocyte cytoplasmic diameter and PVS size.

Conclusion: The morphologic abnormalities in oocytes that failed to cleave after ICSI are not significantly different from those observed in the general population of human oocytes. The oocyte cytoplasmic diameter was found to significantly inversely correlate with PVS size.

Keywords: Morphologic features; morphometric measurements; human oocytes; failed; cleave; intracytoplasmic sperm injection; ICSI (Siriraj Med J 2026;78(1):1-10)

INTRODUCTION

A normal human metaphase II (MII) oocyte generally shows a rounded and clear zona pellucida, a small perivitelline space (PVS) that contains a single oval polar body (or first polar body [PBI]), and a light cytoplasm with moderate granulation and no cytoplasmic inclusions.^{1,2} However, most retrieved oocytes after controlled ovarian stimulation have some morphologic abnormalities, including ooplasmic and/or extracytoplasmic features.^{3,4} Whether the presence of these visible oocyte morphologic abnormalities can adversely influence the outcome of *in vitro* fertilization (IVF) and intracytoplasmic sperm injection (ICSI) or not has not yet been conclusively established. Some authors suggest that oocytes may be successfully fertilized via ICSI regardless of their morphologic features.^{5,6} Other authors suggested that oocyte morphology influences embryo quality and development. One previous study showed that the grade of oocyte (based on PBI morphology, PVS size, and the presence of intracytoplasmic inclusions) correlates with oocyte developmental potential after ICSI.⁷ Another study found the added effect of oocyte morphologic anomalies, like cytoplasmic granularity, refractile bodies, vacuoles, inclusions, and central cytoplasmic granulation, to be significantly associated with impaired embryo quality, but the pregnancy rates were not adversely affected.⁸ However, a contradictory

conclusion was obtained by a different study, which found that the same features mentioned above had no significant effect on the *in vitro* development of embryos, but that they were associated with lower implantation and pregnancy rates when the embryos developed from oocytes with these cytoplasmic defects.⁹

In the present study, the morphologic and morphometric features and measurements of oocytes that failed to cleave following ICSI were investigated. The results of this study will improve our understanding of whether the presence of morphologic and/or morphometric abnormalities influence the fertilization failure observed in these oocytes by comparing them with the prevalence of similar abnormalities observed in human oocytes before ICSI as mentioned in the literature.

MATERIALS AND METHODS

Fifty-two women, aged 20 to 44 years, were included in this prospective observational study during January 2023 to July 2023 study period. These women had controlled ovarian stimulation with the antagonist protocol, using GnRH antagonist and recombinant FSH. Recombinant FSH was used for its proved safety and efficacy in IVF practice.¹⁰ A total of 142 oocytes that failed to show the first mitotic division (cleavage) after ICSI were enrolled. Study oocytes were collected on day-2 post-

injection and immediately examined and photographed using an inverted light microscope (Olympus IX71; Olympus Corporation, Tokyo, Japan) fitted with a digital camera system that is connected to a personal computer loaded with digital imaging software. Photography and microscopic examination of the morphologic parameters were performed under x200 magnification. The protocol for this study was approved by the Institutional Review Board of Kamal Al- Sameraie Hospital for Infertility Management and In Vitro Fertilization, Baghdad, Iraq (COA no. 879/2022), and all female patient volunteers provided written informed consent permitting the use of their failed oocytes in this study.

Oocyte morphometry

Oocyte morphometric measurements were performed using ImageJ software (ij153-win-java8 version; National Institutes of Health, Bethesda, MD, USA). The measurements included oocyte diameter, polar body (PB) size, perivitelline space (PVS) size, and zona pellucida (ZP) thickness. Oocyte size was estimated by measuring the oocyte cytoplasmic diameter (ooplasmic diameter). This was performed by calculating the mean of 4 different cytoplasmic diameter measurements for each oocyte, and each cytoplasmic diameter measurement was taken at a location at least 45° away from any of the other cytoplasmic diameter measurements. The area occupied by the polar body in the oocyte image was used as an indicator of PB size. The size of the PVS was also estimated by measuring its area in the oocyte image. This was performed by subtracting the oocyte image area from the area bounded by the inner surface of the ZP. ZP thickness was measured as the distance between its outer and inner surfaces. To obtain more accurate results, ZP thickness was measured at 8 different locations around its circumference and the mean measurement was recorded.

Oocyte morphology

The morphologic features of the oocytes evaluated in this study include the following: **a.** Cytoplasmic granulation: According to the pattern of cytoplasmic granules, oocytes were divided into one of the following four granulation categories¹¹: fine granulation (FG), dispersed granulation (DG), central granulation (CG), or uneven granulation (UG); **b.** Cytoplasmic color (light or dark); **c.** The presence or absence of specific intracytoplasmic structures, including refractile bodies, smooth endoplasmic reticulum [sER] aggregates, vacuoles, and pronuclei; and, **d.** Extracytoplasmic features, including PB fragmentation and PVS granulation.

Sample size calculation and statistical analysis

The sample size for this study was calculated using Yamane's formula (1967) $n = N/(1+N(e)^2)$ where n: sample size, N: population size, e: margin of error (p=0.05) at 95% confidence interval and 30% expected frequency. The Epi Info application (Centers for Disease Control and Prevention [CDC], Atlanta, Georgia, USA) was used to apply these parameters and the calculated sample size was 140-148. The enrolled sample in the present study was N=142.

The results of this study were analyzed using SPSS Statistics version 26 (SPSS, Inc., Chicago, IL, USA) to confirm or deny statistical significance. The continuous data are expressed as mean ± standard deviation, and a correlation between continuous measurements was detected by Pearson's correlation coefficient (r). T-test and analysis of variance (ANOVA) were used to determine the statistical significance of association between non-continuous data. A probability value of p<0.05 was considered to reflect statistical significance.¹²

RESULTS

Microscopic examination of the 142 oocytes for the investigated features and parameters revealed the following morphometry and morphology data.

Oocyte morphometry

The oocyte diameter (excluding the ZP) ranged from 90.66 µm to 137.79 µm, with a mean of 119.15 µm. Out of the 124 oocytes included, 122 (98.4%) oocytes had a diameter less than 130 µm (the upper normal limit of metaphase II [MII] human oocyte diameter), and only two (1.6%) exceeded 130 µm (Fig 1a, Fig 2a, b). The thickness of oocyte ZP ranged from 12.86 µm to 33.69 µm, with an average of 19.29 µm. Nine (7.2%) oocytes had a ZP thickness greater than the upper normal limit of 24.9 µm, and no oocytes had a ZP thickness below the lower normal limit of 8.57 µm (Fig 1b, Fig 2c, d). The size of the PVS (as estimated by the area in the image) of the included oocytes showed a wide range of variation, ranging from 765 µm² to 6,448 µm², with an average of 3,119.08 µm² (Fig 1c, Fig 2a, b). All of the studied oocytes had at least one visible PB. The size of the first polar body (PBI) (as estimated by its area in the image) showed broad variation, ranging from 53.56 to 703.65 µm², with an average of 225.48 µm² (Fig 1d). Fragmented PBI was observed in 33 oocytes (26.6%). A second polar body (PBII) was identified in only 18 oocytes (14.5%). One oocyte had a giant PB (Fig 3b, c, d).

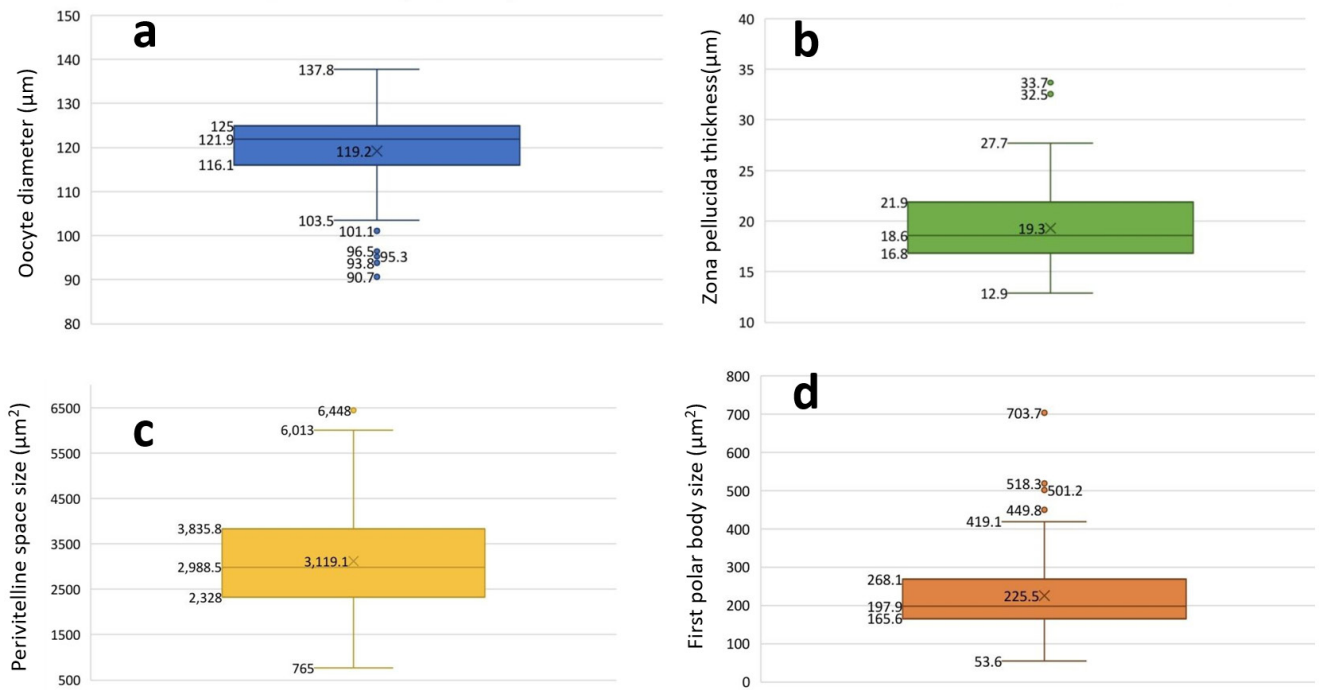


Fig 1. Overall descriptions of oocyte diameter (a), zona pellucida thickness (b), perivitelline space size (c), and first polar body size (d).

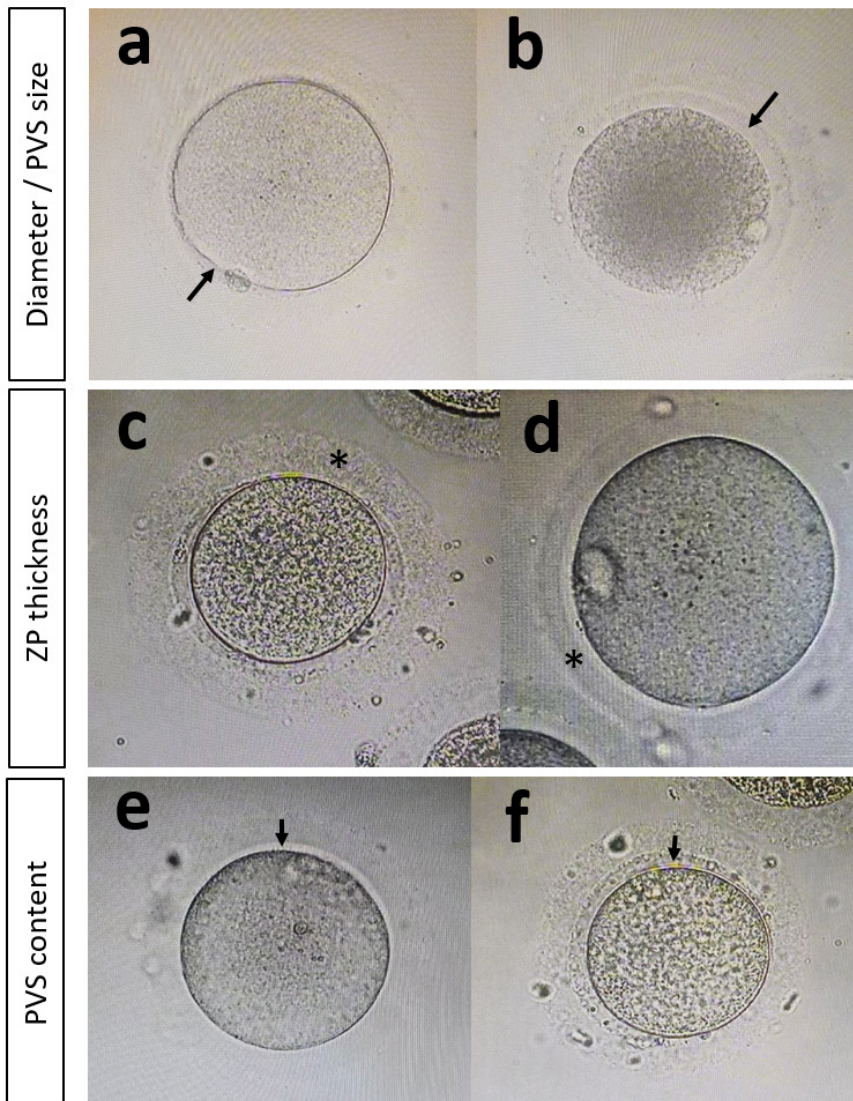


Fig 2. Variations in oocyte morphology and measurements, including oocyte with large diameter and small perivitelline space (PVS) size (a), oocyte with small diameter and large PVS size (b), thick zona pellucida (ZP) (c), thin ZP (d), clear PVS (e), and PVS with fragmentations (f). Arrows indicate PVS. (magnification x200)

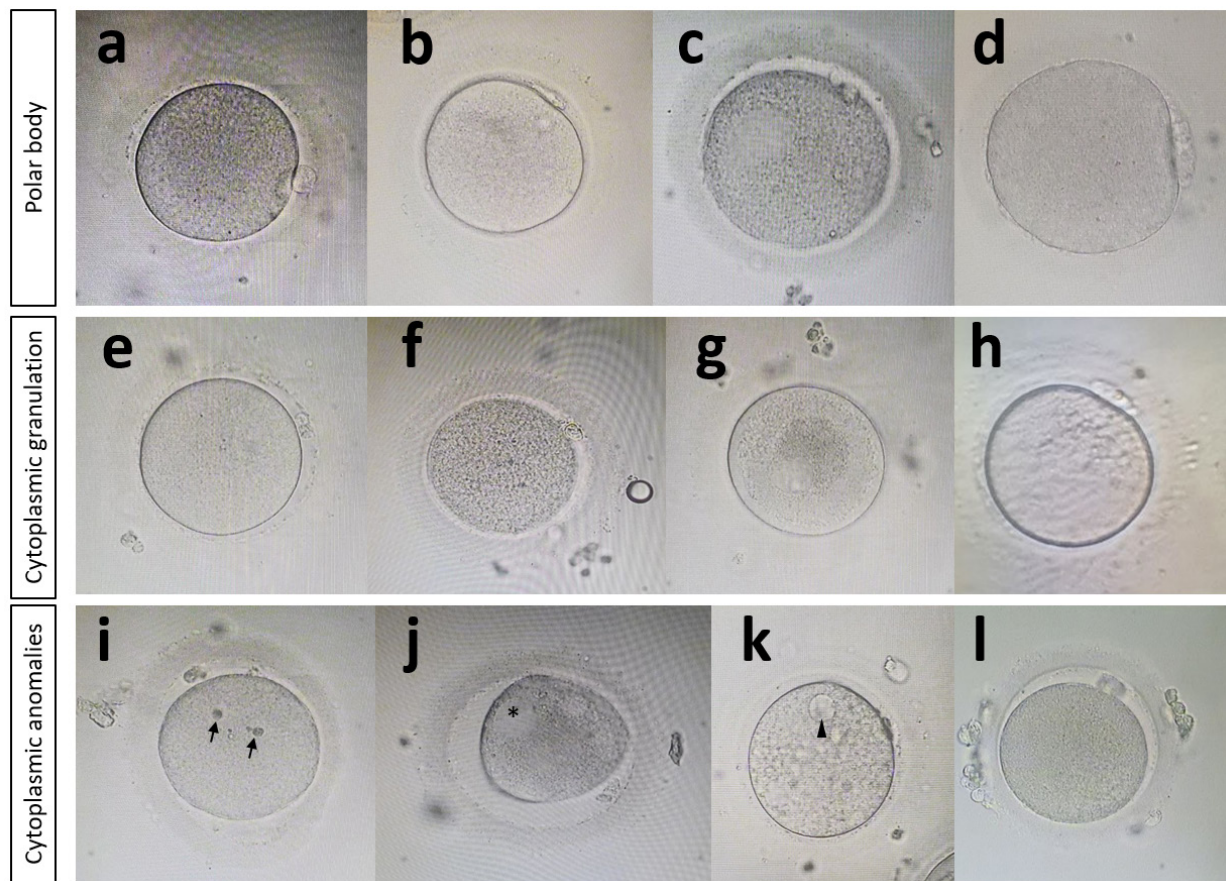


Fig 3. Polar body variations, including regular polar body (PB) (a), fragmented PB (b), double polar bodies (c), and giant PB (d); cytoplasmic granulation patterns: fine (e), dispersed (f), central (g), and uneven (h); cytoplasmic abnormalities: refractile bodies (arrows) (i), smooth endoplasmic reticulum (sER) aggregates (asterisks) (j), vacuoles (arrow head) (k), and dark cytoplasm (l). (magnification x200)

Oocyte morphology

Regarding the pattern of cytoplasmic granularity, the normal fine granulation (FG) pattern of the cytoplasm was seen in 53 (42.7%) oocytes, while the remaining 71 (57.3%) oocytes had one of the abnormal cytoplasmic granulation patterns, including dispersed (50 oocytes; 40.3%), central (18 oocytes; 14.5%), and uneven (3 oocytes; 2.4%) (Fig 3e, f, g, h). Concerning the other morphologic features, refractile bodies were observed in the cytoplasm of 41 oocytes (33%), aggregates of smooth endoplasmic reticulum (sER) were seen in 7 oocytes (5.6%), cytoplasmic vacuoles were observed in 7 oocytes (5.6%), and dark-colored cytoplasm was seen in 18 (14.5%) of oocytes (Fig 3i, j, k, l). PVS with fragmentations was found in 59 (47.6%) oocytes (Fig 2f).

Correlations and associations between morphologic and/or morphometric features

There was a statistically significant moderately inverse linear correlation between oocyte diameter and PVS size (Fig 4). No statistically significant correlation was found between other measurable morphologic features,

including ZP thickness, PVS size, or PBI size. Larger oocyte diameter was significantly associated with the presence of fragmentations in the PVS, and smaller oocyte diameter was significantly associated with uneven cytoplasmic granulation, and with dark-colored oocytes (Fig 5a). Larger PBI size was significantly associated with PB fragmentation (Fig 5b). Smaller ZP thickness was significantly associated with uneven granulation pattern of cytoplasm. Larger PVS size was associated with dark oocytes, and with the presence of a second polar body (PBII) (Fig 5c). Light cytoplasmic color was associated with significantly higher rates of fine cytoplasmic granulation, and dark cytoplasmic color was associated with significantly higher rates of dispersed granulation (Fig 5d).

DISCUSSION

The aim of this study was to investigate the specific morphologic features in an oocyte population that failed to cleave after ICSI, and to compare the prevalence of those features with the features and prevalence observed in the general oocyte population described in the literature.

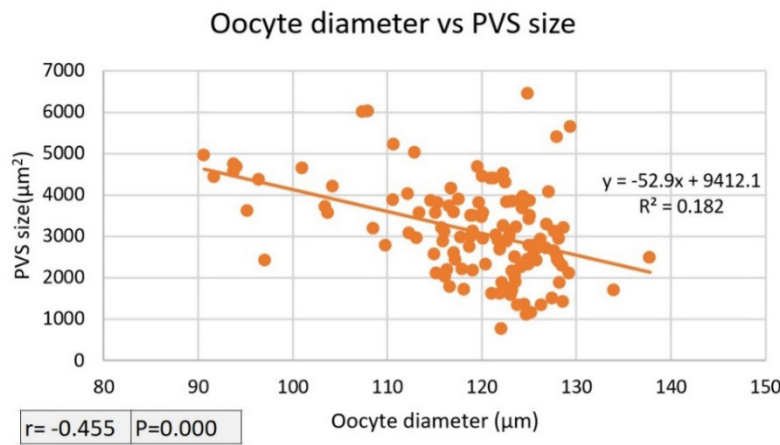


Fig 4. Linear correlation between oocyte diameter and perivitelline space (PVS) size.

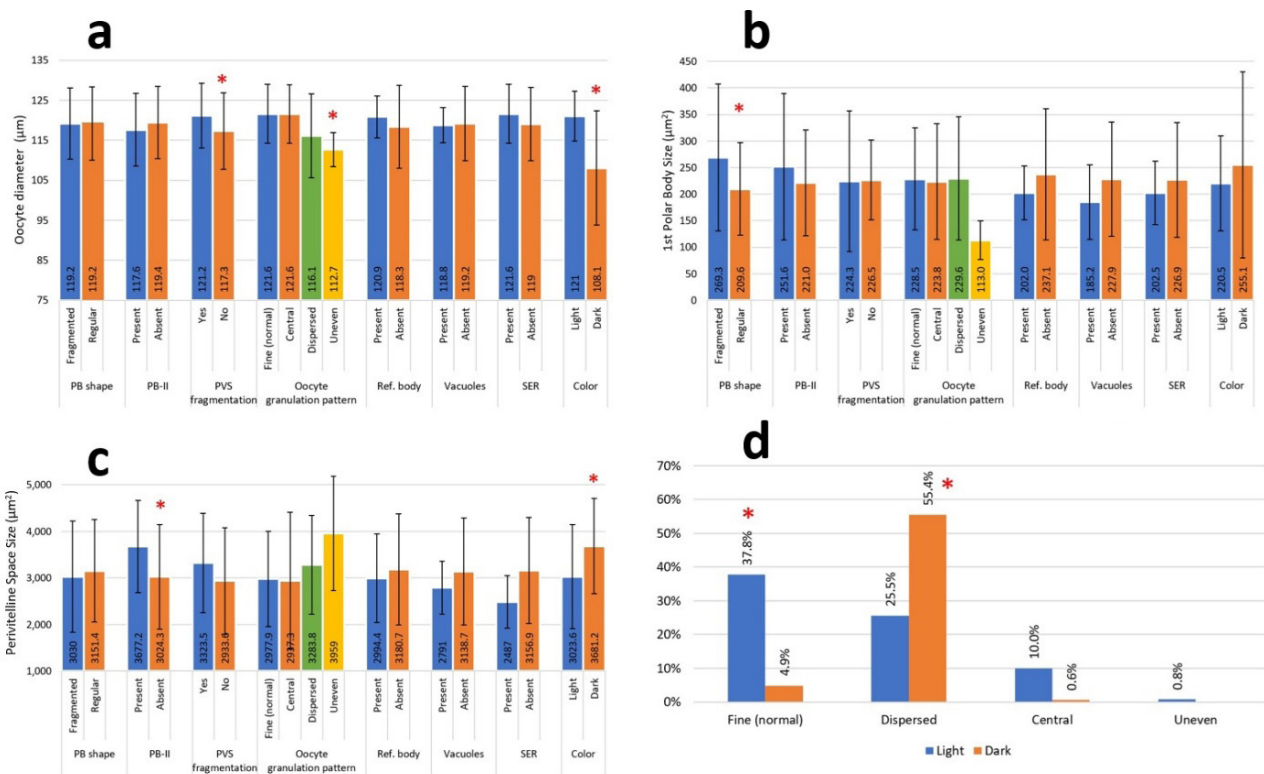


Fig 5. Associations among oocyte morphologic and morphometric parameters, including association between oocyte diameter and oocyte morphologic features (a), association between first polar body size and oocyte morphologic features (b), association between perivitelline space size and oocyte morphologic features (c), and association between oocyte cytoplasmic granulation and oocyte cytoplasmic color (d). An asterisk indicates statistical significance with a p-value < 0.05.

We also reported the statistically significant correlations/associations that we identified between some oocyte morphologic and/or morphometric features.

Cytoplasmic granularity is a common finding in metaphase II (MII) oocytes; however, the previously published studies in the literature do not report the exact numbers regarding the incidence of cytoplasmic granulations. The 4 patterns of cytoplasmic granulation are reported to occur in highly variable proportions in

oocytes retrieved for IVF. The present study investigated oocytes that failed to cleave, and the cytoplasmic granulation patterns among those oocytes included fine (42.7%), dispersed (40.3%), central (14.5%), and uneven (2.4%). In a large recent study¹¹, fresh oocytes showed cytoplasmic granulation in the following percentages: uneven (62.1%), fine (20.1%), dispersed (9.9%), and central (7.9%). Most of the other studies investigated the pattern of central granulation in particular, and reported a higher incidence

of central granulation compared to the rate found in our study.^{13,14,15} The presence of central granulation pattern had a negative effect on ICSI outcomes in most studies^{13,15-17}; however, one study¹⁴ reported no difference in ICSI outcomes between oocytes with central granulation and morphologically normal oocytes. We did not compare the granulation patterns in failed oocytes with those in successfully cleaved oocytes; however, we did find the incidence of CG pattern to be relatively low in failed oocytes.

The association between fine granulation with light-color cytoplasm, and dispersed granulation with dark-color cytoplasm can be explained by the visual effect of the coarse, large-size granules that characterize dispersed granulation pattern and that give the cytoplasm a darker tint compared to that conferred by fine granules. However, not all dark-color oocytes had a dispersed cytoplasmic granulation, and no similar association was mentioned in the studies we searched during our literature review.

The current literature describes the presence of specific cytoplasmic dysmorphisms, including refractile bodies, sER aggregates, and vacuoles, in the oocytes retrieved for IVF, but none of those studies mention the specific rate of incidence for each one. Refractile bodies were commonly seen in our study (33.3% of studied oocytes), which is a higher rate than the previously reported rate for oocytes before performing ICSI (26.6% according to Takahashi, *et al.* 2019.¹⁸ Smooth endoplasmic reticulum aggregates and cytoplasmic vacuoles were rare (both 5.6%), but were within the range mentioned in the literature (4-23% according to Wang, *et al.* 2023.¹⁹ The prevalence of cytoplasmic vacuolation in our study (5.6%) is also within the range previously reported for MII oocytes (5-12% according to Fancsovit, *et al.* 2011.²⁰ The effect of the presence of these morphologic abnormalities on ICSI outcome is related to the number and severity of these dysmorphisms rather than their mere existence.²

The mean oocyte cytoplasmic diameter in our study was comparable to the diameter described in the literature for MII oocytes retrieved for intracytoplasmic sperm injection.²¹⁻²⁴ While all of these studies described the oocyte diameter in all oocytes collected for ICSI, our study included only oocytes that failed to cleave after ICSI, and our results show that the diameter of failed oocytes is not significantly different from that of oocytes that were successfully fertilized.

There was a moderate inverse correlation between ooplasmic diameter and the size of the PVS in our study. This was most evident in oocytes with a diameter <100 μm , which was the oocyte subpopulation that had the largest size of PVS. A possible explanation is the early

degeneration of these oocytes, which results in oocyte shrinkage and increased PVS size. We were unable to find a similar previously reported correlation in the literature to which we could compare our result.

Giant oocytes are characterized as having both approximately twice the size of normal oocytes and abnormal ploidy, which is defined as diploid, triploid, or tetraploid instead of the normal haploid number of chromosomes. Kitasaka, *et al.* (2022)²⁴ set a diameter of >130 μm to define giant oocytes. In our study, two oocytes had a diameter slightly larger than 130 μm ; however, they didn't have extra sets of chromosomes when examined by immunofluorescence stain. They were, therefore, not categorized as giant oocytes. Larger oocyte diameter was found to be significantly associated with higher rate of fragmentation in the PVS in our study. Fragmentation in the PVS has been associated by some authors to high doses of follicle-stimulating hormone (FSH) used during ovarian hyperstimulation in IVF cycles.²⁵ Another study found association between FSH use and a number of oocyte morphologic and morphometric criteria, including larger ooplasmic diameter.²⁶ So our finding may be explained by the use of FSH during controlled ovarian hyperstimulation.

Smaller oocyte diameter was significantly associated with darker-color oocytes, and also with uneven oocyte cytoplasmic granulation in our study. The first association may be due to early degeneration and shrinkage of the oocyte. The data and findings from the very few studies in darker-color oocyte cytoplasm are not enough to support or deny this assumption. The same can be said about the second association in addition to the small number of oocytes with uneven cytoplasmic granulation (3 oocytes), which is insufficiently robust enough to draw confident and reliable conclusions.

The mean ZP thickness of oocytes in this study is consistent with the ZP thickness data reported in the literature.^{27,28} Those studies measured ZP thickness in the entire cohort of oocytes collected for ICSI, whereas our study included only oocytes that failed to cleave. This supports the assumption that ZP thickness is a parameter that will likely not differ significantly between those that failed to cleave and the general oocyte cohort.

The method used to estimate the size of the PVS in this study (by obtaining the area of the PVS on the oocyte 2-dimensional image) is probably more accurate than what is described by some authors. Shi, *et al.* (2016)²⁸ and Faramarzi, *et al.* (2017)²⁹ measured the maximum distance between the ooplasm and the inner surface of the ZP to estimate the PVS size. Alternatively, Yoshida and Niimura (2011)³⁰ subtracted the ooplasmic diameter from

the inner ZP diameter and took half of that measurement as the PVS size. Another study assessed and measured the PVS size subjectively.²⁵ The wide variation in the PVS size observed in our study is also described in many other studies.^{28,30-33} Approximately one-third of all retrieved oocytes show a large PVS^{7,34,35}; however, the published literature doesn't mention a numerical measurement to define what the term "large PVS" actually characterizes. In our study, oocytes with a normal-looking PVS size measured less than 3000 μm^2 , so we considered oocytes with a PVS size >3000 μm^2 to have a large PVS. Accordingly, 60 (48.4%) out of 124 oocytes had a large PVS in our study, and PVS fragmentation was seen in 59 (47.6%) oocytes. These findings suggest a higher chance of failed oocytes having PVS abnormalities (i.e., large PVS and/or PVS fragmentation) compared to all oocytes. This result agrees with previous studies that found a relationship between a large PVS or PVS granulation and a low fertilization rate^{33,34} and disagrees with the studies that found no effect of the size or fragmentation of the PVS on the fertilization rate.³¹ In our study, a larger PVS was found to be associated with dark-colored cytoplasm, and also with the presence of 2 polar bodies. The first finding may be due to early oocyte degeneration that causes both darker ooplasm and ooplasmic shrinkage (and hence larger PVS) since large PVS has been associated with oocyte degeneration in previous studies.⁴ As for the second finding, the extrusion of a second polar body requires more space to accommodate it, so this finding is rational from a mathematical perspective.

The size of every polar body observed in this study was measured to investigate for giant polar body phenomenon, which was observed in one oocyte. Moreover, we found larger PBI size to be significantly associated with PBI fragmentation. A polar body tends to fragment over time, so many authors consider a fragmented PB to be a sign that an oocyte has exceeded its optimal maturity.^{31,35,36} This may explain the association between large (overly mature) polar bodies and PBI fragmentation.

The most notable limitation of this study is the relatively small number of oocytes included in our investigation and analysis. Despite our finding of several important statistically significant correlations or associations, further study of oocyte morphology in a much larger sample of oocytes is needed to shore up the findings of this study, and to further elucidate characteristics like giant oocytes and giant polar bodies.

CONCLUSIONS

Morphologic abnormalities in oocytes that failed to cleave after ICSI showed no significant differences

compared to the general population of human oocytes. Central cytoplasmic granulation is less frequently encountered, and dispersed cytoplasmic granulation is associated with dark cytoplasmic color. Refractile bodies are more commonly observed in failed oocytes. The oocyte cytoplasmic diameter significantly inversely correlates with the PVS size.

Data Availability Statement

The data supporting the findings of our study are available upon request from the corresponding author, Ali Mohsin Alwaeli, with the following contact information: ali.alwaeli@uomustansiriyah.edu.iq

ACKNOWLEDGEMENTS

The authors gratefully acknowledge the female patients who generously agreed to allow their failed oocytes to be investigated in this study; the embryology lab staff of Kamal Al-Sameraie Hospital for Infertility Management and In Vitro Fertilization; and Assistant Professor Dr. Sameh S. Akkila for his assistance with statistical analysis.

DECLARATIONS

Grants and Funding Information

This was an unfunded study.

Conflict of Interest

All authors declare no personal or professional conflicts of interests.

Registration Number of Clinical Trial

None.

Author Contributions

Conceptualization and methodology, A.M.A.; Investigation, A.M.A. and S.S.A.; Formal analysis, M.H.A.; Visualization and writing – original draft, A.M.A.; Writing – review and editing, M.H.K. All authors have read and agreed to the final version of the manuscript.

Use of Artificial Intelligence

No form of AI was used to conduct or report the results of this study.

Ethics Approval

Our study was approved by the Institutional Review Board of Kamal Al-Sameraie Hospital for Infertility Management and In Vitro Fertilization, Baghdad, Iraq under approval number (COA no. 879/2022), and all female patient volunteers provided written informed

consent permitting the use of their failed oocytes in this study.

REFERENCES

1. Ebner T, Moser M, Tews G. Is oocyte morphology prognostic of embryo developmental potential after ICSI? *Reprod Biomed Online*. 2006;12:507–12.
2. Balaban B, Urman B. Effect of oocyte morphology on embryo development and implantation. *Reprod Biomed Online*. 2006;12:608–15.
3. Ebner T, Yaman C, Moser M, Sommergruber M, Feichtinger O, Tews G. Prognostic value of first polar body morphology on fertilization rate and embryo quality in intracytoplasmic sperm injection. *Hum Reprod*. 2000;15:427–30.
4. Mikkelsen AL, Lindenberg S. Morphology of in-vitro matured oocytes: Impact on fertility potential and embryo quality. *Hum Reprod*. 2001;16:1714–8.
5. De Sutter P, Dozortsev D, Qian C, Dhont M. Oocyte morphology does not correlate with fertilization rate and embryo quality after intracytoplasmic sperm injection. *Hum Reprod*. 1996;11:595–7.
6. Balaban B, Urman B, Sertac A, Alatas C, Aksoy S, Mercan R. Oocyte morphology does not affect fertilization rate, embryo quality and implantation rate after intracytoplasmic sperm injection. *Hum Reprod*. 1998;13:3431–3.
7. Xia, P. Intracytoplasmic sperm injection: Correlation of oocyte grade based on polar body, perivitelline space and cytoplasmic inclusions with fertilization rate and embryo quality. *Hum Reprod*. 1997;12:1750–5.
8. Chamayou S, Ragolia C, Alecci C, Storaci G, Maglia E, Russo E, et al. Meiotic spindle presence and oocyte morphology do not predict clinical ICSI outcomes: A study of 967 transferred embryos. *Reprod Biomed Online*. 2006;13(5):661–7.
9. Serhal PF, Ranieri DM, Kinis A, Marchant S, Davies M, Khadum IM. Oocyte morphology predicts outcome of intracytoplasmic sperm injection. *Hum Reprod*. 1997;12(6):1267–70.
10. Phophong P, Choavaratana R, Suppinyopong S, Loakirkkiat P, Karavakul C. Comparison of Human Menopausal Gonadotrophin and Recombinant Follicle-Stimulating Hormone in In-Vitro Fertilisation and Pregnancy Outcome. *Siriraj Med J*. 2020;53(11):805–10.
11. Hu J, Molinari E, Darmon SK, Zhang L, Patrizio P, Barad DH, et al. Predictive value of cytoplasmic granulation patterns during in vitro fertilization in metaphase II oocytes: part II, donor oocyte cycles. *Fertil Steril*. 2021;116(5):133–40.
12. Assi MH, Al-Rubai AJ, Alwaeli AM. Effect of Anthropometric Parameters on Quadriceps Femoris (Q) Angle: An Analytical Cross-Sectional Study from Iraq. *Al-Rafidain J Med Sci*. 2024;7(2):61–65.
13. Kahraman S, Yakın K, Dönmez E, Şamlı H, Bahçe M, Cengiz G, et al. Relationship between granular cytoplasm of oocytes and pregnancy outcome following intracytoplasmic sperm injection. *Hum Reprod*. 2000;15(11):2390–3.
14. Xiao-fang Yi, Hong-Lin Xi, Si-Lin Zhang, Yang J. Relationship between the positions of cytoplasmic granulation and the oocytes developmental potential in human. *Sci Rep*. 2019;10(9):7215.
15. Sun F, Cun J, Huang R, Chen Y, Verwoerd G, Yu Y. Different occurrence rates of centrally located cytoplasmic granulation in one cohort oocytes show distinctive embryo competence and clinical outcomes. *Reprod Biol*. 2022;22(3):100649.
16. Merviel P, Cabry R, Chardon K, Haraux E, Scheffler F, Mansouri N, et al. Impact of oocytes with CLCG on ICSI outcomes and their potential relation to pesticide exposure. *J Ovarian Res*. 2017;10(1):42.
17. Zhang L, Zeng L, Liu H, Jia H, Wu Y, He C. Effects of Oocyte Cytoplasmic Central Granulation on Embryonic Development, Blastocyst Formation, and Pregnancy Outcome in Technology and Its Mechanism. *Cell Mol Biol (Noisy-le-grand)*. 2022;68(5):161–9.
18. Takahashi H, Otsuki J, Yamamoto M, Saito H, Hirata R, Habara T, et al. Clinical outcomes of MII oocytes with refractile bodies in patients undergoing ICSI and single frozen embryo transfer. *Reprod Med Biol*. 2019;19(1):75–81.
19. Wang M, Gao L, Yang Q, Long R, Zhang Y, Jin L, et al. Does smooth endoplasmic reticulum aggregation in oocytes impact the chromosome aneuploidy of the subsequent embryos? A propensity score matching study. *J Ovarian Res*. 2023;16(1):59.
20. Fancsovits P, Murber A, Gilán ZT, János Rigó Jr, Urbancsek J. Human oocytes containing large cytoplasmic vacuoles can result in pregnancy and viable offspring. *Reprod BioMed Online*. 2011;23(4):513–6.
21. Balakier H, Bouman D, Sojecki A, Librach C, Squire JA. Morphological and cytogenetic analysis of human giant oocytes and giant embryos. *Hum Reprod*. 2002;17(9):2394–401.
22. Romão GS, Araújo MC, de Melo AS, Navarro P, Ferriani R, Dos Reis RM. Oocyte diameter as a predictor of fertilization and embryo quality in assisted reproduction cycles. *Fertil Steril*. 2010;93(2):621–5.
23. Weghofer A, Kushnir VA, Darmon SK, Jafri H, Lazzaroni-Tealdi E, Zhang L, et al. Age, body weight and ovarian function affect oocyte size and morphology in non-PCOS patients undergoing intracytoplasmic sperm injection (ICSI). *PLoS One*. 2019;14(10):e0222390.
24. Kitasaka H, Konuma Y, Tokoro M, Fukunaga N, Asada Y. Oocyte cytoplasmic diameter of >130 mm can be used to determine human giant oocytes. *F S Sci*. 2022;3(1):10–17.
25. Yu EJ, Ahn H, Lee JM, Jee B, Kim SH. Fertilization and embryo quality of mature oocytes with specific morphological abnormalities. *Clin Exp Reprod Med*. 2015;42(4):156–62.
26. Taheri F, Mehriz A, Khalili MA, Halvaei I. The influence of ovarian hyperstimulation drugs on morphometry and morphology of human oocytes in ICSI program. *Taiwan J Obstet Gynecol*. 2018;57(2):205–10.
27. Balakier H, Sojecki A, Motamedi G, Bashar S, Mandel R, Librach C. Is the zona pellucida thickness of human embryos influenced by women's age and hormonal levels? *Fertil Steril*. 2012;98(1):77–83.
28. Shi SL, Yao GD, Jin HX, Song WY, Zhang FL, Yang HY, et al. Correlation between morphological abnormalities in the human oocyte zona pellucida, fertilization failure and embryonic development. *Int J Clin Exp Med*. 2016;9(1):260–7.
29. Faramarzi A, Khalili MA, Omidi M. Morphometric analysis of human oocytes using time lapse: does it predict embryo developmental outcomes? *Human Fertility*. 2019;22(3):171–6.
30. Yoshida N, Niimura S. Size of the perivitelline space and incidence of polyspermy in rabbit and hamster oocytes. *Reprod Med Biol*. 2011;10(1):31–41.
31. Balaban B, Urman B. Effect of oocyte morphology on embryo development and implantation. *Reprod Biomed Online*. 2006;12(5):608–15.
32. Hassa H, Aydın Y, Taplamacıoğlu F. The role of perivitelline

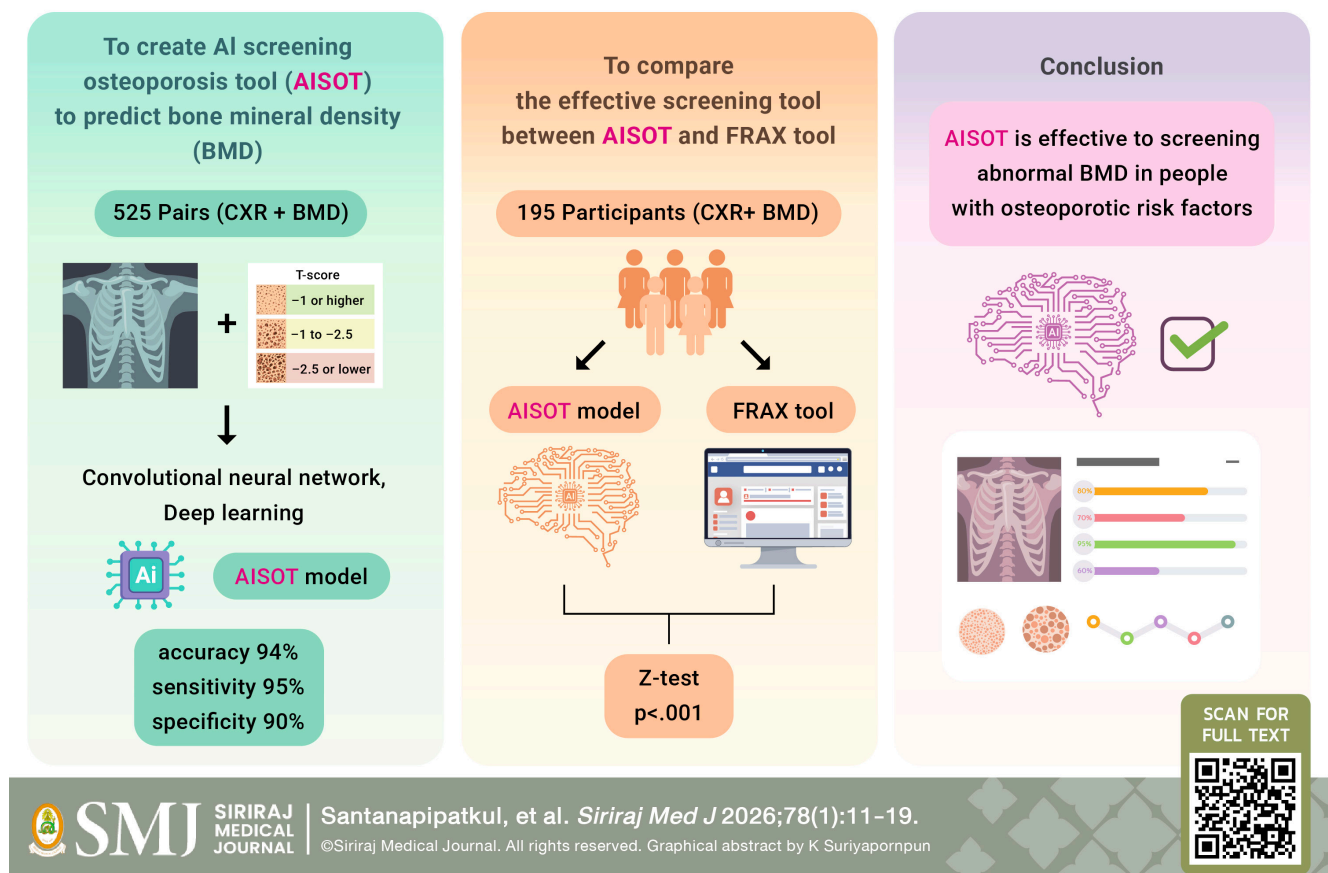
- space abnormalities of oocytes in the developmental potential of embryos. *J Turk Ger Gynecol Assoc.* 2014;15(3): 161-3.
33. Zanetti BF, Braga D, Setti A, Figueira R, Iaconelli A, Borges E. Is perivitelline space morphology of the oocyte associated with pregnancy outcome in intracytoplasmic sperm injection cycles? *Eur J Obstet Gynecol Reprod Biol.* 2018;231:225-9.
34. Rienzi L, Ubaldi FM, Iacobelli M, Minasi MG, Romano S, Ferrero S, et al. Significance of metaphase II human oocyte morphology on ICSI outcome. *Fertil Steril.* 2008;90(5):1692–700.
35. Rienzi L, Balaban B, Ebner T, Mandelbaum J. The oocyte. *Hum Reprod.* 2012;27(Suppl 1):i2-21.
36. Ciotti PM, Notarangelo L, Morselli-Labate AM, Felletti V, Porcu E, Venturoli S. First polar body morphology before ICSI is not related to embryo quality or pregnancy rate. *Hum Reprod.* 2004;19(10):2334–9.

Application of Artificial Intelligence for Osteoporosis Screening Using Chest Radiographs

Polasan Santanapipatkul, M.D.^{1,*}, Lakkana Jirapong, M.D.², Anchalee Chumjam, M.D.³, Nantika Wannasoupol, M.D.², Rapeepat Narkbunnam, M.D.⁴

¹Department of Orthopedic Surgery, Samut Sakhon Hospital, Samut Sakhon Province, Thailand, ²Department of Radiology, Samut Sakhon Hospital, Samut Sakhon Province, Thailand, ³Department of Otorhinolaryngology, Samut Sakhon Hospital, Samut Sakhon Province, Thailand, ⁴Department of Orthopedic Surgery, Faculty of Medicine Siriraj Hospital, Mahidol University, Bangkok, Thailand.

Application of Artificial Intelligence for Osteoporosis Screening Using Chest Radiographs



ABSTRACT

Objective: To create the artificial intelligence screening osteoporosis tool (AISOT) to predict bone mineral density (BMD) using chest radiographs and to describe statistics characterizing the tool's effectiveness and satisfaction of the tool usage.

Materials and Methods: All 525 BMD examinations individually paired with chest radiographs during the years 2022–2023. The AISOT was developed based on deep learning concept on chest radiograph images to predict BMD value. Both BMD observed and predicted values were classified osteoporosis condition by using T-scores of preclinical guidelines. The AISOT demonstrated the accuracy, sensitivity, specificity at 94% (95% CI: 84–99%), 95% (95% CI: 83–99%) and 90% (95% CI: 56–99%) respectively. The AISOT model was tested with 195 participants. The research instrument was a questionnaire developed by the researcher including personal health history, observed and predicted BMD values, FRAX tool osteoporosis evaluation and AISOT satisfaction. Z-test was utilized to compare statistics characterized the tool effectiveness.

Results: The AISOT vs the FRAX tool comprised accuracy at 74% (95% CI: 67–80%) vs 51% (95% CI: 44–58%) ($p < .001$); sensitivity at 61% (95% CI: 52–70%) vs 24% (95% CI: 17–33%) ($p = .012$); specificity at 93% (95% CI: 85–98%) vs 92% (95% CI: 84–97%) ($p > .05$); PPV at 94% vs 83% ($p = .015$); NPV at 61% vs 44% ($p = .016$). AISOT satisfaction was at very satisfied level (mean = 4.81, SD = 0.434).

Conclusions: AISOT is effective for screening abnormal BMD in people with osteoporotic risk factors. Future study of various settings will enhance its credibility.

Keywords: AI; BMD; osteoporosis; screening; chest radiograph (Siriraj Med J 2026;78(1):11-19)

INTRODUCTION

Osteoporosis is caused by decreasing systemic development of bone mineral density (BMD).¹ Osteoporosis typically remains as asymptomatic bone disease causing lack of concern to diagnose until bone fracture.² Elderly or lack of hormone balancing is more likely to stimulate the weakening process of the bone structure more rapidly.² Incidence of Osteoporosis in Thailand is around 20% in women and 10% in men, the age-adjusted incidence of hip fracture increased by 2% per year is rising from about 192.9 (males: 110.8; females: 272.1) to about 253.³ (males: 135.9; females: 367.9) per 100,000 person-year.³ In some cases even small accident could affect hip fracture that may cause a death around 12%.⁴

To detect osteoporosis, dual energy x-ray absorptiometry is the gold standard for examine BMD.⁵ Lower BMD means higher chance to categorize as osteopenia to osteoporosis indicated higher severity.^{5,6} There is a limitation of BMD examination due to high cost and limited availability. Even in Samutsakhon hospital, dual energy x-ray absorptiometry locates so far from the main hospital making it difficult to perform BMD.

To gain service reimbursement coverage from the government, criteria stated by Osteoporosis Institute of Thailand (OIT) must be met strictly.^{7,8} For example, in male group the age must be older than 70 years. On the other hand, in female group the age must be older than 65 years old based on hormone deficiency condition. As

stated by OIT, women at age less than 65 years who often eat meat without routinely exercise are likely to expose to osteoporosis incidence at 80–90%.⁷ This implies that there are some people who do not meet the criteria but can still have abnormal bone mineral density.

According to the study done by Sachin Sharma, artificial intelligence (AI) was immersed to medical area to distinguish infected lung by Corona virus from others. Based on the same pattern, chest radiography (comprised several chest bones) could be used along with AI software to predict BMD referring to osteoporosis classification.⁹ Therefore, the artificial intelligence screening osteoporosis tool (AISOT) was the main topic to serve research question in this study as can AISOT predict BMD accurately?

Fracture Risk Assessment Tool (FRAX) was developed by John A. Kanis, represented Sheffield University. The FRAX tool was widely used around 69 nationalities 34 languages availability to screen risk to have bone fracture.¹⁰ The result from the FRAX tool was reported into 2 statements as in 10 year forward 1) the percentage of chance to have hip fracture (> 20% must start osteoporosis treatment) 2) the percentage of chance to have other important bone fracture such as spine etc. (> 3% must start osteoporosis treatment). To be evaluated by this tool did not need to input BMD value from the examination along with 12-item questionnaire related to fracture risk factors.

Effective and convenience osteoporosis screening tool could help determine the risk group to early detect abnormal BMD. Therefore, to compare differences of the characteristic statistics represent effective screening tool between the AISOT and FRAX tool (as its standard) would be useful.

Objectives

1. To create the AISOT to predict BMD.
2. To compare differences of the characteristic statistics represent effective screening tool between AISOT and FRAX tool.
3. To study satisfaction about AISOT utilization.

Research questions

1. Can AISOT predict BMD accurately?
 2. Are there any significant differences between the characteristic statistics signifying effective screening tool of AISOT and FRAX tool?
 3. How were samples satisfied by AISOT utilization?
- Characteristic statistics of effective screening tool include sensitivity, specificity, accuracy, positive predictive value (PPV) and negative predictive value (NPV).

MATERIALS AND METHODS

A total of 525 BMD examinations during year from 2022 to 2023 personal-match paired with chest radiographs (within the interval of 1-year before and after period of the BMD examination date) were randomized through computer system. Eighty percent (423) out of the total chest radiographs were randomized and were employed as train set. Each 51 (10%) of the rest chest radiographs was used as valid set and test set to complete the model illustration to become osteoporosis screening tool.

The process of AI software program creation first taking place at each chest radiograph was transformed to pixel 8 bit pattern follow by value range 0-255, 128 x128 pixels. Then normalized value range was sent to convolutional neural network, then paired with BMD observe resulted from BMD examination and was turned to be algorithm coding.

According to BMD examination result, there were 3-group classification of osteoporosis condition as normal, osteopenia and osteoporosis. Based on the two by two table of screening test design, the osteoporosis must be categorized into 2 groups. Therefore, two models were generated based on criteria as follows:

Model 1: BMD \leq -1 VS BMD $>$ -1
 (Osteopenia + Osteoporosis) (Normal)

Model 2: BMD \leq -2.5 VS BMD $>$ -2.5
 (Osteoporosis) (Osteopenia + Normal)

The Model 1 characterized as normal vs osteopenia and osteoporosis indicated accuracy at 94% with the best benefit of sensitivity at 95% and specificity at 90% based on receiver operating characteristic (ROC) curve. Predicted BMD values were calculated.

To achieve deeper understanding regarding comparing effective screening tool performance between AISOT and FRAX tool, a total of 195 volunteers were recruited for the study. Inclusion and exclusion criteria were illustrated base on academic considerations to reduce bias in the study.

Inclusion criteria

1. Age 50 years or older who have had chest radiograph within 1 year. In case of age less than 50 years old, needed at least one of the following requirements.

1.1 Female had surgery to remove both of the ovaries or was diagnosed with low estrogen hormone condition at prior stage of menopause or taking aromatase inhibitor drug.

1.2 Male reported on androgen deprivation therapy.

1.3 Individuals who met at least one of the following criteria:

- Had a fragility fracture from a minor accident.
- Taking a glucocorticoid drug at a dose equivalent to 5 mg. of prednisolone daily for longer than 3 months.
- Reported at least one parent experienced a hip fracture though was a small accident.
- Maintained BMI $<$ 20 kg/m²
- Had a height lost of at least 4 cm or a loss of 2 cm per year compared to previous height
- Chest radiograph showed radiographic osteopenia or vertebral fracture

2. Held medical health benefit reimbursement for BMD examination.

3. Willing to participate in the study.

Exclusion criteria

1. Chest area operation history.
2. Diagnosed with bone cancer or cancer in any other organs with bone metastasis.
3. Diagnosed abnormal chest bones.

Both BMD (observed and predicted values) results have been classified to osteoporosis condition based on T-scores of preclinical guidelines (recommended by World Health Organization). Also, osteoporosis condition of each volunteer was classified by using FRAX tool. The comparison of the characteristic statistics represent effective screening tool between the AISOT and FRAX tool was done by using Z-test.

Research instruments

1. The AISOT developed by the researcher based on deep learning, convolutional neural network and transferring learning theory. The AISOT characterized the accuracy at 94% with sensitivity at 0.95 and specificity at 0.90 based on ROC curve (Table 3).

2. Questionnaires created by the researcher including

Part 1: Demographic data and 14 closed questions of osteoporosis risk factors

Part 2: Satisfaction questionnaire with 5 point Likert scale including 7 items

Data collection

After approval by ethical committee (SKH REC 153/2567/V.1), related divisions were approached to collaborate. Consent forms were completed by samples after agreement to participate in this research study. Questionnaire (part 1) was done by each participant. The researcher determined osteoporosis condition for each participant (face-to-face) by applying chest radiograph to AISOT. The results were kept in the system of each participant account with blinding concern to contaminate other research process. The information regarding BMD examination including appointment date, place and time were delivered to the participant. Each participant finished BMD examination. On the day appointment, each participant was educated regarding the result of BMD examination compared to AISOT at outpatient department. Satisfaction questionnaire (part 2) was done by participant. Further treatment was provided to each participant if needed.

Statistical analyses

The data were analyzed by using descriptive statistics relevant to show effective tool and tool usage satisfaction. The Z-test (inferential statistics) was utilized to signify two proportions significant differences.¹¹

RESULTS

A total of 195 volunteers were classified as 120 (61.5%) hospital staff and 75 (38.5%) local health care providers. The majority of cases were female 186 (95.4%) participants. The mean of age was 59.09 (S.D. = 7.54) years old with the majority (55.9%) at the range of 50-59 years, minimum at 40 and maximum at 85 years old. Most of them (61.5%) held BMI less than 25 (kg/m²). Around 20% have reported experienced bone fracture with 6.2% having father who experienced bone fracture as same as mother side around 6.7%. Around 2.6% reported having Rheumatoid arthritis. Around 1% of all participants had fragile bone condition, malabsorption

of intestine, chronic liver disease, on steroid drug daily. The majority of female (89.7%) were in menopause hormone stage (Table 1).

After using the AISOT model to predict BMD in the samples, the tool resulted accuracy at 74% (95% CI: 67- 80%); sensitivity and specificity, PPV, NPV were at 61% (95% CI: 52-70%), 93% (95% CI: 85-98), 94% (95% CI: 86-97%), and 61% (95% CI: 55-66%) in order. The Likelihood Ratios for positive and negative tests were at 9.32 (95% CI: 3.95- 22.02) and 0.41 (95% CI: 0.33- 0.52) (Table 3).

After using BMD observe value result of each participant along with other independent risk factor to predict the osteoporosis condition, the result showed that FRAX tool accuracy was at 51% (95% CI: 44- 58%). With the same order according to the AISOT, the results of FRAX tool were at 24% (95% CI: 17-33%), 92% (95% CI: 84-97%), 83% (95% CI: 68-92%), 44% (95% CI: 41-47%), 3.09 (95% CI: 1.35- 7.08) and 0.82 (95% CI: 0.73- 0.93) for sensitivity, specificity, PPV, NPV, the likelihood ratios for positive and negative tests in sequence (Table 3).

The proportion comparisons between the results of these tools showed that accuracy was highly significantly different ($Z = 3.359$, $p < .001$) and sensitivity, PPV and NPV were significantly different ($Z = 5.290$, $p = .012$; $Z = 0.94$, $p = .015$; and $Z = 2.407$, $p = .016$). Specificity was not significantly different (Table 4). The Pre-test probability was at 0.61. Post-test probability was at 0.94 (Table 3). This means that The AISOT increased the likelihood to find osteoporosis cases improve from 61 to 94% (33% increased) meanwhile FRAX tool has been improved seeking cases around 21% (61% to 82%).

For tool satisfaction, participants responded very satisfied to the AISOT regarding reduce difficulty (mean = 4.82, SD. = .426), safe time to perform (mean = 4.83, SD. = .418), safe cost (mean = 4.81, SD. = .430), very convenient to use (mean = 4.80, SD. = .438), support treatment planning (mean = 4.80, SD. = .438), increase knowledge to help other people (mean = 4.81, SD. = .434), in general (mean = 4.81, SD. = .434).

DISCUSSION

The AISOT was established to predict BMD. The AISOT was promising screening tool due to low cost, ease of use, rapid assessment and reasonable precision (74%) result. Seeking osteoporosis as soon as possible for early treatment was the main goal in this study. The discussion of AISOT as effective screening tool will be discussed as follows:

Osteoporosis, mainly cause of bone fracture referring to severe morbidity or mortality in some cases.⁷ This

TABLE 1. Demographic data of samples (N = 195).

Demographic data	Number	Percentage (%)
Status (Hospital staff/ Health care volunteers)	120/75	61.5/38.5
Gender (Male/Female)	9/186	4.6/95.4
Age		
40 - 49	9	4.6
50 - 59	109	55.9
60 - 69	55	28.2
70 - 79	18	9.2
80 and above	4	2.1
Mean = 59.09 (S.D. = 7.54) Minimum = 40 Maximum = 85		
BMI (kg/m ²)		
18.49 and less	10	5.1
18.50 - 22.99	71	36.4
23.00 - 24.99	39	20.0
25.00 – 29.99	58	29.7
30.00 and above	17	8.7
Bone fracture experience* (Yes/No)	38/155	19.7/80.3
Does father have hip fracture* (Yes/No)	12/181	6.2/93.8
Does mother have hip fracture* (Yes/No)	13/180	6.7/93.3
Rheumatoid arthritis* (Yes/No)	5/188	2.6/97.4
Type I Diabetes* (Yes/No)	2/191	1.0/99.0
Secondary osteoporosis* (Yes/No)	2/191	1.0/99.0
Hyperthyroidism* (Yes/No)	8/185	4.1/95.9
Hormone deficiency* (Yes/No)	6/187	3.1/96.9
Chronic malnutrition* (Yes/No)	0/193	0.0/100.0
Absorption disorder* (Yes/No)	2/191	1.0/99.0
Chronic liver disease* (Yes/No)	2/191	1.0/99.0
Steroid daily intake* (Yes/No)	3/190	1.6/98.4
Only female with menopause** (Yes/No)	165/19	89.7/10.3

*n = 193; **n=186

TABLE 2. Diagnosis of osteoporosis classified by BMD with AISOT result and FRAX result.

		BMD		
		Positive	Negative	Total
AISOT (FRAX)	Positive	73 (29)	5 (6)	78 (35)
	Negative	46 (90)	71 (70)	117 (160)
Total		119	76	195

Abbreviations: BMD, bone mineral density; AISOT, artificial intellectual screening osteoporosis tool; FRAX, fracture risk assessment tool

TABLE 3. The statistics characterized screening tool effectiveness of osteoporosis classified by AISOT, FRAX and the original created AISOT.

Statistics	AISOT (95% CI) (n=195)	FRAX (95% CI)	Original (n=525)
Sensitivity	0.61 (0.52, 0.70)	0.24 (0.17, 0.33)	0.95 (0.83, 0.99)
Specificity	0.93 (0.85, 0.98)	0.92 (0.84, 0.97)	0.90 (0.56, 0.99)
Accuracy	0.74 (0.67, 0.80)	0.51 (0.44, 0.58)	0.94 (0.84, 0.99)
Positive predictive value (PPV)	0.94 (0.86, 0.97)	0.83 (0.68, 0.92)	0.97 (0.86, 0.99)
Negative predictive value (NPV)	0.61 (0.55, 0.66)	0.44 (0.41, 0.47)	0.82 (0.53, 0.95)
Likelihood Ratios for positive test	9.32 (3.95, 22.02)	3.09 (1.35, 7.08)	9.51 (1.48, 61.15)
Likelihood Ratios for negative test	0.41 (0.33, 0.52)	0.82 (0.73, 0.93)	0.05 (0.01, 0.21)
Prevalence or Pre-test probability	0.61 (0.54, 0.68)	0.80 (0.67, 0.90)	
Pre-test odds	1.56	1.56	
Post-test odds	14.58	4.83	
Post-test probability	0.94	0.82	

Abbreviations: BMD, bone mineral density; AISOT, artificial intelligence screening osteoporosis tool; FRAX, fracture risk assessment tool

TABLE 4. The statistics characterized screening tool effectiveness of osteoporosis classification using Z test for proportional comparison.

Statistics	AISOT	FRAX	Z	p
Sensitivity	0.61	0.24	5.290	.012
Specificity	0.93	0.92	.268	> .05
Accuracy	0.74	0.51	3.359	< .001
Positive predictive value (PPV)	0.94	0.83	.94	.015
Negative predictive value (NPV)	0.61	0.44	2.407	.016

Abbreviations: AISOT, artificial intelligence screening osteoporosis tool; FRAX, fracture risk assessment tool

AISOT was established and was expected to utilize in osteoporosis risk group, 50-year-old or older, to find actual osteoporosis cases. The finding of accuracy at 74% was congruent with some previous studies have held same concept of using AI working on chest radiographs in screening but difference settings. For example, from 31 prior studies the accuracy was ranged from 66.1% to 97.9% (this finding was 74%). Sensitivity and specificity was ranged from 67.4% to 100.0% (this finding was 61%), and 60.0% to 97.5% (this finding was 93%) respectively.¹² This indicates that AI has potential to classify chest radiographs detailed similarly. Deeper insight of AI utilization in technology (how AI works better) along with clinical screening (earlier detection) will be a challenge for further research study. The improvement of finding real cases with AISOT utilization compared to without the AISOT was 33% (61% to 94%).

As a part of health check-up procedures, chest radiography usually have done annually refer to higher chance to access. The AISOT working on the chest radiography to seek high risk cases of osteoporosis for further investigations. Even if chest radiography was not available, to do so it is affordable and accessible in most health care places.¹³ As far as the AISOT was utilized, the benefits range from early detection to early treatment with very low side effect. However, the AISOT has some acknowledged limitations as follows:

Due to limited participants for the study, sample selection contained sampling bias because they were selected based on inclusion criteria then volunteers were involved with no effect of randomization process.¹⁴ Lack of external validation in the study may cause less promise of same potentially model's performance reported in the research result. In prospective future research, having greater number of sample size with various datasets from multicenter and using randomized sampling technique will gain more credibility, validity and reliability to generalize the research application.

Recently, FRAX tool has been popular in many countries.⁹ In this study the prevalence of osteoporosis was 61%. High prevalence of disease could affect the sensitivity value.¹⁵ In this study, the FRAX tool held the sensitivity at 24% lower than that of the AISOT with statistically significant difference. ($p = .012$). Unlike the specificity between the AISOT and FRAX tools (0.93 VS 0.92) showed that there is no significant difference. The explanation could be less availability of the Dual energy x-ray absorptiometry as a result the cutoff point used to serve high rate of true negative cases. Also, the likelihood ratios for positive test (less affected by the prevalence rate compare to positive predictive value) between the

AISOT and FRAX tools were at 9.32 VS 3.09. This means the AISOT was better classification of positive outcome. Contrasting likelihood ratios for negative test, the FRAX tool was at 0.82 better than the AISOT was at 0.41.

According to the Fagan's Nomogram,¹⁶ the result showed pre-test probability was 0.61, pre-test odds at 1.56, post-test odds at 35.15, post-test probability at 0.97, this means the AISOT help to screen abnormal BMD 28% higher than without the tool (Fig 1).

In term of research utilization, there are many factors need to consider as follows:

1. Osteoporosis was not identified as life threatening disease based on the disease progression like cancer but it could cause death in some cases based on accident definition like unpredictable occurrence.

2. Similar to most diseases, the concept of early detection to access early treatment definitely gains advantages. Osteoporosis treatment before fracture occurs referring to operation or cervix cancer screening before metastasis stage are agreed to gain obvious advantages.

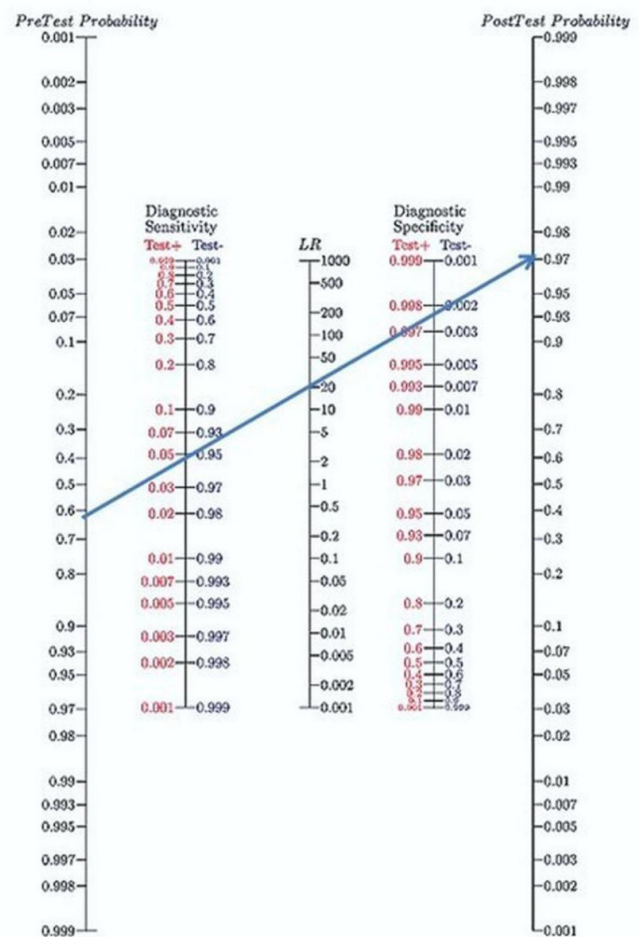


Fig 1. Fagan's Nomogram

3. To apply the AISOT in the high risk group as seniors will find the cases more than utilize in other group. However, national policy should be developed to serve the positive screening results to prevent negative health care service frustration.

4. National health care policy should be served the progression of the research finding such as health check-up yearly especially in non-high risk group with AISOT screening application and BMD examination regarding the positive result should be considered in the future.

CONCLUSION

The AISOT is a useful tool for screening abnormal BMD in people with osteoporosis risk factors due to no harm. Further prospective study with multicenter settings will help to perform sample selection with randomization. Lack of bias and error will obviously indicate better AISOT's performance to gain its credibility, validity and reliability to become popular clinical utilization.

Data Availability Statement

The data that support the findings of this study are not publicly available due to privacy and ethical restrictions related to the Personal Data Protection Act (PDPA) of Thailand. Data may be available from the corresponding author (Polasan Santanapipatkul) upon reasonable request and with permission from the Siriraj Institutional Review Board.

ACKNOWLEDGEMENT

The authors thank Parichard Gooch for her invaluable assistance and support.

DECLARATIONS

Grants and Funding Information

This article received no specific grant from any funding agency in the public, commercial, or not-for-profit sectors.

Conflict of Interest

All the authors confirm that they have no personal or professional conflicts of interest to declare relating to any aspect of this research study.

Registration Number of Clinical Trial

TCTR20241218007

Author Contributions

Conceptualization and methodology, P.S, A.C., L.J. and N.W. ; Investigation, P.S., A.C. and L.J. ; Formal analysis, A.C. and L.J. ; Visualization and writing –

original draft, P.S. ; Writing – review and editing, P.S., A.C. and L.J. ; Supervision, R.N. All authors have read and agreed to the final version of the manuscript.

Use of Artificial Intelligence

Artificial intelligence was not used in the preparation of the manuscript. All study concepts, analysis, interpretation, and writing were carried out by the authors.

REFERENCES

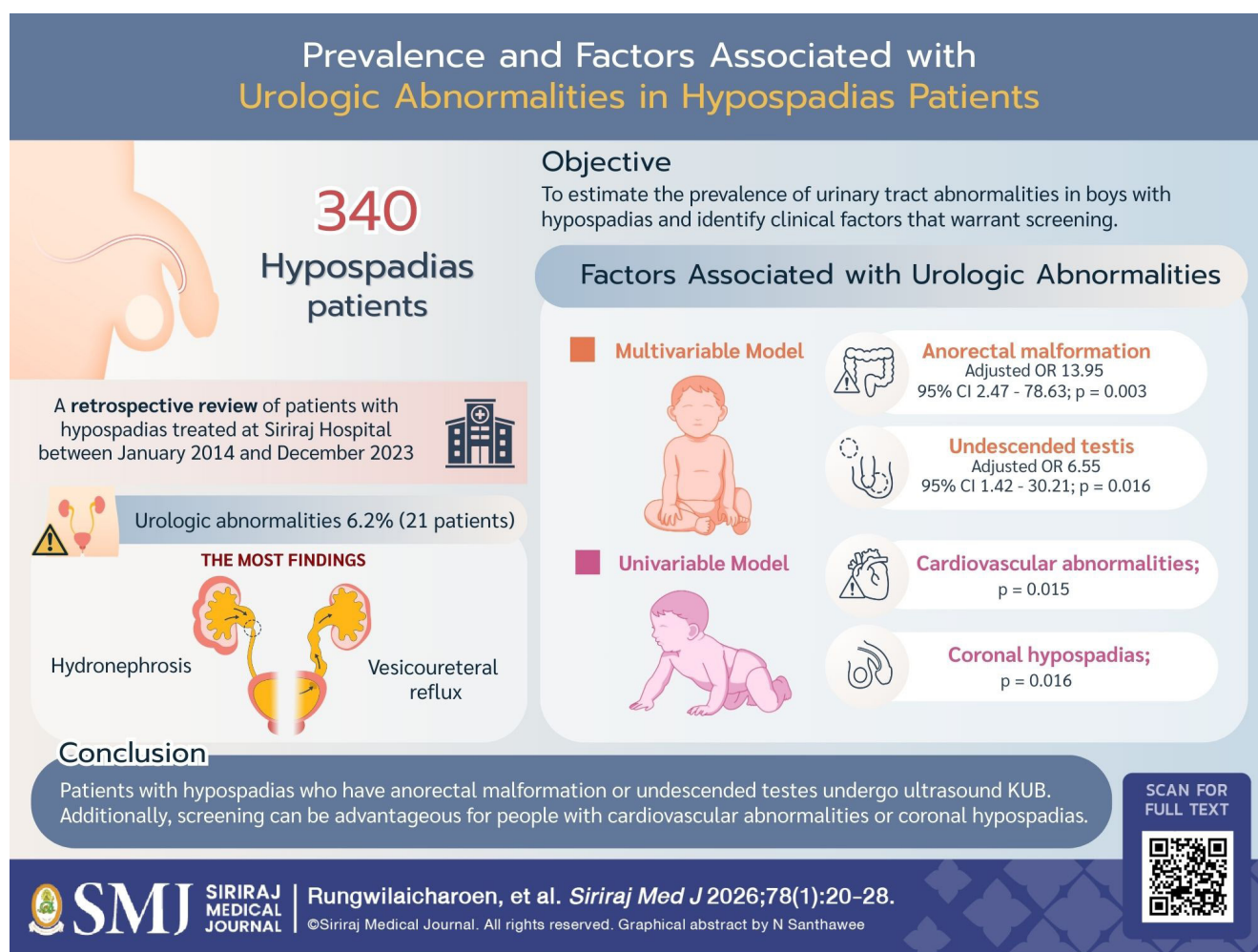
- National Institute of Arthritis and Musculoskeletal and Skin Diseases. Osteoporosis. [Internet] 2022 [cited 2024 Dec 15]. Available from: [https://www.niams.nih.gov/health-topics/osteoporosis#:~:text=Osteoporosis%20is%20a%20bone%20disease,of%20fractures%20\(broken%20bones\)](https://www.niams.nih.gov/health-topics/osteoporosis#:~:text=Osteoporosis%20is%20a%20bone%20disease,of%20fractures%20(broken%20bones)).
- Taechakraichana N. Treatment and Prevention of Osteoporosis in Menopause. *Siriraj Med J* [Internet]. 2005 [cited 2025 Oct 9]; 57(12):555-6. Available from: <https://he02.tci-thaijo.org/index.php/sirirajmedj/article/view/245661>
- Charoengnam N, Pongchaiyakul C. Current issues in evaluation and management of osteoporosis in Thailand. *Osteoporos Sarcopenia*. 2023;9(2):53-9.
- Pongchaiyakul C, Songpattanasilp T, Taechakraichana N. Burden of Osteoporosis in Thailand. *J Med Assoc Thai*. 2008;91(2):261-7.
- Nuti R, Brandi ML, Checchia G, Di Munno O, Dominguez L, Falaschi P, et al. Guidelines for the management of osteoporosis and fragility fractures. *Intern Emerg Med*. 2019;14(1):85-102.
- Johns Hopkins Medicine. Bone Densitometry. [Internet]. (n.d.) [cited 2024 Jan 10]. Available from: [https://dmsic.moph.go.th/index/detail/1385](https://www.hopkinsmedicine.org/health/treatment-tests-and-therapies/bone-mithal-a, Bansal B, Kyer CS, Ebeling P. The Asia-Pacific Regional Audit-Epidemiology, Costs, and Burden of Osteoporosis in India 2013: A report of International Osteoporosis Foundation. <i>Indian J Endocrinol Metab</i>. 2014;18(4):449-54.
Drug and Medical Supply Information Center, Ministry of Public Health. Osteoporosis Screening (W 316). [Internet] 2011 [cited 2024 Jan 20]. Available from: <a href=)
- Sharma S. Drawing insights from COVID-19-infected patients using CT scan images and machine learning techniques: a study on 200 patients. *Environ Sci Pollut Res Int*. 2020;27(29):37155-37163.
- Whitlock RH, Leslie WD, Shaw J, Rigatto C, Thorlacius L, Komenda P, et al. The Fracture Risk Assessment Tool (FRAX®) predicts fracture risk in patients with chronic kidney disease. *Kidney Int*. 2019;95(2):447-54.
- Webb R. Two proportion Z-test and confidence interval. [Internet]. 2023. [cited 2024 Dec 20]. Available from: [https://stats.libretexts.org/Bookshelves/Introductory_Statistics/Mostly_Harmless_Statistics_\(Webb\)/09%3A_Hypothesis_Tests_and_Confidence_Intervals_for_Two_Populations/9.03%3A_Two_Proportion_Z-Test_and_Confidence_Interval](https://stats.libretexts.org/Bookshelves/Introductory_Statistics/Mostly_Harmless_Statistics_(Webb)/09%3A_Hypothesis_Tests_and_Confidence_Intervals_for_Two_Populations/9.03%3A_Two_Proportion_Z-Test_and_Confidence_Interval)
- Liu RW, Ong W, Makmur A, Kumar N, Low XZ, Shuliang G, et al. Application of artificial intelligence methods on osteoporosis classification with radiographs—A Systematic Review. *Bioengineering (Basel)*. 2024;11(5):484.
- RadiologyInfo.org. Chest X-ray. Radio Society of North America.

- [Internet]. 2025. [cited 2024 Dec 12]. Available from: <https://www.radiologyinfo.org/en/info/chestrad>
14. Jonathan AC Sterne, Miguel A Hernán, Alexandra McAleenan, Barnaby C Reeves, Julian PT Higgins. Cochrane Handbooks for Systematic Reviews of Interventions: Assessing Risk of Bias in a Non-randomized Study. [Internet]. (n.d.). [cited 2024 Dec 12]. Available from: <https://www.cochrane.org/authors/handbooks-and-manuals/handbook/current/chapter-25>
 15. Murad MH, Lin L, Chu H, Hasan B, Alsibai RA, Abbas AS, et al. The association of sensitivity and specificity with disease prevalence: analysis of 6909 studies of diagnostic test accuracy. *CMAJ*. 2023;195(27):E925-E931.
 16. Caraguel CG, Vanderstichel R. The two-step Fagan's nomogram: ad hoc interpretation of a diagnostic test result without calculation. *Evid Based Med*. 2013;18(4):125-8.

Prevalence and Factors Associated with Urologic Abnormalities in Hypospadias Patients

Donlaporn Rungwilaicharoen, M.D., Ravit Ruangtrakool, M.D.*

Division of Pediatric Surgery, Department of Surgery, Faculty of Medicine Siriraj Hospital, Mahidol University, Bangkok, Thailand.



*Corresponding author: Ravit Ruangtrakool

E-mail: sisuped@mahidol.ac.th

Received 9 October 2025 Revised 22 October 2025 Accepted 11 November 2025

ORCID ID: <http://orcid.org/0000-0001-8162-2941>

<https://doi.org/10.33192/smj.v78i1.278201>



All material is licensed under terms of the Creative Commons Attribution 4.0 International (CC-BY-NC-ND 4.0) license unless otherwise stated.

ABSTRACT

Objective: To estimate the prevalence of urinary tract abnormalities in boys with hypospadias and identify clinical factors that warrant screening.

Materials and Methods: A retrospective review was conducted of patients with hypospadias treated at Siriraj Hospital between January 2014 and December 2023. No standardized radiographic screening protocol was applied.

Results: Urinary tract abnormalities were identified in 6.2% (21/340) of patients with hypospadias. The most prevalent findings were vesicoureteral reflux (VUR) and hydronephrosis, primarily non-obstructive, non-reflux hydronephrosis. Ultrasound KUB was a valuable screening tool (n = 95), detecting 19 urinary tract abnormalities and 13 additional abnormalities. Analysis of KUB-related anomalies in hypospadias showed no direct relationship between urethral opening and the frequency of urinary tract abnormalities, except in coronal hypospadias, which demonstrated a higher rate of anomalies. On multivariable binary logistic regression, anorectal malformation (adjusted OR 13.95, 95% CI 2.47 - 78.63; p = 0.003) and undescended testis (adjusted OR 6.55, 95% CI 1.42 - 30.21; p = 0.016) predicted KUB abnormalities in patients with hypospadias. In the univariable model, cardiovascular abnormalities and coronal hypospadias were also significantly associated with urinary tract abnormalities (p = 0.015 and p = 0.006, respectively), with medium to high effect sizes.

Conclusion: Of patients with hypospadias, 6.2% had anomalies of the urinary tract. It is advised that patients with hypospadias who additionally have anorectal anomalies or undescended testes undergo ultrasound KUB. Additionally, screening can be advantageous for patients with cardiovascular abnormalities or coronal hypospadias.

Keywords: Hypospadias; kidney-ureter-bladder (KUB); ultrasonography; urogenital anomalies; voiding cystourethrogram. (Siriraj Med J 2026;78(1):20-28)

INTRODUCTION

Hypospadias is the most prevalent abnormality of the male urogenital tract.¹ The reported incidence of associated urinary tract anomalies in patients with hypospadias varies widely, from 1.7%² to 40%.³ This variation is largely attributed to differences in diagnostic methods used to detect urinary tract abnormalities. Earlier studies, particularly those conducted before 1976, often reported higher prevalence rates, likely because intravenous pyelography (IVP) was the primary diagnostic tool.⁴ In contrast, more recent studies using ultrasonography as the main screening method have reported a much lower prevalence of associated abnormalities, approximately 1.7%.²

The role of ultrasonography in screening for urological abnormalities in patients with hypospadias remains controversial, with three main viewpoints: 1. All patients with hypospadias should undergo screening for urological abnormalities.^{5,6} 2. Screening should be reserved for patients with severe hypospadias or other associated abnormalities,⁴ and 3. No screening is necessary for any patient with hypospadias, regardless of its severity.^{7,8}

The aim is to estimate the prevalence of urinary tract abnormalities in hypospadias and identify factors that warrant screening, such as the severity of hypospadias or the presence of associated abnormalities.

MATERIALS AND METHODS

This study was approved by the Institutional Review Board of Siriraj (COA no. Si 320/2024). We retrospectively reviewed all patients with hypospadias admitted for further evaluation and surgical treatment at the Divisions of Pediatric Surgery and Urology, Department of Surgery, Faculty of Medicine Siriraj Hospital, Mahidol University, between January 2014 and December 2023. Patients were excluded if they lacked complete follow-up medical records, had bladder exstrophy or cloacal exstrophy, or had disorders of sex development.

In this investigation, the type of hypospadias was classified based on the position of the urethral opening prior to surgical chordee correction in cases where chordee was present. The decision to perform additional urological testing, such as ultrasound kidney-ureter-bladder (KUB), voiding cystourethrogram (VCUG), IVP, or a combination of these, varied by surgeon. This decision was typically guided by the suspected lesion and the results of the initial KUB ultrasonography, in the absence of a clear standardized investigative protocol.

Demographics and clinical data were systematically collected, including type of hypospadias, genital anomalies, KUB anomalies, and other congenital anomalies.

For statistical analysis, qualitative variables were compared between groups using Fisher's exact test or

Pearson's χ^2 test. Associations between exposures (types of hypospadias, kinds of genital malformations, and other anomalies) and outcomes (KUB anomalies) were assessed by calculating odds ratios (OR). Univariable models reported unadjusted ORs with 95% confidence intervals (CI), evaluating each independent variable separately without adjustment for confounders. Variables with $p < 0.10$ entered the multivariable logistic regression alongside clinically relevant covariates. Model fit was assessed with the Hosmer–Lemeshow test and pseudo- R^2 . Variables were further analyzed in multivariable logistic regression models to account for the impact of confounding factors, yielding adjusted ORs with 95% CI.

All analyses were performed using the PASW Statistics program (SPSS for Windows, version 26.0, SPSS Inc., Chicago, Illinois, USA). A p -value lower than 0.05 was considered statistically significant.

RESULTS

Among 340 patients with hypospadias enrolled between January 2014 and December 2023, KUB abnormalities were identified in 21 patients (6.2%). The precise location

of the urethral opening was not recorded in two patients. Based on the penoscrotal junction as the reference point, 196 patients had hypospadias distal to the junction: 27 glandular hypospadias, 25 coronal, 47 distal penile, 81 midshaft, and 16 proximal penile. A further 142 patients had hypospadias from the penoscrotal junction to the perineum: 133 penoscrotal, 8 scrotal, and 1 perineal. Details of congenital urinary system abnormalities by urethral position are shown in [Table 1](#).

KUB abnormalities occurred in 13/196 patients with urethral openings distal to the penoscrotal junction (6.6%) and in 8/142 patients with openings from the junction onward (5.6%). The most frequent abnormalities were hydronephrosis (usually non-obstructive, non-reflux, though some cases were obstructive) and vesicoureteral reflux. Additional kidney abnormalities included two cases of renal agenesis and one hypoplastic kidney in patients whose urethra opened distal to the penoscrotal junction. The types of hypospadias were categorized based on the urethra's position and the frequency of urinary tract abnormalities, as shown in [Table 2](#).

TABLE 1. Comparison of the prevalence of KUB anomalies in hypospadias with a urethral opening* distal to the penoscrotal junction ($n = 196$) versus hypospadias with a urethral opening between the penoscrotal junction and the perineum ($n = 142$).

KUB anomalies** ($n = 21$); n (%)	Distal to penoscrotal junction ($n = 13$); n (%)	Penoscrotal junction to perineum ($n = 8$); n (%)
Hydronephrosis (non-obstructive, non-reflux)	5 (38.5)	4 (50.0)
Hydronephrosis (obstructive hydronephrosis)	1 (7.7)	1 (12.5)
Vesicoureteral reflux	7 (53.8)	2 (25.0)
Renal agenesis	2 (15.4)	0 (0)
Bladder diverticulum	2 (15.4)	0 (0)
Prostatic utricle cyst	1 (7.7)	2 (25.0)
Horseshoe kidney	0 (0)	1 (12.5)
Medullary nephrocalcinosis	1 (7.7)	0 (0)
Hypoplastic kidney	1 (7.7)	0 (0)
Patent urachus	1 (7.7)	0 (0)
Neurogenic bladder	1 (7.7)	0 (0)
Hydroureter	1 (7.7)	0 (0)
Incomplete double collecting system	1 (7.7)	0 (0)

*In two of the 340 hypospadias individuals, the exact position of the urethral opening was not noted.

**Patients may have more than one abnormality.

TABLE 2. Percentage and frequency of KUB abnormalities by the type of hypospadias.

Type of hypospadias	KUB anomalies** (n = 21)	No KUB anomalies** (n = 317)	Total (n = 338)*	p-value
Glandular; n (%)	1 (4.8)	26 (8.2)	27 (8.0)	1.000
Coronal; n (%)	5 (23.8)	20 (6.3)	25 (7.4)	0.013
Shaft of Penis; n (%)	7 (33.3)	137 (43.2)	144 (42.6%)	0.510
Distal penile	3 (14.3)	44 (13.9)	47 (13.9)	1.000
Midshaft	3 (14.3)	78 (24.6)	81 (24.0)	0.419
Proximal penile	1 (4.8)	15 (4.7)	16 (4.7%)	1.000
Penoscrotal Junction to Perineum; n (%)	8 (38.1)	134 (42.2)	142 (42.0)	0.883
Penoscrotal	8 (38.1)	125 (39.4)	133 (39.3)	1.000
Scrotal	0 (0)	8 (2.5)	8 (2.4)	
Perineal	0 (0)	1 (0.3)	1 (0.3)	
Total; n (%)	21 (6.2)	317 (93.8)	338 (100.0)	

*In two of the 340 hypospadias individuals, the exact position of the urethral opening was not noted.

**Patients may have more than one abnormality.

Among 340 patients, urethral position was missing for 2; thus, **Table 2** totals 338. As per **Table 2**, the prevalence of KUB abnormalities was comparable across most hypospadias subtypes, except for coronal hypospadias, where five of 25 patients were affected (20%), a significantly higher rate compared with other groups ($p = 0.013$).

Ultrasound KUB was the most commonly performed test for urinary tract abnormality screening, either alone ($n = 75$), in conjunction with VCUG ($n = 18$), or with IVP ($n = 2$). VCUG was the second most common, performed either alone ($n = 10$) or with ultrasound KUB plus VCUG ($n = 18$). Only one patient underwent IVP as a standalone test. Radiologic modalities identifying urinary and associated anomalies are presented in **Table 3**.

Hydronephrosis was successfully diagnosed by ultrasound KUB. The most common diagnosis was non-obstructive, non-reflux hydronephrosis (two patients on ultrasound KUB alone, two on ultrasound KUB + VCUG, and two on ultrasound KUB + IVP). Vesicoureteral reflux was diagnosed in five patients with ultrasound KUB + VCUG and in one patient on ultrasound KUB alone. Other related abnormalities included hydroceles ($n=8$) and undescended testes ($n=4$), also detectable by ultrasound KUB alone. Among 95 patients who underwent initial ultrasound KUB, 19 urinary tract anomalies and 13 additional anomalies were identified.

Urinary tract abnormalities appear to be more common in patients with hypospadias who also present with related conditions. Urinary tract abnormalities are more common in patients with hypospadias with certain types of related malformations. **Table 4** summarizes the association between urinary tract anomalies and related malformations in other organs.

According to **Table 4**, among patients with hypospadias and undescended testes, three of 16 (18.75%) patients demonstrated KUB abnormalities. This association was nearly statistically significant ($p = 0.068$).

In the group with extra-urinary malformations, KUB abnormalities were statistically significant in seven of 27 patients with hypospadias and the “Vertebral defects, Anal atresia, Cardiac defects, Tracheo-esophageal fistula, Renal anomalies, and Limb abnormalities” association (VACTERL association) ($p < 0.001$). Additionally, three out of seven individuals with anorectal malformations and hypospadias ($n = 7$) had KUB abnormalities, also statistically significant ($p = 0.006$).

Patients with hypospadias and cardiovascular anomalies showed a higher prevalence of urinary tract abnormalities. Specifically, four of 20 patients demonstrated KUB abnormalities ($p = 0.027$). These were more common in patients with non-cyanotic heart defects compared with those with cyanotic heart diseases.

TABLE 3. Radiological techniques used to detect all anomalies, including KUB anomalies and other anomalies.

Investigation	Total (n = 340); n (%)	KUB anomalies* (n = 21); n (%)	Other abnormalities* (n = 210); n (%)	No abnormalities (n = 109); n (%)
US KUB**; n (%)	75 (22.1)	7 (33.3)	13 (6.2)	55 (50.5)
Hydronephrosis (non-obstructive, non-reflux)		2 (28.6)		
Hydronephrosis (outflow tract obstruction)		1 (14.3)		
Hypoplastic kidney		1 (14.3)		
Medullary nephrocalcinosis		1 (14.3)		
Vesicoureteral reflux		1 (14.3)		
Prostatic utricle cyst		1 (14.3)		
Hydrocele			8 (61.5)	
Undescended testis			4 (30.8)	
Retractile testis			1 (7.7)	
Indirect inguinal hernia			2 (15.4)	
Varicocele			1 (7.7)	
VCUG; n (%)	10 (2.9)	1 (4.8)	0 (0)	9 (8.3)
Bladder diverticulum		1 (100.0)		
IVP; n (%)	1 (0.3)	1 (4.8)	0 (0)	0 (0)
Hydronephrosis (outflow tract obstruction)		1 (100.0)		
US KUB** + VCUG; n (%)	18 (5.3)	10 (47.6)	0 (0)	8 (7.3)
Hydronephrosis (non-obstructive, non-reflux)		2 (20.0)		
Vesicoureteral reflux		5 (50.0)		
Renal agenesis		1 (10.0)		
Prostatic utricle cyst		2 (20.0)		
Patent urachus		1 (10.0)		
US KUB** + IVP; n (%)	2 (0.6)	2 (9.5)	0 (0)	0 (0)
Hydronephrosis (non-obstructive, non-reflux)		2 (100.0)		
Horseshoe kidney		1 (50.0)		
Extrarenal pelvis		1 (50.0)		

*The patient may have many deformities, and there may be abnormalities in the urinary system or other systems together.

**US KUB = Ultrasound KUB

TABLE 4. Association between urinary tract malformations and other organ anomalies in patients with hypospadias.

Other anomalies	Total (n = 340); n (%)	KUB anomalies* (n = 21); n (%)	No KUB anomalies* (n = 317); n (%)	p-value
Other genital anomalies; n (%)	62 (18.2)	6 (28.6)	56 (17.7)	0.240
Undescended testis	16 (4.7)	3 (14.3)	13 (4.1)	0.068
Bifid scrotum	10 (2.9)	1 (4.8)	9 (2.8)	0.476
Shawl scrotum	6 (1.8)	1 (4.8)	5 (1.6)	0.320
Indirect inguinal hernia	12 (3.5)	1 (4.8)	11 (3.5)	0.541
Hydrocele	21 (6.2)	1 (4.8)	20 (6.3)	1.000
Extra-urinary anomalies; n (%)	32 (9.4)	7 (33.3)	25 (7.9)	0.002
• VACTERL association; n (%)	27 (7.9)	7 (33.3)	20 (6.3)	<0.001
• Vertebral anomalies; n (%)	1 (0.3)	0 (0)	1 (0.3)	1.000
- Spinal lipoma	1	0	1	
• Anorectal malformation; n (%)	7 (2.1)	3 (14.3)	4 (1.3)	0.006
• Low type	1	1		
- ARM with anocutaneous fistula	1	1		
• Non-low type	6	2	4	
- ARM with rectoprostatic urethra fistula	1	1		
- ARM with rectobladder neck fistula	2	1	1	
- ARM with rectobulbar urethra fistula	1		1	
- ARM without Fistula	1		1	
- ARM with non-low type fistula (unknown location)	1		1	
• Cardiovascular anomalies; n (%)	20 (5.9)	4 (19.0)	16 (5.0)	0.027
• Non-cyanotic heart disease				
- Atrial Septal Defect (ASD)	5	3	2	
- Patent Ductus Arteriosus (PDA)	6	2	4	
- Ventricular Septal Defect (VSD)	6	1	5	
- Mitral Valve Regurgitation (MR)	2	1	1	
- Aortopulmonary Septal Defect (APSD)	1		1	
• Cyanotic heart disease				
- Severe Pulmonary Valve Stenosis (PS)	1		1	
- Tetralogy of Fallot (TOF)	5	1	4	
- Pulmonary atresia (PA)	1		1	
- Complete Atrioventricular Canal Defect (CAVC)	1		1	
- dextro-Transposition of the Great Arteries (dTGA)	1		1	
• Tracheoesophageal anomalies; n (%)	2 (0.6)	0 (0)	2 (0.6)	1.000
- EA type C	2		2	
• Other anomalies; n (%)	6 (1.8)	2 (9.5)	4 (1.3)	0.047
• Head & Neck anomalies; n (%)	4 (1.2)	2 (9.5)	2 (0.6)	0.020
- Cleft lip & Cleft palate	1	1		
- Bifid uvula	1	1		
- Microcephaly	2	1	1	
- Craniosynostosis	1		1	
• GI tract anomalies; n (%)	2 (0.6)	0 (0)	2 (0.6)	1.000
- Hirschsprung's disease	1		1	
- Hypertrophic pyloric stenosis	1		1	

*The patient may have many deformities, and there may be abnormalities in the urinary system or other systems together.

Urinary tract abnormalities were also significantly more frequent in patients with head and neck conditions linked to hypospadias, such as microcephaly, bifid uvula, and cleft lip and cleft palate ($p = 0.020$).

Taken together, this study suggests that certain significant factors, such as coronal-type hypospadias, undescended testes, anorectal malformations, cardiovascular anomalies, and head and neck abnormalities, are associated with an increased risk of urinary tract abnormalities in patients with hypospadias. As a result, screening for these abnormalities should be considered. Table 5 presents the results of univariate and multivariable binary logistic regression analyses using the aforementioned components.

When assessing the relationship between hypospadias and KUB anomalies, the univariable analysis showed that coronal-type hypospadias, undescended testes, anorectal malformations, cardiovascular anomalies, and head and neck anomalies were all statistically significant predictors. However, only undescended testes and anorectal malformation were statistically significant when correlated with KUB abnormalities in the multivariable model, as shown in Table 5. This may be attributable to the effect sizes of these factors, which ranged from medium to large. With a larger sample of patients presenting with coronal hypospadias or cardiovascular anomalies, these associations might reach statistical significance in multivariable analysis.

DISCUSSION

Even though hypospadias is the most prevalent urogenital tract abnormality in boys¹, there is ongoing discussion on whether all patients should undergo routine screening for related urogenital tract abnormalities. The

urinary system can be screened for abnormalities using a variety of techniques. Historically, IVP was the primary screening method,⁴ yielding a high reported incidence of anomalies. Reported rates have varied widely, from 1.7%² to 56%.^{3,7} largely due to differences in diagnostic techniques. More recently, ultrasound KUB has become the preferred initial screening tool. However, identifying a urinary tract anomaly does not always alter clinical management.⁸

Current perspectives on ultrasound screening in hypospadias patients fall into three categories: 1. Screening all patients, as some studies reported urological anomalies^{5,6} ranging from 13.26%⁵ to 18.46%⁶, 2. Selective screening, limited to patients with severe hypospadias or other abnormalities⁴, and 3. No routine screening, even in severe hypospadias^{2,7,8}, given the relatively low prevalence and the predominance of clinically insignificant anomalies.^{2,7}

In this study, 6.2% (21/340) of hypospadias patients had urinary tract malformations, most commonly hydronephrosis (mainly non-obstructive and non-reflux) and vesicoureteral reflux. These findings align with previous research that these two disorders are the most prevalent abnormalities of the urinary tract.⁷ Although kidney malposition (pelvic kidney and horseshoe kidney) has been frequently described elsewhere⁷, it was rare in our series, while sporadic renal agenesis was noted, which was extremely uncommon in earlier studies.⁷

Ultrasound KUB was the primary screening method. Either an ultrasound KUB examination was performed alone ($n = 75$), followed by either an ultrasound KUB and VCUG combination ($n = 18$) or an ultrasound KUB and IVP combination ($n = 2$). If an abnormality was discovered. According to guidelines, 19 urinary tract

TABLE 5. Univariate and multivariable binary logistic regression analyses of variables linked to KUB abnormalities in patients with hypospadias.

Factors	Univariable model		Multivariable model	
	Unadjusted OR (95% CI)	<i>p</i> -value	Adjusted OR (95% CI)	<i>p</i> -value
Coronal hypospadias	4.641 (1.542, 13.963)	0.006	3.691 (0.990, 13.758)	0.052
Undescended testis	3.923 (1.025, 15.018)	0.046	6.550 (1.420, 30.213)	0.016
Anorectal malformation	13.125 (2.729, 63.119)	0.001	13.945 (2.473, 78.631)	0.003
Cardiovascular anomalies	4.456 (1.343, 14.789)	0.015	3.323 (0.745, 14.825)	0.115
Head & Neck anomalies	16.684 (2.227, 125.005)	0.006	1.456 (0.090, 23.466)	0.791

anomalies were found in hypospadias patients who had their first KUB ultrasonography ($n = 95$), or 20% of the total. This is comparable to the findings of *Gupta L.*⁶, who found that 18.46% of patients had an ultrasound-detected urinary tract abnormality.⁶ Ultrasound was also used in this investigation to identify other anomalies in 13 other systems. This suggests that ultrasonography screening is highly beneficial and an effective method for identifying patients who are more likely to have abnormalities of the urinary system.⁵

Researchers also found urinary tract malformations in 6.2% (21/340) of hypospadias patients, consistent with previous studies. Given this low prevalence, additional criteria, such as hypospadias type, associated genital anomalies, or other organ deformities, are needed to better identify patients who require screening for urinary tract malformations.

The type of hypospadias remains a contentious factor when determining the need for KUB anomaly screening. Traditionally, proximal hypospadias, extending from the penoscrotal junction to the scrotum or perineum, was thought to be associated with a higher incidence of urinary tract malformations compared with hypospadias that extend distal to the penoscrotal junction.^{4,5} *Davenport*⁴ found that severe hypospadias was associated with a higher incidence of urinary tract malformations, with positive ultrasound rates of 5.4% for coronal hypospadias, 11.1% for distal shaft hypospadias, 28.5% for proximal shaft hypospadias, and 20.0% for perineal hypospadias cases. However, the present study found no direct correlation between urethral opening location and urinary tract abnormalities, consistent with earlier reports that showed no association between hypospadias position and overall urinary tract deformities.^{7,8,11} Similarly, no correlation was observed between the incidence of vesicoureteral reflux^{3,9}, hydronephrosis^{3,10,11}, or kidney malposition^{6,11} and hypospadias position as determined by the urethral opening. The researchers were unable to explain why the coronal hypospadias group in this study had a considerably higher incidence of urinary tract deformities than other groups ($p = 0.013$). In comparison to other research, the degree of hypospadias in this study was typically more severe. The distal part of the penis shaft with combined coronal and glandular hypospadias was only visible in 52 out of 338 patients (15.38%) in this study. In contrast, in studies conducted elsewhere, most hypospadias patients had their urethral opening distal to the mid-shaft of the penis. Therefore, caution is warranted when interpreting the association between coronal hypospadias and urinary tract anomalies, which might only occur in this cohort composition.

Researchers also examined whether hypospadias patients with associated anomalies had a higher incidence of urinary tract malformations, which would justify further KUB radiologic screening.

Although not statistically significant ($p = 0.068$), patients with hypospadias and contemporaneous undescended testes showed more urinary tract anomalies compared with those without. This study excluded patients with Disorders of Sex Development, preventing direct comparison with prior studies. Disorders of Sex Development is considered a confounding factor, as multiple previous studies from various institutions have shown that hypospadias with undescended testes often represents manifestations of Disorders of Sex Development, warranting automatic ultrasound KUB evaluation.

Urinary tract anomalies were significantly more common in patients with hypospadias and anorectal malformations ($p = 0.006$). Apart from the author's previous research on genitourinary anomalies in anorectal malformation and urological investigations,¹² no prior studies have addressed this problem, and the proposed pathophysiological explanation remains unclear. Similarly, urinary tract abnormalities were significantly more prevalent in patients with cardiac abnormalities and hypospadias ($p = 0.027$), particularly in those with hypospadias and non-cyanotic heart disorders, than in those with cyanotic heart diseases.

When the prevalence and contributing factors of urinary tract malformations (KUB anomalies) in hypospadias patients were examined using the univariable model, all factors - including the coronal type of hypospadias, undescended testes, anorectal malformation, cardiovascular anomalies, and head and neck anomalies - were found to be statistically significant.

To account for confounding factors, the researcher entered several variables into a multivariable logistic regression model. Then, the researcher computed the adjusted OR with a 95% CI. Using a multivariable model, it was discovered that only anorectal malformation and undescended testes were statistically significant ($p = 0.003$ and $p = 0.016$, respectively). The multivariable model did not exhibit statistical significance, but the univariable model column showed that cardiovascular abnormalities and coronal hypospadias were statistically significant. This condition may be corrected by the medium to large effect sizes of coronal hypospadias and cardiovascular abnormalities. If the study included a large enough sample group, it might be possible to find statistically significant KUB anomalies in hypospadias patients in the coronal hypospadias and cardiovascular abnormalities in a multivariable model.

CONCLUSION

Urinary tract abnormalities were observed in 6.2% of patients with hypospadias. Our data support selective ultrasound KUB in hypospadias with anorectal malformation or undescended testis; screening may also be considered with coronal meatus or cardiovascular anomalies, acknowledging wide CIs and potential selection effects.

Data Availability Statement

The datasets generated and analyzed in this study are not publicly available. However, they can be accessed upon reasonable request made to a corresponding author.

LIMITATIONS

1. The decision to conduct further urological testing is necessary, such as ultrasound KUB, VCUG, IVP, or a combination of these techniques. Every surgeon approaches this in a unique way. In the absence of a standardized protocol, the choice depends largely on the suspected lesion and findings of the initial ultrasound KUB. Developing a universal protocol is difficult, as current textbooks present divergent recommendations.

2. In Thailand, minor or glandular hypospadias cases typically do not undergo distal hypospadias surgery. Therefore, compared with studies conducted internationally, particularly in Western nations, the patients in this study presented with more severe forms of hypospadias.

3. This study reflects the experience of a single institution, which also serves as a referral center for hypospadias. While it represents the largest single-center study of its kind in Thailand, the findings may not be fully generalizable to other contexts.

4. The absence of long-term follow-up data limited the ability to identify urinary tract abnormalities that might present later in adolescence or adulthood.

ACKNOWLEDGEMENTS

The researcher would like to thank Dr. Sasima Tongyai from the Division of Clinical Epidemiology, Department of Research and Development, Faculty of Medicine Siriraj Hospital, Mahidol University for her continuous help with data processing and statistical analysis.

DECLARATIONS

Grants and Funding Information

Not applicable.

Conflict of Interest

All the authors confirm that they have no personal

or professional conflicts of interest to declare relating to any aspect of this research study.

Registration Number of Clinical Trial

Not applicable.

Author Contributions

Conceptualization and methodology, D.R., R.R.; Formal analysis, D.R., R.R.; Visualization and writing – original draft, R.R.; Writing – review and editing, D.R., R.R.; Supervision, R.R.; All authors have read and agreed to the final version of the manuscript.

Use of Artificial Intelligence

Artificial intelligence was not used in the preparation of the manuscript. All study concepts, analysis, interpretation, and writing were carried out by the authors.

REFERENCES

1. Sujjantararat P. Pediatric urology: What's new? *Siriraj Med J.* 2007;59(5):259-63.
2. Cerasaro TS, Brock WA, Kaplan GW. Upper urinary tract anomalies associated with congenital hypospadias: Is screening necessary? *J Urol.* 1986;135(3):537-8.
3. Shima H, Ikoma F, Terakawa T, Satoh Y, Nagata H, Shimada K, et al. Developmental anomalies associated with hypospadias. *J Urol.* 1979;122:619-21.
4. Davenport M, MacKinnon AE. The value of ultrasound screening of the upper urinary tract in hypospadias. *Br J Urol.* 1988;62: 595-6.
5. Friedman T, Shalom A, Hoshen G, Brodovsky S, Tieder M, Westrich M. Detection and incidence of anomalies associated with hypospadias. *Pediatr Nephrol.* 2008;23:1809-16.
6. Gupta L, Sharma S, Gupta DK. Is there a need to do routine sonological, urodynamic study and cystourethroscopic evaluation of patients with simple hypospadias? *Pediatr Surg Int.* 2010;26: 971-6.
7. Chariatte V, Ramseyer P, Cachat F. Urological screening for upper and lower urinary tract anomalies in patients with hypospadias: A systematic literature review. *Evid Based Med.* 2013;18(1):11-20.
8. Snodgrass W. Hypospadias. In: Hulbert WC, Rabinowitz R, Mevorach RA, editors. *Pediatric Urology for the Primary Care Physician.* New York: Springer; 2014.p.229-35.
9. Wu WH, Chuang JH, Ting YC, Lee SY, Hsieh CS. Developmental anomalies and disabilities associated with hypospadias. *J Urol.* 2002;168:229-32.
10. Moore CC. The role of routine radiographic screening of boys with hypospadias: a prospective study. *J Pediatr Surg.* 1990;25: 339-41.
11. Kelly D, Harte FB, Roe P. Urinary tract anomalies in patients with hypospadias. *Br J Urol.* 1984;56:316-8.
12. Pengvanich P, Mungnirandr A, Ruangtrakool R. Associated genitourinary abnormalities in low-type anorectal malformation and urological investigations. *J Med Assoc Thai.* 2017; 100(3): S95-S100.

The Correlation between Chest X-ray and Cardiac Magnetic Resonance Imaging in the Assessment of Left Atrial Enlargement

Satchana Pumprueg¹, M.D.¹, Methat Meechuen², M.S.², Thananya Boonyasirinant^{1,*}, M.D.^{1,*}

¹Division of Cardiology, Department of Medicine, Faculty of Medicine Siriraj Hospital, Mahidol University, Bangkok, Thailand, ²Research Department, Faculty of Medicine Siriraj Hospital, Mahidol University, Bangkok, Thailand.

Accuracy of Left atrial enlargement assessed using CXR is not accurate as CMR



This is the first study validating CXR parameters against CMR for detecting LAE, revealing that conventional radiographic signs have limited diagnostic performance. Despite its accessibility and routine use, CXR demonstrated low sensitivity and specificity for LAE compared with CMR.



Population & Setting



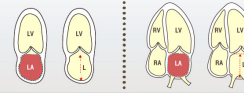
110 patients

who underwent CMR and had a posteroanterior CXR within 6 months.

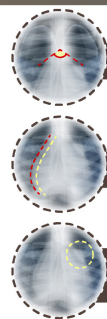


Intervention

Left atrial volume was calculated by



the biplane area-length method and indexed to body surface area



CXR signs assessed were the subcarinal angle

double density sign

left atrial appendage prominence ("third contour")

Sensitivity, specificity, and diagnostic accuracy were calculated against CMR-defined LAE.



Outcomes

CMR identified LAE in **85 patients** (77.3%)

The third contour had the highest sensitivity

78.8%

but poor specificity

8.0%

whereas a subcarinal angle > 90°

92.0%

had the highest specificity

8.2%

with low sensitivity

Overall diagnostic accuracy for individual or combine CXR signs was 27.3%–62.7%, with no correlation between CXR findings and CMR-derived left atrial volume index (all $P > 0.05$).

SCAN FOR FULL TEXT



Pumprueg, et al. *Siriraj Med J* 2026;78(1):29-38.

©Siriraj Medical Journal. All rights reserved. Graphical abstract by Y Krimouy

*Corresponding Author: Thananya Boonyasirinant

E-mail: drthananyaa@yahoo.com

Received 22 October 2025 Revised 13 November 2025 Accepted 13 November 2025

ORCID ID: <http://orcid.org/0000-0002-9149-3407>

<https://doi.org/10.33192/smj.v78i1.278423>



All material is licensed under terms of the Creative Commons Attribution 4.0 International (CC-BY-NC-ND 4.0) license unless otherwise stated.

ABSTRACT

Objective: Left atrial enlargement (LAE) is common in cardiovascular disease and is associated with heart failure, atrial fibrillation, and stroke. Chest X-ray (CXR) is widely available; however, its diagnostic value for LAE has not been validated against cardiac magnetic resonance imaging (CMR). We evaluated the correlation and diagnostic performance of conventional CXR signs for detecting LAE using CMR as the reference standard.

Materials and Methods: We retrospectively analyzed 110 patients who underwent CMR and had a posteroanterior CXR within 6 months. Left atrial volume was calculated by the biplane area-length method and indexed to body surface area. CXR signs assessed were the subcarinal angle, double density sign, and left atrial appendage prominence (“third contour”). Sensitivity, specificity, and diagnostic accuracy were calculated against CMR-defined LAE.

Results: CMR identified LAE in 85 patients (77.3%). The third contour had the highest sensitivity (78.8%) but poor specificity (8.0%), whereas a subcarinal angle > 90° had the highest specificity (92.0%) with low sensitivity (8.2%). Overall diagnostic accuracy for individual or combined CXR signs was 27.3%–62.7%, with no correlation between CXR findings and CMR-derived left atrial volume index (all $P > 0.05$).

Conclusions: To our knowledge, this is the first study validating CXR parameters against CMR for detecting LAE, revealing that conventional radiographic signs have limited diagnostic performance. Despite its accessibility and routine use, CXR demonstrated low sensitivity and specificity for LAE compared with CMR.

Keywords: Left atrial enlargement; cardiac magnetic resonance imaging; chest X-ray (Siriraj Med J 2026;78(1):29-38)

INTRODUCTION

Left atrial enlargement (LAE) is common across cardiovascular conditions, including heart failure, valvular heart disease, and atrial fibrillation.^{1,2} It also occurs in disorders linked to cardiovascular pathology, such as hypertension, obesity, and obstructive sleep apnea.^{3,4}

LAE can be assessed with chest X-ray (CXR), electrocardiogram (ECG), echocardiography, cardiac magnetic resonance (CMR), or cardiac computed tomography (CT). Despite limitations, CXR remains simple, accessible, and widely used.^{5,6} Radiographic criteria include measuring the subcarinal angle, evaluating left atrial prominence along the left heart border (“third contour”), and identifying the double density sign. CMR provides highly precise chamber quantification, including the left atrium, right atrium, left ventricle, and right ventricle.⁷⁻⁹

LAE is strongly associated with increased risk of heart failure, stroke, and atrial fibrillation, as well as elevated cardiovascular mortality.¹⁰⁻¹³ Consequently, accurate left atrial sizing is essential for risk stratification, outcome prediction, and disease monitoring.

Prior studies have compared LAE assessment by electrocardiogram with CMR^{14,15}, but none have directly compared CXR with CMR. Therefore, we investigated the diagnostic performance of conventional CXR signs for detecting LAE, using CMR as the reference standard.

MATERIALS AND METHODS

Study population

We consecutively enrolled 110 patients who underwent CMR at the Division of Cardiology, Department of Medicine, Faculty of Medicine Siriraj Hospital, Mahidol University, Bangkok, Thailand. Eligibility required a posteroanterior upright CXR of adequate quality performed within 6 months before or after the CMR examination. Patients with significant valvular heart disease, post-cardiothoracic surgery, or pulmonary conditions affecting lung volume (such as atelectasis or pleural effusion) were excluded. Baseline clinical characteristics and medical history were obtained from medical records. The study protocol was approved by the Siriraj Institutional Review Board.

CMR acquisition and measurements

Acquisition

CMR examinations were performed on a 1.5T Achieva XR scanner (Philips, Best, Netherlands). After localizer scouts, cine steady-state free precession balanced turbo field echo images were obtained in 2-, 3-, and 4-chamber and short-axis views. Imaging parameters were: repetition time/echo time/number of excitations, 3.7/1.8/1; slice thickness, 8 mm with no gap; flip angle, 60°; and 25 cardiac phases per cardiac cycle. Field of view was 350×320 mm for long-axis and 270×320 mm for short-axis views, with reconstructed voxel size 1.25×1.25×8 mm³

Left atrial volume measurement and indexing

CMR images were analyzed offline using cardiovascular imaging software (Extended Brilliance Workspace; Philips Healthcare, Best, Netherlands). The left atrial volume was derived with the biplane area-length method at end-atrial diastole, including the left atrial appendage and excluding the 4 pulmonary veins. The left atrial area was manually contoured on mid-atrial slices in 2- and 4-chamber cine views. The atrioventricular junction was defined by a line connecting the mitral valve insertion points. The atrial long-axis length was measured as the perpendicular distance from the midpoint of the mitral annular plane to the superior left atrial border. Left atrial volume (LAV) was calculated by the biplane area-length formula:

$$\text{LAV} = (8 \times A_1 \times A_2) / (3\pi \times L).$$

A_1 and A_2 denote maximal planimetered left atrial areas from the vertical and horizontal long-axis views, and L denotes the long-axis length. The LAV index (LAVI) was obtained by normalizing LAV to body surface area.

Reproducibility and additional left ventricular metrics

To assess intra- and interobserver variability, the primary investigator repeated measurements after 1 week in 20 randomly selected patients; an independent investigator performed the same measurements. Left ventricular end-diastolic volume (LVEDV), left ventricular end-systolic volume (LVESV), left ventricular ejection fraction (LVEF), and left ventricular mass index were measured according to current guidelines.

CXR acquisition and measurements

CXRs were performed using standard technique with posteroanterior projection. Patients with uninterpretable films owing to inappropriate exposure, severe kyphoscoliosis, severe pulmonary disease, or inadequate inspiration were excluded. Three left atrial enlargement signs were evaluated: left atrial appendage prominence ("third contour"), double density sign, and subcarinal angle. Third contour was defined as protrusion of the left heart border between the left pulmonary artery and the ventricular border, graded as 1+ (slight protrusion) or 2+ (obvious protrusion). The double density sign was a curvilinear line along the right heart border with a distance from the mid-inferior left bronchus to that border > 7 cm. The subcarinal angle was measured on a dedicated workstation.

Statistical analysis

Analyses were performed with PASW Statistics version 18 (SPSS Inc, Chicago, IL, USA). Categorical variables are

presented as counts and percentages; continuous variables are expressed as mean (SD) for normally distributed data and median (IQR) for nonnormally distributed data. Normality was assessed with the Kolmogorov–Smirnov test. We calculated accuracy, sensitivity, specificity, positive and negative likelihood ratios, and positive and negative predictive values for each criterion and for all 3 combined, using CMR-derived LAVI as the reference. Group comparisons used the chi-square test or Fisher's exact test for categorical variables, and Student's t test or the Mann–Whitney U test for continuous variables, as appropriate. A P value < 0.05 was considered statistically significant.

RESULTS*Baseline characteristics*

A total of 110 patients were included in the analysis. The mean age was 68.8 ± 10.1 years, and 40.0% were male. Mean body mass index and body surface area were 25.8 ± 4.8 kg/m² and 1.67 ± 0.20 m², respectively. Hypertension, dyslipidemia, diabetes mellitus, and coronary artery disease were present in 87.3%, 83.6%, 42.7%, and 36.4%, respectively. Current smoking was reported in 16.4% of participants. The mean systolic and diastolic blood pressures were 137.0 ± 21.3 mm Hg and 68.0 ± 11.3 mm Hg, respectively (Table 1).

CMR findings

CMR demonstrated a median LVEDV of 122.8 mL (IQR 101.8–154.4 mL) and a median LVESV of 36.8 mL (IQR 23.3–56.5 mL). The mean LVEF was $65.9\% \pm 16.6\%$, and the mean LAVI was 52.6 ± 17.8 mL/m² (Table 2). Using cutoffs of LAVI > 40 mL/m² for men and > 39 mL/m² for women, LAE was present in 85 patients (77.3%). Among CMR-derived volumetric parameters, LAVI correlated significantly with LVEDV but not with LVESV or LVEF.

CXR findings

On CXR, a third contour was presented in 81.8% of patients (score 1+ to 2+), whereas 18.2% had no visible contour (score 0). A prominent third contour (score 2+) was identified in 20.9% of patients, and a double density sign in 13.6% of patients. The mean subcarinal angle was $73.4 \pm 11.7^\circ$, with 42.7% exceeding 75° and 8.2% exceeding 90° .

Using subcarinal angle thresholds of > 75° and > 90° , the presence of any radiographic criterion (third contour, double density sign, or widened subcarinal angle) was noted in 88.2% and 82.7% of patients, respectively. The combined presence of all 3 findings was detected in

TABLE 1. Baseline characteristics.

Variables	Values	LAVI > 40 mL/m ² in men or >39 mL/m ² in women (n = 85)	LAVI ≤ 40 mL/m ² in men or ≤ 39 mL/m ² in women (n = 25)	p - value
Age (years)	68.8 ± 10.1	70.0 ± 10.1	64.9 ± 9.4	0.028
Male gender	44 (40.0%)	35 (41.2%)	9 (36.0%)	0.642
Height (cm)	157.7 ± 8.6	156.8 ± 8.7	160.8 ± 7.8	0.042
Weight (kg)	64.2 ± 13.7	64.2 ± 12.9	64.1 ± 16.5	0.966
Body mass index (kg/m ²)	25.8 ± 4.8	26.1 ± 4.6	24.7 ± 5.3	0.191
Body surface area (m ²)	1.7 ± 0.2	1.7 ± 0.2	1.7 ± 0.2	0.720
Systolic BP (mmHg)	137.0 ± 21.3	140.0 ± 21.4	127.0 ± 17.9	0.007
Diastolic BP (mmHg)	68.0 ± 11.7	67.7 ± 11.5	69.3 ± 10.4	0.533
Hypertension	96 (87.3%)	78 (91.8%)	18 (72.0%)	0.016
Dyslipidemia	92 (83.6%)	77 (90.6%)	15 (60.0%)	0.001
Diabetes mellitus	47 (42.7%)	36 (42.4%)	11 (44.0%)	0.884
Coronary artery disease	40 (36.4%)	33 (38.8%)	7 (28.0%)	0.323
Smoking	18(16.4%)	13 (15.3%)	5 (20.0%)	0.552

Data are mean ± SD or n (%).

Abbreviations: LV = left ventricular; LAVI = left atrial volume index; cm = centimeter; kg = kilogram; BP = blood pressure; mL = milliliter; mL/m² = milliliter per square meter

TABLE 2. CMR-derived left ventricular and left atrial parameters.

Variables	Values	LAVI > 40 mL/m ² in men or >39 mL/m ² in women (n = 85)	LAVI ≤ 40 mL/m ² in men or ≤ 39 mL/m ² in women (n = 25)	p - value
LV end diastolic volume (ml)	122.8 (101.8 - 154.4)	135.0 (104.5-155.5)	106.7 (87.0-121.1)	0.001
LV end systolic volume (ml)	36.8 (23.3 - 56.5)	40.5 (25.5-59.7)	30.4 (18.7-43.5)	0.052
LV ejection fraction (%)	65.9 ± 16.6	65.3 ± 17.2	67.7 ± 14.3	0.525
LA volume index (ml/m ²)	52.6 ± 17.8	58.8 ± 15.2	31.8 ± 6.3	-

Data are mean ± SD or median (percentile 25th – percentile 75th).

Abbreviations: LV = left ventricular; LA = left atrial; LAVI = left atrial volume index; mL = milliliter; mL/m² = milliliter per square meter

9.1% of patients for the $> 75^\circ$ threshold and in 3.6% for the stricter $> 90^\circ$ threshold (Table 3). None of the CXR parameters—including third contour, double density sign, or subcarinal angle thresholds—correlated significantly with CMR-defined LAE (all $P > 0.05$).

Diagnostic performance of CXR parameters

The diagnostic performance of CXR parameters for detecting LAE (LAVI > 40 mL/m² in men and > 39 mL/m² in women) is summarized in Table 4.

When evaluated individually, the presence of a

TABLE 3. Radiographic characteristics of chest X-ray findings.

Variables	Values	LAVI > 40 mL/m ² in men or >39 mL/m ² in women (n = 85)	LAVI ≤ 40 mL/m ² in men or ≤ 39 mL/m ² in women (n = 25)	p - value
3rd Contour				
0	20 (18.2%)	18 (21.2%)	2 (8.0%)	0.285
1	67 (60.9%)	49 (57.6%)	18 (72.0%)	
2	23 (20.9%)	18 (21.2%)	5 (20.0%)	
3rd Contour				
0	20 (18.2%)	18 (21.2%)	2 (8.0%)	0.236
1 - 2	90 (81.8%)	67 (78.8%)	23 (92.0%)	
3rd Contour				
0 - 1	87 (79.1%)	67 (78.8)	20 (80.0%)	0.899
2	23 (20.9%)	18 (21.2%)	5 (20.0%)	
Double density sign				
0	95 (86.4%)	75 (88.2%)	20 (80.0%)	0.325
1	15 (13.6%)	10 (11.8%)	5 (20.0%)	
Subcarinal angle	73.35 \pm 11.67	73.41 \pm 11.57	73.16 \pm 12.27	0.925
≤ 75	63 (57.3%)	50 (58.8%)	13 (52.0%)	0.544
> 75	47 (42.7%)	35 (41.2%)	12 (48.0%)	
≤ 90	101 (91.8%)	78 (91.8%)	23 (92.0%)	1.00
> 90	9 (8.2%)	7 (8.2%)	2 (8.0%)	
Subcarinal angle >75 & Double density sign & 3rd Contour				
0	100 (90.9%)	78 (91.8%)	22 (88.0%)	0.692
1	10 (9.1%)	7 (8.2%)	3 (12.0%)	
Subcarinal angle >90 & Double density sign & 3rd Contour				
0	106 (96.4%)	82 (96.5%)	24 (96.0%)	1.00
1	4 (3.6%)	3 (3.5%)	1 (4.0%)	
Subcarinal angle >75 or Double density sign or 3rd Contour				
0	13 (11.8%)	12 (14.1%)	1 (4.0%)	0.291
1	97 (88.2%)	73 (85.9%)	24 (96.0%)	
Subcarinal angle >90 or Double density sign or 3rd Contour				
0	19 (17.3%)	17 (20.0%)	2 (8.0%)	0.232
1	91 (82.7%)	68 (80.0%)	23 (92.0%)	

Abbreviations: LAVI = left atrial volume index; cm = centimeter; mL = milliliter; mL/m² = milliliter per square meter

TABLE 4. Diagnostic performance of CXR parameters compared with CMR-defined LAE.

Variables	Sensitivity (95% CI)	Specificity (95% CI)	LR+ (95% CI)	LR- (95% CI)	PPV (%) (95% CI)	NPV (%) (95%CI)	Accuracy (95% CI)
3rd Contour (1 – 2)							
Xxx	78.8%	8.0%	0.9%	2.7%	74.4%	10.0%	62.7%
xxx	(68.6-86.9)	(1.0-26.0)	(0.7-1.0)	(0.7-10.6)	(64.2-83.1)	(1.2-31.7)	(53.7-71.8)
3rd Contour (2)							
Xxx	21.2%	80.0%	1.1%	1.0%	78.3%	23.0%	34.6%
xxx	(13.1-31.4)	(59.3-93.2)	(0.4-2.6)	(0.8-1.2)	(56.3-92.5)	(14.6-33.2)	(25.7-43.4)
Double density sign							
Xxx	11.8%	80.0%	0.6%	1.1%	66.7%	21.1%	27.3%
xxx	(5.8-20.6)	(59.3-93.2)	(0.2-1.6)	(0.9-1.4)	(38.4-88.2)	(13.4-30.6)	(19.0-35.6)
Subcarinal angle							
> 75	41.2%	52.0%	0.9%	1.1%	74.6%	20.6%	43.6%
	(30.6-52.4)	(31.3-72.2)	(0.5-1.4)	(0.8-1.7)	(59.7-86.1)	(11.5-32.7)	(34.4-52.9)
> 90	8.2%	92.0%	1.0%	1.0%	77.8%	22.8%	27.3%
	(3.4-16.2)	(74.0-99.0)	(0.2-4.7)	(0.9-1.1)	(40.0-97.2)	(15.0-32.2)	(19.0-35.6)
Subcarinal angle >75 & Double density sign & 3rd Contour							
Xxx	8.2%	88.0%	0.7%	1.0%	70.0%	22.0%	11.8%
xxx	(3.4-16.2)	(68.8-97.5)	(0.2-2.5)	(0.9-1.2)	(34.8-93.3)	(14.3-31.4)	(5.8-17.9)
Subcarinal angle >90 & Double density sign & 3rd Contour							
Xxx	3.5%	96.0%	0.9%	1.0%	75.0%	22.6%	24.6%
xxx	(0.7-10.0)	(79.6-99.9)	(0.1-8.1)	(0.9-1.1)	(19.4-99.4)	(15.1-31.8)	(16.5-32.6)
Subcarinal angle >75 or Double density sign or 3rd Contour							
Xxx	85.9%	4.0%	0.9%	3.5%	75.3%	7.7%	67.3%
xxx	(76.6-92.5)	(0.1-20.4)	(0.8-1.0)	(0.5-25.8)	(65.5-83.5)	(0.2-36.0)	(58.5-76.0)
Subcarinal angle >90 or Double density sign or 3rd Contour							
Xxx	80.0%	8.0%	0.9%	2.5%	74.7%	10.5%	63.6%
xxx	(69.9-87.9)	(1.0-26.0)	(0.7-1.0)	(0.6-10.1)	(64.5-83.3)	(1.3-33.1)	(54.7-72.6)

Abbreviations: PPV = positive predictive value; NPV = negative predictive value

third contour showed the highest sensitivity, 78.8% (95% CI, 68.6–86.9), but very low specificity, 8.0% (95% CI, 1.0–26.0). Conversely, a subcarinal angle $> 90^\circ$ provided the highest specificity, 92.0% (95% CI, 74.0–99.0), but poor sensitivity, 8.2% (95% CI, 3.4–16.2). Using a lower threshold, subcarinal angle $> 75^\circ$ showed moderate sensitivity, 41.2% (95% CI, 30.6–52.4), and specificity, 52.0% (95% CI, 31.3–72.2). The double density sign demonstrated low sensitivity, 11.8% (95% CI, 5.8–20.6), but good specificity, 80.0% (95% CI, 59.3–93.2). Overall diagnostic accuracy was 27.3%–62.7%, indicating poor discriminative ability of CXR markers for CMR-defined LAE.

Combining all 3 criteria (subcarinal angle $> 75^\circ$, double density sign, and third contour) yielded a sensitivity of 8.2% with specificity of 88.0%. Using a stricter combination with subcarinal angle $> 90^\circ$ further decreased sensitivity to 3.5% while achieving specificity to 96.0%.

Clinical predictors of left atrial enlargement

Patients were stratified by CMR-defined LAE (LAVI > 40 mL/m² in men and > 39 mL/m² in women). Those with LAE were older than those without LAE (70.0 ± 10.1 vs 64.9 ± 9.4 years; $P = 0.028$) and had higher systolic blood pressure (140.0 ± 21.4 vs 127.0 ± 17.9 mm Hg; $P = 0.007$). No significant differences were seen in sex, body mass index, or other cardiovascular risk factors between groups, except for associations between body mass index and the presence of a third contour or subcarinal angle $> 90^\circ$ (Table 5).

DISCUSSION

To our knowledge, this is the first study to evaluate CXR for diagnosing LAE using CMR as the reference standard. The prevalence of LAE was high (77.3%), likely reflecting a high burden of comorbidity, particularly hypertension. Prior studies have demonstrated links between elevated blood pressure and higher LAVI.¹⁶⁻¹⁸ Among CXR signs, the third contour was most prevalent. Prominent left atrial appendage, double density sign, and subcarinal angle $> 90^\circ$ occurred in 20.9%, 13.6%, and 8.2% of patients, respectively. The low prevalence of these findings is explored below.

Prominent left atrial appendage (third contour)

This sign was most prevalent in our cohort. The sensitivity, specificity, and accuracy were 21.2%, 80.0%, and 34.6%, respectively, indicating low overall diagnostic performance. Prior work demonstrated better accuracy in mitral valve disease, particularly rheumatic heart disease.^{19,20} No patients in our cohort had rheumatic

heart disease. In nonrheumatic LAE, pulmonary artery prominence and ventricular enlargement may obscure the left atrial appendage shadow, rendering the sign undetectable.

Double density sign

The double density sign in the right retrocardiac area showed sensitivity of 11.8%, specificity of 80.0%, and accuracy of 21.3%. Its low prevalence contrasts with prior work; Higgins et al reported universal presence in patients with echocardiographic LAE. Interpretation challenges and variable film quality likely contributed. A curvilinear line over the right cardiac shadow can appear without cardiac disease, while adjacent structures, particularly the right pulmonary vein, can mimic the left atrial border, explaining the interstudy differences.

Widened subcarinal angle

Despite the high prevalence of LAE, only 8.2% of patients had a subcarinal angle $> 90^\circ$. The sensitivity, specificity, and accuracy were 8.2%, 92.0%, and 27.3%, respectively. This likely reflects that 90° represents the upper limit of normal reported previously²¹, so many patients with LAE have angles $< 90^\circ$. Reported thresholds vary across studies^{22,23}, likely due to difficulty plotting the left main bronchus axis as it courses beneath the aortic arch. Using a lower cutoff of $> 75^\circ$ increased the proportion of patients meeting the angle criterion to 42.7%, with sensitivity, specificity, and accuracy of 41.2%, 52.0%, and 43.6%, respectively.

When any one of the 3 CXR criteria was considered positive, sensitivity was high but specificity was unacceptably low. Conversely, requiring all 3 criteria yielded high specificity but unacceptably low sensitivity. With all 3 criteria combined, sensitivity was 8.2% using the $> 75^\circ$ angle threshold and 3.5% using the $> 90^\circ$ threshold, while specificity reached 88.0% and 96.0%, respectively.

The study found that the sensitivity and specificity of classical CXR signs for LAE were low. Whether combination of other parameter such as electrocardiogram findings would improve the outcomes is not known.

CONCLUSIONS

This study demonstrated limited diagnostic performance of conventional radiographic signs. Despite its accessibility and routine use, CXR showed low sensitivity and specificity compared with CMR.

Limitations

This study has several limitations. First, the enrolled population had a high prevalence of LAE, which may

TABLE 5. Factors associated with CXR parameters (sex, BMI, age).

Factor	Sex		p- value	BMI		Age	
	Male	Female		Mean ± SD	p - value	Mean ± SD	p - value
X-ray parameter							
3rd Contour							
0	11 (55.0%)	9 (45.0%)	0.306	24.1 ± 3.7*	0.018	68.4 ± 13.0	0.958
1	24 (35.8%)	43 (64.2%)		26.8 ± 5.3**		68.8 ± 9.1	
2	9 (39.1%)	14 (60.9%)		24.5 ± 3.3		69.4 ± 10.8	
3rd Contour							
0	11 (55.0%)	9 (45.0%)	0.130	24.1 ± 3.7	0.074	68.4 ± 13.0	0.866
1 - 2	33 (36.7%)	57 (63.3%)		26.2 ± 4.9		68.9 ± 9.5	
3rd Contour							
0 - 1	35 (40.2%)	52 (59.8%)	0.924	26.1 ± 5.1	0.135	68.7 ± 10.0	0.766
2	9 (39.1%)	14 (60.9%)		24.5 ± 3.3		69.4 ± 10.8	
Double density sign							
0	38 (40.0%)	57 (60.0%)	1.00	25.5 ± 4.3	0.211	68.6 ± 9.9	0.539
1	6(40.0%)	9 (60.0%)		27.9 ± 6.9		70.3 ± 11.9	
Subcarinal angle							
≤ 75	29 (46.0%)	34 (54.0%)	0.135	25.1 ± 4.7	0.058	69.6 ± 10.4	0.336
> 75	15 (31.9%)	32 (68.1%)		26.8 ± 4.7		67.7 ± 9.8	
≤ 90	41 (40.6%)	60 (59.4%)	0.739	25.4 ± 4.5	0.011	68.8 ± 10.2	0.877
> 90	3 (33.3%)	6 (66.7%)		29.6 ± 6.2		69.3 ± 9.9	
Subcarinal angle >75 & Double density sign & 3rd Contour							
0	40 (40.0%)	60 (60.0%)	1.00	25.6 ± 4.6	0.302	68.9 ± 10.1	0.864
1	4 (40.0%)	6 (60.0%)		27.3 ± 6.5		68.3 ± 11.7	
Subcarinal angle >90 & Double density sign & 3rd Contour							
0	42 (39.6%)	64 (60.4%)	1.00	25.6 ± 4.5	0.351	68.8 ± 10.1	0.739
1	2 (50.0%)	2 (50.0%)		30.6 ± 9.1		70.5 ± 11.9	
Carinal Angle >75 or Double Contour or 4th Curve							
0	7 (15.9%)	6 (9.1%)	0.278	23.7 ± 4.4	1.00	71.1 ± 11.7	0.397
1	37 (84.1%)	60 (90.9%)		26.1 ± 4.8		68.5 ± 10.0	
Subcarinal angle >90 or Double density sign or 3rd Contour							
0	10 (22.7%)	9 (13.6%)	0.217	24.2 ± 3.7	0.103	67.6 ± 12.8	0.647
1	34 (77.3%)	57 (86.4%)		26.1 ± 4.9		69.1 ± 9.6	

*p-value < 0.05 of Multiple comparison between 3rd Contour (0) vs 3rd Contour (1).

**p-value < 0.05 of Multiple comparison between 3rd Contour (1) vs 3rd Contour (2).

Abbreviation: BMI = body mass index

have influenced the diagnostic performance of CXR parameters; including more patients with normal left atrial size would improve generalizability. Second, CXRs were performed within 6 months of CMR rather than on the same day; however, only clinically stable patients were included to minimize temporal variation. Third, analysis was restricted to posteroanterior views; adding lateral views might have improved sensitivity. Finally, image interpretation by 2 experienced cardiologists may not capture interobserver variability across a broader range of readers.

Data Availability Statement

The datasets generated and analyzed during the current study are not publicly available due to patient confidentiality but are available from the corresponding author on reasonable request.

ACKNOWLEDGMENT

The authors thank Ms. Khemajira Karaketklang for her valuable assistance with statistical analysis.

DECLARATIONS

Grants and Funding Information

This research received no specific grant from any funding agency in the public, commercial, or not-for-profit sectors.

Conflicts of Interest

The authors declare that there are no conflicts of interest.

Registration Number of Clinical Trial

Not applicable.

Author Contributions

Conceptualization and methodology, S.P, M.M., and T.B. ; Investigation, S.P, M.M., and T.B. ; Formal analysis, S.P, M.M., and T.B. ; Visualization and writing – original draft, S.P. and T.B. ; Writing – review and editing, S.P, M.M., and T.B. ; Funding acquisition, S.P, M.M., and T.B. ; Supervision, S.P, M.M., and T.B. All authors have read and agreed to the final version of the manuscript.

Use of Artificial Intelligence

The authors did not use any generative artificial intelligence tools in the preparation, writing, or analysis of this manuscript.

Ethics Approval

The study protocol was approved by the Siriraj Institutional Review Board, Faculty of Medicine Siriraj Hospital, Mahidol University, Bangkok, Thailand (731/2554 [EC3]).

REFERENCES

- Haykal R, Kassar A, Chamoun N, Akoum N. The left atrium in heart failure with preserved ejection fraction: What we know and what we do not know. *Heart Rhythm O2*. 2025;6(7):1028–38.
- Thomas L, Abhayaratna WP. Left Atrial Reverse Remodeling: Mechanisms, Evaluation, and Clinical Significance. *JACC Cardiovasc Imaging*. 2017;10(1):65–77.
- Janwanishstaporn S, Boonyasirinant T. Correlation between aortic stiffness and left atrial volume index in hypertensive patients. *Clin Exp Hypertens*. 2016;38(2):160–5.
- Jaturapisanukul S, Kaolawanich Y, Meechuen M, Boonyasirinant T. Correlation between Obesity and Left Atrial Enlargement in Patients Using Cardiac Magnetic Resonance. *Siriraj Med J*. 2025;77(2):130–6.
- Higgins CB, Reinke RT, Jones NE, Broderick T. Left atrial dimension on the frontal thoracic radiograph: a method for assessing left atrial enlargement. *AJR Am J Roentgenol*. 1978;130(2):251–5.
- Quinton SJ, Ker JA, Rheeder P, Deffur A. The reliability of chest radiographs in predicting left atrial enlargement. *Cardiovasc J Afr*. 2010;21(5):274–9.
- El Mathari S, Hopman L, Bouchnaf C, Heidendael JF, Nederveen AJ, van Ooij P, et al. Clinical implications of different methods to assess left atrial remodeling: A comparative study between echocardiography and cardiac magnetic resonance imaging for left atrial volume index quantification. *Int J Cardiol*. 2024;414:132443.
- Maceira AM, Cosín-Sales J, Roughton M, Prasad SK, Pennell DJ. Reference left atrial dimensions and volumes by steady state free precession cardiovascular magnetic resonance. *Journal of Cardiovascular Magnetic Resonance*. 2010;12(1):65.
- Mahmod M, Bull S, Kailayanathan T, Davis TA, Borlotti A, Popescu IA, et al. Left atrial volume quantification by transthoracic echocardiography versus cardiovascular magnetic resonance: a systematic review and meta-analysis. *Int J Cardiovasc Imaging*. 2025;41(9):1657–69.
- Cho MS, Park HS, Cha MJ, Lee SR, Park JK, Kim TH, et al. Clinical impact of left atrial enlargement in Korean patients with atrial fibrillation. *Sci Rep*. 2021;11(1):23808.
- Khan MA, Yang EY, Zhan Y, Judd RM, Chan W, Nabi F, et al. Association of left atrial volume index and all-cause mortality in patients referred for routine cardiovascular magnetic resonance: a multicenter study. *J Cardiovasc Magn Reson*. 2019;21(1):4.
- Njoku A, Kannabhiran M, Arora R, Reddy P, Gopinathannair R, Lakkireddy D, et al. Left atrial volume predicts atrial fibrillation recurrence after radiofrequency ablation: a meta-analysis. *Europace*. 2018;20(1):33–42.
- Essayagh B, Antoine C, Benfari G, Messika-Zeitoun D, Michelena H, Le Tourneau T, et al. Prognostic Implications of Left Atrial Enlargement in Degenerative Mitral Regurgitation. *J Am Coll Cardiol*. 2019;74(7):858–70.
- Tsao CW, Josephson ME, Hauser TH, O'Halloran TD, Agarwal A, Manning WJ, et al. Accuracy of electrocardiographic criteria

- for atrial enlargement: validation with cardiovascular magnetic resonance. *J Cardiovasc Magn Reson*. 2008;10(1):7.
15. Bureekam S, Boonyasirinant T. Accuracy of left atrial enlargement diagnosed by electrocardiography as compared to cardiac magnetic resonance in hypertensive patients. *J Med Assoc Thai*. 2014;97 Suppl 3:S132–8.
 16. Matsuda M, Matsuda Y. Mechanism of left atrial enlargement related to ventricular diastolic impairment in hypertension. *Clin Cardiol*. 1996;19(12):954–9.
 17. Cioffi G, Mureddu GF, Stefenelli C, de Simone G. Relationship between left ventricular geometry and left atrial size and function in patients with systemic hypertension. *J Hypertens*. 2004;22(8):1589–96.
 18. Eshoo S, Ross DL, Thomas L. Impact of mild hypertension on left atrial size and function. *Circ Cardiovasc Imaging*. 2009;2(2):93–9.
 19. Kelley MJ, Elliott LP, Shulman ST, Ayoub EM, Victorica BE, Gessner IH. The significance of the left atrial appendage in rheumatic heart disease. *Circulation*. 1976;54(1):146–53.
 20. Kaye J, Meyer MJ, Van Lingen B, McGregor M, Braudo JL. The radiological diagnosis of mitral valve disease. *Br J Radiol*. 1953;26(305):242–51.
 21. Murray JG, Brown AL, Anagnostou EA, Senior R. Widening of the tracheal bifurcation on chest radiographs: value as a sign of left atrial enlargement. *AJR Am J Roentgenol*. 1995;164(5):1089–92.
 22. Alavi SM, Keats TE, O'Brien WM. The angle of tracheal bifurcation: its normal mensuration. *Am J Roentgenol Radium Ther Nucl Med*. 1970;108(3):546–9.
 23. Haskin PH, Goodman LR. Normal tracheal bifurcation angle: a reassessment. *AJR Am J Roentgenol*. 1982;139(5):879–82.

Incidence and Factors Associated with Perioperative Respiratory Adverse Events in Pediatric Patients with Upper Respiratory Tract Infection Undergoing Surgery Under General Anesthesia: A Retrospective Cohort Study

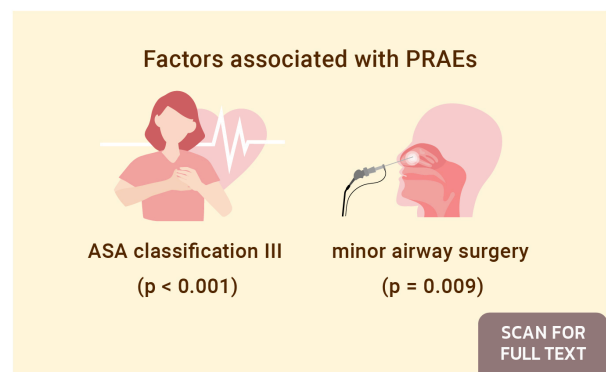
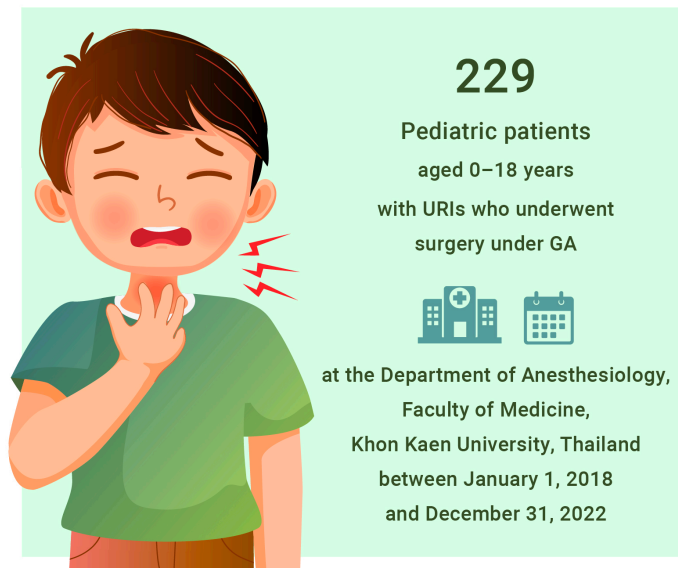
Sutida Boonkamjad, R.N.¹, Darunee Sripadungkul, M.D.^{2,*}, Cattleya Kasemsiri, M.D.², Prathana Wittayapairoch, M.D.², Panaratana Ratanasuwan, M.D.²

¹Nurse Anesthetist Division, Department of Nursing, Srinagarind Hospital, Faculty of Medicine, Khon Kaen University, Khon Kaen, Thailand,

²Department of Anesthesiology, Faculty of Medicine, Srinagarind Hospital, Khon Kaen University, Khon Kaen, Thailand.

Incidence and factors associated with perioperative respiratory adverse events in pediatric patients with upper respiratory tract infection

Preoperative management should carefully assess pediatric patients with URI and implement strategies to prevent PRAEs.



SCAN FOR FULL TEXT



*Corresponding author: Darunee Sripadungkul

E-mail: daruneeta@kku.ac.th

Received 29 September 2025 Revised 15 November 2025 Accepted 19 November 2025

ORCID ID: <http://orcid.org/0000-0003-2228-2224>

<https://doi.org/10.33192/smj.v78i1.277950>



All material is licensed under terms of the Creative Commons Attribution 4.0 International (CC-BY-NC-ND 4.0) license unless otherwise stated.

ABSTRACT

Objective: The primary objective is to determine the incidence of perioperative respiratory adverse events (PRAEs) in pediatric patients with upper respiratory tract infections (URIs) undergoing general anesthesia (GA); the secondary objective is to identify associated risk factors, including the COLDS score.

Materials and Methods: This retrospective cohort study included pediatric patients aged 0–18 years with URIs who underwent surgery under GA at the Department of Anesthesiology, Faculty of Medicine, Khon Kaen University, Khon Kaen, Thailand, between January 1, 2018, and December 31, 2022.

Results: A total of 229 pediatric patients were analyzed, with a PRAE incidence of 3.9%. In univariable logistic regression analysis, the American Society of Anesthesiologists (ASA) classification III, severe URI, underlying respiratory disease, endotracheal tube use, emergency surgery, and minor airway surgery (compared with other surgery types) were identified as factors associated with PRAEs. In multivariable analysis, only ASA classification III compared with ASA classification II (adjusted odds ratio [OR] 83.33; 95% CI, 7.10 to 1363.56; $p < 0.001$) and minor airway surgery compared with other surgery types (adjusted OR 18.54; 95% CI, 1.97 to 237.98; $p = 0.009$) remained significantly associated with PRAEs.

Conclusion: The incidence of PRAEs in pediatric patients with URIs undergoing GA was 3.9%. ASA classification III and minor airway surgery were associated with PRAEs. Careful preoperative assessment and targeted prevention strategies are recommended for pediatric patients with URIs to reduce PRAEs.

Keywords: Anesthesia; children; factors; pediatric; perioperative respiratory adverse events; upper respiratory tract infections (Siriraj Med J 2026;78(1):39-50)

Previous presentation in conferences

Part of this study was previously presented as a poster presentation at the SANCON-ASPA 2025 Conference: Scaling New Heights in Pediatric Anesthesia and Beyond (24th Annual Conference of the Society of Anesthesiologists of Nepal and 21st Meeting of the Asian Society of Paediatric Anesthesiologists), held in Kathmandu, Nepal, on April 5, 2025. The abstract was presented under the title “Incidence of perioperative respiratory events in children with upper respiratory tract infections.”

INTRODUCTION

Upper respiratory tract infections (URIs) are the most common medical issue in pediatric surgical patients and the leading cause for postponing surgery.^{1,2} Postponing surgery can cause stress for the child, parents, surgeon, and hospital.^{1,2} URIs are typically caused by viral infections.¹⁻⁴ Children under four years old may experience an average of eight episodes of URIs per year, each lasting up to two weeks.¹ The incidence of URIs decreases as children age, with older children and adults averaging about two to four URIs per year.^{1,2,4} However, airway hypersensitivity can persist for approximately two to six weeks.^{2,5} To diagnose an active URI, a child must exhibit at least two of the following symptoms: rhinorrhea, nasal congestion, sneezing, cough, sore or scratchy throat, malaise, or fever exceeding 38°C.^{1,6} These symptoms should have manifested within two weeks of the perioperative period and must be confirmed by a parent.^{6,7} The severity of pediatric URI is commonly categorized as mild, moderate, or severe according to clinical presentation, though criteria vary by reference.^{1,2} For severe URIs, studies recommend

postponing surgery until the child has been symptom-free for two weeks, followed by a re-evaluation.¹⁻³ Identifying high-risk children preoperatively is challenging.^{7,8} Due to their anatomical and physiological characteristics and frequent URIs, children are vulnerable to perioperative respiratory adverse events (PRAEs).⁷ The incidence of PRAEs is between 24% and 30% in children with a current and/or recent URI, compared to 8% to 17% in children without a URI.⁵ Common PRAEs under general anesthesia (GA) include desaturation, breath holding, laryngospasm, bronchospasm, and coughing. Laryngospasm, bronchospasm, and persistent hypoxemia can lead to severe complications and death.^{7,9} Factors associated with PRAEs in children with URIs include age, respiratory comorbidities, URI severity, passive smoking, COLDS score, type of surgery, anesthetic technique, and anesthesiologist experience, though criteria may vary by clinical setting.^{3,7,10,11}

We hypothesized that the incidence of PRAEs in our pediatric patients would be low due to the hospital policy of postponing elective surgery for severe URIs

until patients are symptom-free for at least two weeks and have been re-evaluated. Our hospital has no prior information about the incidence of PRAEs or the factors associated with PRAEs in children with URI. Therefore, the primary objective of this study is to determine the incidence of PRAEs among pediatric patients with URI undergoing surgery under GA. The secondary objective is to identify the factors associated with PRAEs in these pediatric patients. The findings will provide guidelines for anesthetic services and improve the efficacy of anesthesiology practices for children with URIs undergoing surgery under GA.

MATERIALS AND METHODS

This retrospective cohort study involves pediatric patients aged 0-18 years with URIs who were scheduled for surgery under GA at the Department of Anesthesiology, Faculty of Medicine, Khon Kaen University, Khon Kaen, Thailand. Ethical approval was obtained from Khon Kaen University's Ethics Committee (HE671456), and the requirement for written informed consent was waived by the Institutional Ethics Committee. Before commencement, the study was also registered in the Thai Clinical Trial Registry (TCTR20250109001). The study adhered to the Strengthening the Reporting of Observational Studies in Epidemiology (STROBE) guidelines in order to ensure comprehensive and transparent reporting of the observational data.

Patient population

We included all pediatric patients aged 0-18 years with URIs undergoing surgery under GA at Srinagarind Hospital between January 1, 2018, and December 31, 2022. Both elective and emergency surgeries were included. Patients whose records did not contain sufficient documentation were excluded.

Data collection

The database consisted of anesthesia records and medical records. The anesthesia records provided data on pre-anesthesia evaluation, intraoperative care, post-anesthesia care, and post-anesthesia visits. These records contained preoperative, intraoperative, and postoperative data. The medical records contained patient characteristics, operative notes, and events after anesthesia. We compared the groups with PRAEs and No-PRAEs group.

The first section assessed patient characteristic data consisting of gender, age, body weight, height, the American Society of Anesthesiologists (ASA) physical status, comorbidities including cardiovascular disease, respiratory disease, central nervous system disease, hematologic disease, kidney disease, coagulopathy, and

obesity (body mass index (BMI) \geq 95th percentile for children of the same age and weight).⁷ We also recorded underlying respiratory diseases, including asthma, allergic rhinitis, bronchopulmonary dysplasia, tracheal stenosis, presence of a tracheostomy tube pneumonia, and scoliosis. Additionally, we noted parental concern, history of wheezing, and abnormal preoperative chest X-ray (CXR).

In the second section assessed data of preoperative diagnosis of URI including symptoms of URI (runny nose, dry cough, productive cough, mucopurulent secretion, nasal congestion, sore throat, wheezing, rhonchi, fever $> 38^{\circ}\text{C}$, and lethargy). We recorded duration of URI and symptom-free period before surgery. The severity of URI was classified as mild, moderate, or severe.² Mild URI was defined as a recent history of URI without current signs or symptoms within the past 2-4 weeks. Moderate URI was defined as the presence of any URI symptoms, such as a runny nose or dry cough, without wheezing and no systemic symptoms for one or two days before surgery. Severe URI was defined as the presence of any URI symptoms with systemic manifestations, including fever above 38°C , productive cough, mucopurulent secretion, nasal congestion, sore throat, wheezing, pulmonary involvement, and lethargy.² We also documented of COLDS score.^{3,11} The COLDS score is a heuristic preanesthetic risk assessment tool commonly used to predict the incidence of PRAEs in children with URI. It is based on five categories: the severity of current symptoms (none, mild, moderate/severe), the onset of signs (> 4 weeks, 2-4 weeks, < 2 weeks), lung disease (none, mild, moderate/severe), the airway management device (facemask, supraglottic airway (SGA), endotracheal tube (ETT)), and the type of surgery (other, minor airway, major airway). Each category of the COLDS score is assigned 1, 2, or 5 points, resulting in a total score that can range from 5 to 25 points.^{3,11}

The third section assessed operative details, including type of surgical urgency (elective or emergency), and type of surgery detailed.¹¹ Major airway surgery, such as cleft palate repair, rigid bronchoscopy, and maxillofacial surgery. Minor airway surgery, such as tonsillectomy, adenoidectomy, and nasolacrimal duct surgery. Other surgery, such as ear tube insertion.¹¹ We also recorded operative time, and intraoperative blood loss.

The fourth section assessed anesthesia detailed including anesthetic techniques included balanced GA, inhalational GA, total intravenous anesthesia (TIVA) for GA, and sedation, anesthetic agents for induction (sevoflurane, propofol), anesthetic time, and anesthesiologist experience.

The fifth section assessed PRAEs, including incidence and detailed of PRAEs including abnormal breath sounds after anesthesia, breath holding (defined as apnea lasting more than 15 seconds, irregular breathing, or apnea associated with bradycardia or cyanosis),⁷ hypoxemia (defined as oxygen saturation (SpO₂) < 95% lasting more than 30 seconds),⁷ laryngospasm (defined as airway obstruction with abdominal and chest muscle rigidity requiring positive pressure ventilation or administration of succinylcholine),⁷ bronchospasm (defined as increased work of breathing, especially during expiration and wheezing, or requiring bronchodilators),⁷ excessive respiratory secretions requiring ETT suctioning during anesthesia, chest retraction, postoperative diagnosis of pneumonia or bronchitis, abnormal postoperative CXR (atelectasis, pneumonia, bronchiolitis), and need for prolonged oxygen support (> 1 hour postoperative) to maintain SpO₂ > 95%.³ Additionally, we summarized of when PRAEs occurred (during induction, intraoperatively, after extubation, in the PACU, or postoperatively in the ward or intensive care unit (ICU)). Additionally, we noted anesthetic management (suction, steroid, salbutamol inhaler, antibiotic treatment, retained ETT and on ventilator support). We also assessed ICU stay, postoperative hospital stay, and postoperative outcomes (uneventful, on oxygen support, retained ETT, transferred to ICU).

The sixth section assessed factors associated with PRAEs, including patient factors, anesthesia factors, and surgical factors. Patient factors included gender (male, female), age (< 1 year, ≥ 1 year), ASA classification (I, II, III), obesity, severity of URI (mild, moderate, severe), onset of URI before surgery (< 2 weeks, 2-4 weeks, > 4 weeks), and underlying respiratory disease. Anesthesia factors included anesthetic technique (balanced GA, inhalational GA, TIVA for GA, and sedation), anesthetic agents for induction (sevoflurane, propofol), airway device (facemask, SGA, ETT), anesthesiologists' experience, and COLDS score > 10. Surgical factors included type of surgical urgency (elective, emergency), type of surgery (major airway, minor airway, other), and surgical time.

Statistical analysis

Data analysis was performed using STATA for Windows, version 18 (StataCorp, College Station, TX). Descriptive statistics were used to summarize the participants' characteristics. Categorical variables were reported as numbers and percentages, based on the number of participants with non-missing data. Continuous variables were presented as the median and

interquartile range (IQR) for non-normally distributed data, or as the means and standard deviations (SDs) for normally distributed data. The primary analysis focused on the incidence of PRAEs among children with URIs undergoing surgery under GA. Statistical significance was defined as $p < 0.05$. For the secondary analysis, we evaluated the factors associated with PRAEs using univariable and multivariable logistic regression models. Univariable analyses were conducted using chi-square tests or Fisher's exact tests, as applicable, to examine associations between categorical variables. To control for potential confounders, baseline variables that were statistically significant in the univariable analysis ($p < 0.2$) were included in the multivariable model. The final multivariable logistic regression model was constructed using the enter method and refined through sequential backward elimination based on the likelihood ratio test. Variables were retained in the model if they remained significant during the elimination process. The strength of association was expressed as adjusted odds ratios (ORs) with 95% confidence intervals (CIs).

The estimated required sample size for the study was determined using the formula for estimating an infinite population proportion. This calculation was based on a previous study that reported the incidence of PRAEs as 21.50%.¹² Using 25% as the proportion (p), a type I error of 0.05, and a power of 80%, we determined that a sample size of 225 participants was required for this study. This is a retrospective data collection study. Therefore, we aimed to include all patients over a 5-year period. The total population consisted of 229 patients.

RESULTS

A total of 17,183 pediatric patients aged 0–18 years underwent surgery (both elective and emergency cases) under GA. Of these, data were collected from 229 patients with URIs (Fig 1). We analyzed 229 pediatric patients scheduled for surgery under GA.

Patient characteristics

There were 144 males (62.9%). Median age was 4.1 (2.1, 6.4) years, weight was 14.7 (10.9, 22) kg, and height was 100 (85, 116) cm. Most patients (97.4%) were ASA physical status classification II. The most common comorbidities were respiratory disease (100%), central nervous system disease (7.9%), age < 1 year (7.9%), hematologic disease (6.6%), and cardiovascular disease (3.9%). The most common respiratory conditions were asthma (4.8%), allergic rhinitis (3.9%), and presence of a tracheostomy tube (1.3%) (Table 1).

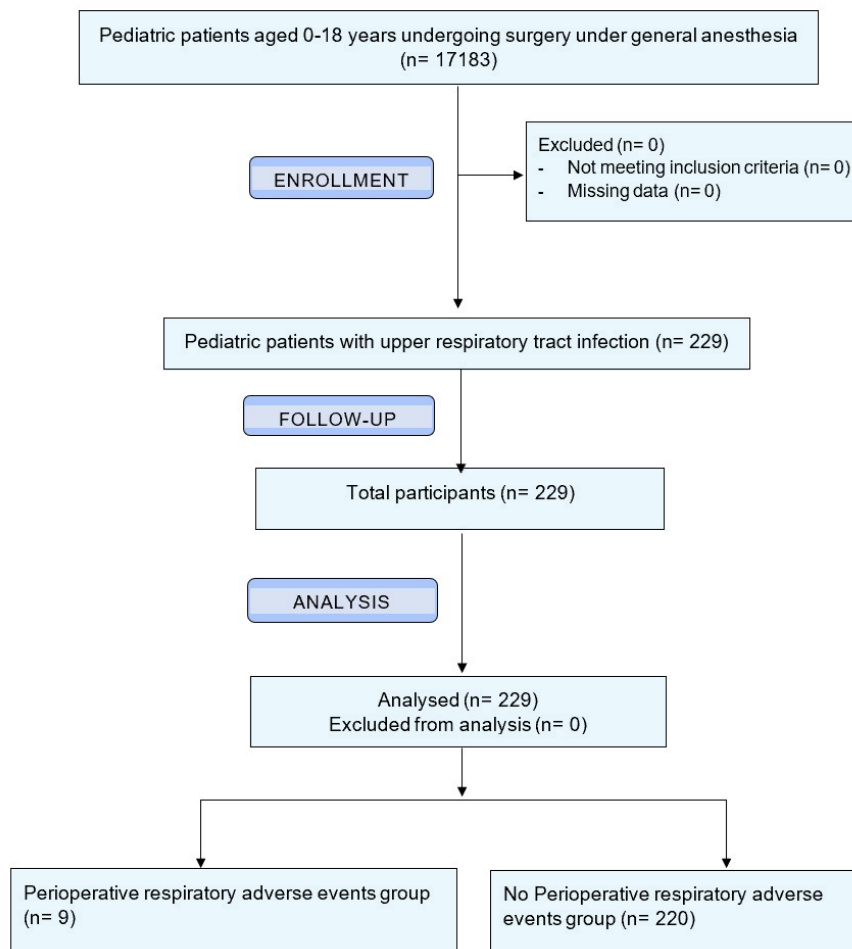


Fig 1. Study flow diagram

Preoperative diagnoses of URI and COLDS score

As shown in [Table 2](#), the most common URI symptoms were runny nose (76.4%), dry cough (32.8%), and mucopurulent secretions (15.7%). The median duration of URI was 3 (2, 3) days. Most patients (50.7%) remained symptomatic before surgery, while 41.9% had 1–6 symptom-free days. Most patients (83.4%) had moderate URI severity.

Based on the COLDS score, most patients (83.4%) had mild URI symptoms, with 96.1% of cases occurring less than two weeks before surgery. Lung disease was absent in 90.0% of patients. Airway devices used included SGA (50.7%), ETT (38.9%), and facemasks (10.5%). Most surgeries were other types (87.3%), with minor and major airway surgeries comprising 7.9% and 4.8%, respectively. The median COLDS score was 12 (11, 14), ranging from 5 to 25. In the PRAEs group, the median score was 15 (15, 17), compared to 11.5 (11, 14) in the No-PRAEs group. A COLDS score above 10 was observed in 90% of patients, including all patients in the PRAEs group. Additionally, 96.1% had parental concern about URI, 1.3% had a history of wheezing, and 3.1% had abnormal preoperative CXR.

Operative details

Almost all cases were elective, with 227 patients (99.1%), while only 2 patients (0.9%) underwent emergency procedures. Major airway surgery was performed in 11 patients (4.8%) including rigid bronchoscopy (3.1%), cleft palate repair (0.9%), and maxillofacial surgery (0.9%). Minor airway surgery was performed in 18 patients (7.9%), consisting of nasolacrimal duct probing (2.6%), cleft lip repair (2.2%), tonsillectomy (1.3%), flexible bronchoscopy (0.9%), and tongue-tie release (0.9%). Other types of surgery were performed in 200 patients (87.3%), including ophthalmologic surgery (24.0%), magnetic resonance imaging (20.1%), general surgery (14.8%), orthopedic surgery (14.0%), urologic surgery (7.4%), ear reconstruction (3.5%), computed tomography (1.3%), radiation therapy (0.9%), neurological surgery (0.9%), and cardiovascular and thoracic surgery (0.4%). The median operative time was 60 (40, 90) minutes, and estimated blood loss 0 (0, 3) ml.

Anesthesia details

The anesthetic techniques used included inhalational GA in 139 patients (60.7%), balanced GA in 77 patients

TABLE 1. Demographic data.

Variables	PRAEs group (n = 9)	No-PRAEs group (n = 220)	Total (n = 229)	p-value
Gender (n (%))				0.730
Male	5 (55.6)	139 (63.2)	144 (62.9)	
Female	4 (44.4)	81 (36.8)	85 (37.1)	
Age (years, median (IQR))	3.3 (1.9, 5.6)	4.2 (2.1, 6.4)	4.1 (2.1, 6.4)	0.691
Age < 1 year (n (%))	1 (11.1)	17 (7.7)	18 (7.9)	0.528
Age ≥ 1 year (n (%))	8 (88.9)	203 (92.3)	211 (92.1)	
Weight (kg, median (IQR))	11.8 (11.3, 23)	15 (10.9, 22)	14.7 (10.9, 22)	0.619
Height (cm, median (IQR))	96 (85, 117)	100.5 (85, 115.5)	100 (85, 116)	0.882
Obesity (n (%))	0 (0)	8 (3.6)	8 (3.5)	> 0.999
ASA classification (n (%))				< 0.001
II	6 (66.7)	217 (98.6)	223 (97.4)	
III	3 (33.3)	3 (1.4)	6 (2.6)	
Comorbidity (n (%))				
Respiratory disease	9 (100.0)	220 (100.0)	229 (100.0)	
Central nervous system disease	2 (22.2)	16 (7.3)	18 (7.9)	0.151
Age < 1 year	1 (11.1)	17 (7.7)	18 (7.9)	0.528
Hematologic disease	3 (33.3)	12 (5.5)	15 (6.6)	0.015
Cardiovascular disease	1 (11.1)	8 (3.6)	9 (3.9)	0.308
Obesity	0 (0.0)	8 (3.6)	8 (3.5)	> 0.999
Liver disease	1 (11.1)	3 (1.4)	4 (1.8)	0.149
Immune system	0 (0.0)	2 (0.9)	2 (0.9)	> 0.999
Endocrine	1 (11.1)	1 (0.5)	2 (0.9)	0.077
Kidney disease	0 (0.0)	1 (0.5)	1 (0.4)	> 0.999
Risk aspiration	0 (0.0)	1 (0.5)	1 (0.4)	> 0.999
Underlying respiratory disease (n (%))				0.001
Asthma	0 (0.0)	11 (5.0)	11 (4.8)	
Allergic rhinitis	1 (11.1)	8 (3.6)	9 (3.9)	
Presence of a tracheostomy tube	2 (22.2)	1 (0.5)	3 (1.3)	
Tracheal stenosis	0 (0.0)	2 (0.9)	2 (0.9)	
Pneumonia	0 (0.0)	2 (0.9)	2 (0.9)	
Bronchopulmonary dysplasia	1 (11.1)	0 (0.0)	1 (0.4)	
Scoliosis	0 (0.0)	1 (0.5)	1 (0.4)	

Abbreviations: PRAEs group, Perioperative respiratory adverse events group; No-PRAEs group, No perioperative respiratory adverse events group; IQR, interquartile range; ASA, the American Society of Anesthesiologists

TABLE 2. Data of preoperative diagnosis of upper respiratory tract infection and COLDS score.

Variables	PRAEs group (n = 9)	No-PRAEs group (n = 220)	Total (n = 229)	p-value
Symptoms (n (%))				
Runny nose	6 (66.7)	169 (76.8)	175 (76.4)	0.443
Dry cough	5 (55.6)	70 (31.8)	75 (32.8)	0.157
Mucopurulent secretion	4 (44.4)	32 (14.6)	36 (15.7)	0.036
Low grade fever	1 (11.1)	27 (12.3)	28 (12.2)	> 0.999
Throat pain	0 (0.0)	6 (2.7)	6 (2.6)	> 0.999
Productive cough	0 (0.0)	2 (0.9)	2 (0.9)	> 0.999
Nasal congestion	1 (11.1)	0 (0.0)	1 (0.4)	0.039
Sneezing	0 (0.0)	1 (0.5)	1 (0.4)	> 0.999
Duration of URI (days, median (IQR))	3 (2, 3)	3 (2, 3)	3 (2, 3)	0.935
Symptom-free period before surgery (days, n (%))				
0	5 (55.6)	111 (50.5)	116 (50.7)	> 0.999
1-6	4 (44.4)	92 (41.8)	96 (41.9)	
7-14	0 (0.0)	17 (7.7)	17 (7.4)	
Severity of URI (n (%))				0.044
Moderate	5 (55.6)	186 (84.6)	191 (83.4)	
Severe	4 (44.4)	34 (15.5)	38 (16.6)	
Current symptom (n (%))				0.044
Mild	5 (55.6)	186 (84.6)	191 (83.4)	
Moderate/ severe	4 (44.4)	34 (15.5)	38 (16.6)	
Onset of URI (days, median (IQR))	3 (2, 7)	4 (2, 7)	4 (2, 7)	0.822
2-4 weeks (n (%))	0 (0.0)	9 (4.1)	9 (3.9)	> 0.999
< 2 weeks (n (%))	9 (100.0)	211 (95.9)	220 (96.1)	
Lung disease (n (%))				0.277
None	7 (77.8)	199 (90.5)	206 (90.0)	
Mild	2 (22.2)	18 (8.2)	20 (8.7)	
Moderate/ severe	0 (0.0)	3 (1.4)	3 (1.3)	
Device (n (%))				0.013
Facemask	0 (0.0)	24 (10.9)	24 (10.5)	
SGA	1 (11.1)	115 (52.3)	116 (50.7)	
ETT	8 (88.9)	81 (36.8)	89 (38.9)	
Type of surgery (n (%))				0.021
Other (including ear tubes)	5 (55.6)	195 (88.6)	200 (87.3)	
Minor airway	3 (33.3)	15 (6.8)	18 (7.9)	
Major airway	1 (11.1)	10 (4.6)	11 (4.8)	
COLDS score (median (IQR), score range 5-25)	15 (15,17)	11.5 (11,14)	12 (11,14)	< 0.001
COLDS score ≤ 10 (n (%))	0 (0.0)	23 (10.5)	23 (10.0)	0.604
COLDS score > 10 (n (%))	9 (100.0)	197 (89.6)	206 (90.0)	

Abbreviations: PRAEs group, Perioperative respiratory adverse events group; No-PRAEs group, No perioperative respiratory adverse events group; URI, upper respiratory tract infection; IQR, interquartile range; SGA, supraglottic airway; ETT, endotracheal tube

(33.6%), TIVA for GA in 10 patients (4.4%), and sedation in 3 patients (1.3%). The agents used for induction were sevoflurane in 153 patients (66.8%) and propofol in 76 patients (33.2%). The median (IQR) anesthetic time was 90 (60, 120) minutes. Anesthetics were administered by anesthesiologists with less than 5 years of experience in 44 patients (19.2%), and by those with 5 or more years of experience in 185 patients (80.8%).

The perioperative respiratory adverse events

The incidence of PRAEs in pediatric patients with URIs undergoing GA was 9 out of 229 (3.9%). The most common PRAEs were abnormal breath sounds after anesthesia, prolonged oxygen requirement, chest retraction, bronchospasm, breath-holding, and hypoxemia. Most events occurred intraoperatively, and during induction, as shown in Table 3. Anesthetic management for PRAEs included: two patients received succinylcholine, salbutamol inhaler, and oxygen support; two received suction, salbutamol inhaler, and oxygen support; two received succinylcholine, suction, and salbutamol inhaler, requiring a retained ETT with ventilator and oxygen support; one received only oxygen support; one received succinylcholine and oxygen support; and one received suction, salbutamol

inhaler, and required a retained ETT with ventilator and oxygen support. In the PRAEs group, the median ICU stay was 1 (0, 1) day.

For all patients, the median postoperative hospital stay was 3 (1, 4) days. For postoperative outcomes, all 220 patients in the No-PRAEs group had uneventful recoveries. Among the nine patients in the PRAEs group, one had an uneventful recovery, two required oxygen support, three needed retained ETT, oxygen support, and ICU admission, and three required both oxygen support and ICU admission. No severe adverse events or fatalities occurred.

The factors associated with perioperative respiratory adverse events

As shown in Table 4, univariable logistic regression analyses were performed to identify factors associated with PRAEs. Patient factors (ASA classification III, severe URI, and underlying respiratory disease), anesthesia factors (use of an ETT compared with an SGA), and surgical factors (emergency surgery and minor airway surgery compared with other surgery types) were all statistically significantly associated with PRAEs ($p < 0.05$), based on ORs with 95% CIs. In the multivariable

TABLE 3. Perioperative respiratory adverse events (N = 9).

Adverse events	n (%)
Abnormal breath sound after anesthesia	8 (88.9)
Need for prolonged oxygen support	8 (88.9)
Chest retraction	7 (77.8)
Bronchospasm	6 (66.7)
Breath holding	6 (66.7)
Hypoxemia	6 (66.7)
Laryngospasm	5 (55.6)
Postoperative diagnosis pneumonia	3 (33.3)
Abnormal postoperative CXR (pneumonia)	3 (33.3)
Excessive respiratory secretion and require ETT suctioning during anesthesia	2 (22.2)
Summary of PRAEs occurred	
During induction	5 (55.6)
Intraoperative	6 (66.7)
After extubation	1 (11.1)
Postoperative at ICU	1 (11.1)

Abbreviations: CXR, chest X-ray; ETT, endotracheal tube; PRAEs, perioperative respiratory adverse events; ICU, intensive care unit

TABLE 4. The factors associated with perioperative respiratory adverse events.

	Factors	Reference	Odds ratio (95% CI)	p-value	Adjusted odds ratio (95% CI)	p-value
Patient factors						
Gender	Female	Male	1.37 (0.36, 5.26)	0.646		
Age	< 1 year	≥ 1 year	1.49 (0.18, 12.65)	0.726		
ASA classification	III	II	36.17 (6.01, 217.52)	< 0.001	83.33 (7.10, 1363.56)	< 0.001*
Bodyweight	Obese	Non obese	2.22 (< 0.01, 16.26)	> 0.999		
Severity of URI	Severe	Moderate	4.38 (1.12, 17.13)	0.034		
Onset of URI before surgery	< 2 weeks	2-4 weeks	0.51 (0.07, > 999)	> 0.999		
Symptom-free period before surgery	0 day	7-14 days	1.04 (0.27, 3.97)	0.959		
Symptom-free period before surgery	1-6 days	7-14 days	NA			
Underlying of respiratory disease	Yes	No	0.02 (< 0.01, 0.20)	0.002		
Abnormal Preoperative CXR	Yes	No	2.56 (< 0.01, 19.20)	> 0.999		
Anesthesia factors						
Anesthetic technique	Inhalational GA	Sedation	0.05 (< 0.01, > 999)	1.000		
Anesthetic technique	Balanced GA	Sedation	0.31 (0.03, > 999)	1.000		
Anesthetic technique	TIVA for GA	Sedation	0.30 (0.01, > 999)	1.000		
Anesthetic agent for induction	Sevoflurane	Propofol	0.61 (0.16, 2.33)	0.474		
Airway device	Facemask	SGA	4.83 (< 0.01, 188.5)	1.000		
Airway device	ETT	SGA	11.25 (1.46, 508.25)	0.012		
Anesthesiologist experience	< 5 years	≥ 5 years	1.21 (0.24, 6.04)	0.818		
COLDS score > 10	> 10	≤ 10	1.43 (0.21, > 999)	0.604		
Anesthesia time	> 60 mins	≤ 60 mins	1.25 (0.25, 6.21)	0.778		
Surgical factors						
Type of surgical urgency	Emergency	Elective	27.37 (1.57, 478.10)	0.049		
Type of surgery	Minor airway	Other	7.80 (1.70, 35.83)	0.008	18.54 (1.97, 237.98)	0.009*
Type of surgery	Major airway	Other	3.90 (0.42, 36.60)	0.234		
Surgical time	≥ 60 mins	< 60 mins	1.55 (0.38, 6.35)	0.536		

Abbreviations: CI, confidence interval; ASA, the American Society of Anesthesiologists; URI, upper respiratory tract infection; CXR, chest x-ray; GA, general anesthesia; TIVA, total intravenous anesthesia; SGA, supraglottic airway; ETT, endotracheal tube; NA, not applicable. *Statistically significant ($p < 0.05$).

logistic regression analyses, only ASA classification III compared with ASA classification II (adjusted OR, 83.33; 95% CI, 7.10 to 1,363.56; $p < 0.001$) and minor airway surgery compared with other surgery types (adjusted OR, 18.54; 95% CI, 1.97 to 237.98; $p = 0.009$) remained statistically significantly associated with PRAEs.

DISCUSSION

This study found that the incidence of PRAEs among pediatric patients with URIs undergoing surgery under GA was 3.9%. In multivariable logistic regression analysis, factors associated with PRAEs were ASA classification III and minor airway surgery.

A retrospective study involving 267 pediatric patients (ages 0–13) with recent URIs undergoing GA reported a PRAE incidence of 8.6% (23 cases).¹³ A prospective observational study of 270 children under 2 years old with oropharyngeal cleft deformity found a PRAE incidence of 1.85% (5 cases).¹⁴ Similarly, our study observed a low PRAE incidence. In contrast, a prospective observational study of 216 children (ages 1–5) with mild to moderate URIs undergoing ambulatory ilioinguinal surgery found a PRAE incidence of 21.3%.³ Another retrospective study of pediatric patients (ages 0–18) with recent URIs undergoing GA reported a PRAE incidence of 21.5%.¹² Our study observed a low incidence of PRAEs, likely because most patients (83.4%) had only moderate URIs, and our hospital policy requires postponing elective surgery for severe URI cases until at least two weeks after full symptom resolution and re-evaluation. Additionally, differences in PRAE incidence across studies may reflect variation in PRAE definitions, URI severity, study design, inclusion criteria, surgery type, and pediatric age range.

For the occurrence of PRAEs, a previous study of ambulatory ilioinguinal surgery found that 78.3% occurred during anesthesia and 21.7% in the PACU.³ Similarly, in our study, 77.8% of PRAEs occurred during anesthesia, with 11.1% occurring after extubation and 11.1% in the ICU. In contrast, a study of airway surgery in children under two years of age with oropharyngeal cleft deformity reported that all cases of PRAEs occurred after extubation.¹⁴ PRAEs occurred most often immediately after tracheal extubation and were much less common during the induction and maintenance phases.⁷ The timing of PRAEs varies depending on patient characteristics (e.g., very young age), the type of surgery (especially airway procedures), the severity of URIs, and the adequacy of perioperative management—from preoperative preparation to intraoperative and postoperative care.^{7,14}

From univariable logistic regression, factors associated with PRAEs included ASA classification III, severe URI,

underlying respiratory disease, use of an ETT (compared with an SGA), emergency surgery, and minor airway surgery (compared with other surgery types), consistent with previous systematic reviews.^{1,2}

In multivariable analysis, the prior study identified respiratory comorbidities, postponement of surgery for less than 15 days, passive smoking, and a COLDS score greater than 10 as predictors of PRAEs.³ Additionally, abnormal findings on preoperative chest imaging and a symptom-free period of 7–13 days were independently associated with PRAEs.¹³ In contrast, our study found that only ASA classification III and minor airway surgery (compared with other surgery types) were significantly associated with PRAEs. This may be attributable to the low incidence of PRAEs in our cohort. Major airway surgery (compared with other types of surgery) was not an independent factor associated with PRAEs, possibly because of the small sample size—only eleven cases of major airway surgery (one in the PRAEs group and ten in the No-PRAEs group)—which may have limited the statistical power to detect a significant association.

ASA classification III is an independent risk factor for PRAEs in children with URIs undergoing GA. These patients have more than a fivefold increased risk of PRAEs compared to those with lower ASA status, likely due to more severe underlying disease and reduced physiological reserve.⁷ Undergoing airway-related procedures further increases the risk of PRAEs by about sixfold compared to non-airway surgeries, mainly because airway manipulation stimulates airway reflexes and increases reactivity, particularly in children with URIs.^{7,13}

The COLDS score is a preanesthetic risk assessment tool commonly used to predict the likelihood of PRAEs in pediatric patients with URIs.¹¹ Previous research identified a COLDS score > 10 as a risk factor for PRAEs in pediatric URI patients.³ However, in our study, the median COLDS score was 12; 90% of patients scored above 10, and all patients with PRAEs exceeded this threshold. Univariable logistic regression showed that a COLDS score > 10 was not significantly associated with PRAEs ($p = 0.604$), possibly due to the low incidence of PRAEs in our cohort. Notably, prior studies have reported a higher cutoff value of 12.5 for the COLDS score when predicting PRAEs.¹² The COLDS score helps assess PRAE risk, but no specific cancellation threshold is established.³ It should guide risk assessment and interventions, with surgery cancellation considered when the COLDS score is high (especially ≥ 10) alongside other clinical factors.³

Perioperative management to prevent PRAEs in pediatric patients can be structured into three parts.^{1,2} Preoperative care focuses on risk assessment, joint decision-

making about surgery timing, experienced teams for high-risk cases, and individualized premedication—favoring alpha-2 agonists, beta-2 agonists for recent URI or bronchospasm risk, and corticosteroids when urgent surgery is needed in severe bronchial hyperreactivity.¹ In the intraoperative phase, propofol is preferred for induction and maintenance; lidocaine or dexmedetomidine may be used adjunctively. Minimize and monitor neuromuscular blockers. Prefer facemask or SGA over ETT. Use sevoflurane or propofol, not desflurane, for maintenance. Apply lung-protective ventilation, opioid-sparing strategies, remove airway devices under deep anesthesia if safe, and consider lateral positioning.¹ In the postoperative phase, continuous respiratory monitoring, staff training, and standardized handover to ensure early detection and response to complications.¹

In our pediatric URI cases, elective surgery for severe URIs is postponed until at least two weeks after symptoms resolve and re-evaluation, per hospital policy.¹⁻³ However, surgery for children with mild to moderate URIs may proceed provided that the procedure's nature and duration are appropriate for the patient's condition, suitable airway equipment is used, and it is performed by an experienced anesthesiologist in a proper institutional setting with full parental cooperation.^{1,2} High-risk patients with recent URI receive nebulized beta-2 agonists preoperatively and are managed in consultation with an expert anesthesiologist. Intraoperatively, propofol is preferred for induction when IV access is available, and sevoflurane is favored over desflurane for maintenance. SGA devices or facemasks are used instead of ETTs whenever possible to reduce airway complications. Deep extubation with an SGA is performed when it is safe. Lung-protective strategies and multimodal analgesia, including regional techniques, are employed for optimal perioperative care. In the postoperative phase, we closely monitor pediatric patients and reserve a bed in the pediatric intensive care unit (PICU) for high-risk cases to ensure early detection and management of complications.

Although this study was carefully designed and evaluated the COLDS score as a preanesthetic risk assessment tool for PRAEs, several limitations should be acknowledged. Ethical requirements necessitated a retrospective cohort design, which may have introduced confounding factors and reliance on potentially incomplete medical records. The single-center setting limits generalizability. The low incidence of PRAEs reduced statistical power, increasing the risk of type II error in both univariable and multivariable analyses. Larger studies are needed to clarify these findings.

Future research should employ a prospective,

multicenter design to more accurately assess the incidence and risk factors for PRAEs in pediatric patients with URIs and minimize bias. Establishing a standardized definition of PRAEs and URI severity is recommended to improve consistency across studies.

CONCLUSIONS

The incidence of PRAEs among pediatric patients with URIs undergoing surgery under GA was 3.9%. ASA classification III and minor airway surgery were factors associated with PRAEs. Preoperative management should carefully assess pediatric patients with URIs and implement strategies to prevent PRAEs.

Data Availability Statement

The datasets generated during and/or analyzed during the current study are available from the corresponding author on reasonable request.

ACKNOWLEDGMENT

We appreciate the support of Kaewjai Thepsuthammarat from the Clinical Epidemiology Unit for biostatistical assistance.

DECLARATIONS

Grants and Funding Information

None.

Conflict of Interest

No potential conflict of interest relevant to this article was reported.

Registration Number of Clinical Trial

This study was registered with the Thai Clinical Trials Registry (TCTR20250109001) on January 9, 2025.

Author Contributions

Conceptualization and methodology, S.B., D.S., C.K., P.W. and P.R.; Investigation, S.B., D.S. and C.K.; Formal analysis: S.B., D.S. and C.K.; Data Curation, S.B., D.S., P.W. and P.R.; Visualization and writing - original draft, S.B., D.S. and C.K.; Writing - review & editing, S.B., D.S. and C.K.; Supervision, D.S. and C.K. All authors have read and agreed to the final version of the manuscript.

Use of Artificial Intelligence

The generative AI tool Perplexity (version sonar-pro) was used solely for grammar and language editing. Professional language editors at the Language Institute of Khon Kaen University also reviewed the final manuscript.

No AI tools were used for data analysis, content generation, or interpretation. The authors remain fully responsible for the study's accuracy and scientific content.

IRB number

This study was approved by the Human Research Ethics Committee of Khon Kaen University in Thailand (HE671456). During this research project, the authors followed the applicable EQUATOR Network (STROBE) guidelines.

REFERENCES

1. Stepanovic B, Regli A, Becke-Jakob K, von Ungern-Sternberg BS. Preoperative preparation of children with upper respiratory tract infection: a focussed narrative review. *Br J Anaesth*. 2024;133(6):1212-21.
2. Lema GF, Berhe YW, Gebrezgi AH, Getu AA. Evidence-based perioperative management of a child with upper respiratory tract infections (URTIs) undergoing elective surgery; A systematic review. *Int J Surg Open*. 2018;12:17-24.
3. Jarraya A, Kammoun M, Ammar S, Feki W, Kolsi K. Predictors of perioperative respiratory adverse events among children with upper respiratory tract infection undergoing pediatric ambulatory ilioinguinal surgery: a prospective observational research. *World J Pediatr Surg*. 2023;6(2):e000524.
4. Pohplook J, Puwarawuttipanit W, Koositamongkol S, Rongrungruang Y. Factors Influencing Severity and Impact of Symptoms in Patients with Upper Respiratory Tract Infection at Community Hospitals and Health-Promoting Hospitals. *Siriraj Med J*. 2021;73(8):510-7.
5. Regli A, Becke K, von Ungern-Sternberg BS. An update on the perioperative management of children with upper respiratory tract infections. *Curr Opin Anesthesiol*. 2017;30(3):362.
6. Malviya S, Voepel-Lewis T, Siewert M, Pandit UA, Riegger LQ, Tait AR. Risk Factors for Adverse Postoperative Outcomes in Children Presenting for Cardiac Surgery with Upper Respiratory Tract Infections. *Anesthesiology*. 2003;98(3):628-32.
7. Wudineh DM, Berhe YW, Chekol WB, Adane H, Workie MM. Perioperative Respiratory Adverse Events Among Pediatric Surgical Patients in University Hospitals in Northwest Ethiopia; A Prospective Observational Study. *Front Pediatr*. 2022;10:827663.
8. Lee S, Reddington E, Koutsogiannaki S, Hernandez MR, Odegard KC, DiNardo JA, et al. Incidence and Risk Factors for Perioperative Cardiovascular and Respiratory Adverse Events in Pediatric Patients With Congenital Heart Disease Undergoing Noncardiac Procedures. *Anesth Analg*. 2018;127(3):724.
9. Ramgolam A, Hall GL, Zhang G, Hegarty M, von Ungern-Sternberg BS. Inhalational versus Intravenous Induction of Anesthesia in Children with a High Risk of Perioperative Respiratory Adverse Events: A Randomized Controlled Trial. *Anesthesiology*. 2018;128(6):1065-74.
10. von Ungern-Sternberg BS, Boda K, Chambers NA, Rebmann C, Johnson C, Sly PD, et al. Risk assessment for respiratory complications in paediatric anaesthesia: a prospective cohort study. *Lancet Lond Engl*. 2010;376(9743):773-83.
11. Lee BJ, August DA. COLDS: A heuristic preanesthetic risk score for children with upper respiratory tract infection. *Pediatr Anesth*. 2014;24(3):349-50.
12. Kim HS, Kim YS, Lim BG, Lee JH, Song J, Kim H. Risk Assessment of Perioperative Respiratory Adverse Events and Validation of the COLDS Score in Children with Upper Respiratory Tract Infection. *Med Kaunas Lith*. 2022;58(10):1340.
13. Lee HJ, Woo JH, Cho S, Oh HW, Joo H, Baik HJ. Risk Factors for Perioperative Respiratory Adverse Events in Children with Recent Upper Respiratory Tract Infection: A Single-Center-Based Retrospective Study. *Ther Clin Risk Manag*. 2020;16:1227-34.
14. Shenoy U, Chirayath B, Narayanan PV, Francis A, Thomas MK, Rajagopal R. Predictors of Perioperative Respiratory Adverse Events in Children Undergoing Surgery for Oropharyngeal Cleft Deformity: A Prospective Observational Study (PRAE-OPCD Study). *Paediatr Anaesth*. 2025;35(12):1024-8.

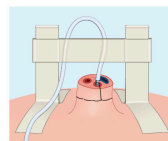
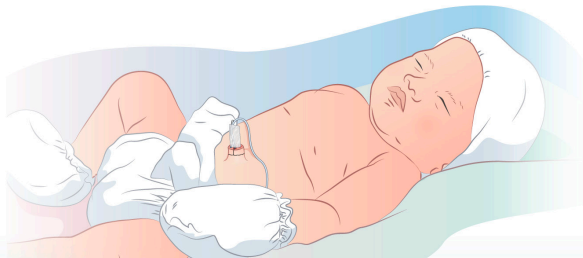
Comparison of Bridging and Contactless Technique for Umbilical Catheter Securement in Preterm Infants: A Pilot Randomized Controlled Trial

Sujitra Terdnueakao, M.D.^{1,2}, Punnanee Wutthigat, M.D.¹, Chanoknan Sriwiset, BNS³, Walaiporn Bowornkitiwong, M.D.^{1,*}

¹Division of Neonatology, Department of Pediatrics, Faculty of Medicine Siriraj Hospital, Mahidol University, Bangkok, Thailand, ²Department of Pediatrics, Samutsakhon Hospital, Samutsakhon, Thailand, ³Department of Pediatrics Nursing, Faculty of Nursing, Mahidol University, Bangkok, Thailand.

Contactless Technique for Umbilical Catheter Securement in Preterm Infants

Contactless technique can be used for umbilical catheter securement.



Conventional method to stabilize umbilical catheter is **bridging technique**. However, there are risks for skin injury.



Contactless technique using Tegaderm to attach catheter to umbilical stump may reduce skin injury. However, data regarding catheter stability are limited.



This pilot RCT was conducted in preterm infants in a tertiary NICU.



Catheter dislodgement rates



skin injuries

were compared between **contactless technique** and **bridging group**.

Conclusion:

There were no significant differences in catheter dislodgement rates and skin injuries between contactless technique and bridging group.

SCAN FOR FULL TEXT



ABSTRACT

Objective: To compare the rate of catheter dislodgement between the bridging technique and contactless technique (CLT) for umbilical catheter securement in preterm infants.

Materials and Methods: This pilot randomized controlled trial enrolled 30 preterm infants who were randomized in a 1:1 ratio into either the bridging or CLT group. The primary outcome was catheter dislodgement. Secondary outcomes included skin injury, procedural duration, and complications such as omphalitis, catheter-related bloodstream infection (CRBSI), and hypothermia.

Results: A total of 15 patients were included in each group. In the CLT group, 25 catheters were placed (12 umbilical arterial catheters (UAC) and 13 umbilical venous catheters (UVC)), while 24 catheters were placed in the bridging group (10 UACs and 14 UVCs). There was no significant difference in catheter dislodgement rates (1 in 25 catheters in the CLT group vs 0 in 24 catheters in the bridging group, $p = 1.00$). There was no CRBSI in either group. Skin injuries were minimal, with one case in the bridging group and none in the CLT group ($p = 1.00$). Repositioning challenges were observed with the CLT after the umbilical stump had dried.

Conclusion: The CLT method demonstrated comparable catheter stability to the bridging technique and may reduce skin injury. It is cost-effective and simple to apply. However, its effectiveness in extremely preterm infants requires further investigation.

Keywords: Umbilical catheterization; securement; preterm infants; skin injury (Siriraj Med J 2026;78(1):51-58)

INTRODUCTION

Umbilical catheterization is a common and essential procedure in neonatal intensive care units (NICUs), particularly for managing critically ill or preterm neonates who require reliable vascular access for fluid resuscitation, medications, and blood sampling.¹ Various securement techniques have been described, with significant variability in clinical practice depending on institutional preferences, staff experience, and patient characteristics.²⁻⁶ One widely used method is the bridging technique, in which adhesive tape is applied to the catheter and affixed to the infant's skin to create a stabilizing bridge. However, this approach has the potential for skin injury due to the adhesive tape especially in very preterm infants.^{4,7} Skin injuries, including erythema, epidermal stripping, and medical adhesive-related skin injury, are particularly common in infants less than 32 weeks' gestation and can result in discomfort, infection risk, and delayed healing.^{7,8} An alternative approach is the anchoring technique, described by South and Magnay³, which avoids direct adhesive contact with the infant's skin. In this method, a purse-string suture is placed around the umbilical stump, and the suture tail is passed through zinc oxide tape wrapping around the catheter and tied securely. This technique has shown favorable outcomes, including the absence of skin injuries and only a few instances of catheter dislodgement, highlighting its potential advantages in minimizing adhesive-related complications.^{2,5} A recent study by D'Andrea et al. found that adding cyanoacrylate glue to suturing reduced catheter dislodgement within

48 hours (1.5% vs. 23.1%, $p < 0.01$), although this benefit diminished thereafter.⁹ However, cyanoacrylate glue may not be available in all centers and can increase procedural costs.

Despite the variety of securement strategies described in the literature, our unit developed a contactless technique (CLT) by modifying the anchoring technique: the umbilical catheter is sutured at the base of the stump and secured onto a transparent dressing (Tegaderm™) rather than directly to the skin. This method avoids adhesive contact and may reduce the risk of skin injury, particularly in very preterm infants with fragile skin. To evaluate this technique, we conducted a pilot randomized controlled trial comparing it with the conventional bridging method. The primary objective was to assess catheter dislodgement rates. Secondary objectives included the incidence of skin injury, procedural duration, and complications following the procedure.

MATERIALS AND METHODS

Study design and population

This study was a single-center, pilot randomized controlled trial conducted in the NICU at Siriraj Hospital, Mahidol University, between 27 May 2024 and 29 Dec 2024. Eligible participants were infants born at a gestational age of less than 37 weeks who required umbilical catheterization for clinical indications, with an anticipated catheter dwell time of at least 24 hours. Infants were excluded if catheter placement was unsuccessful. Enrolled infants were withdrawn if catheter malposition was identified,

if the catheter was not used, or if it was removed within 24 hours of placement. After enrollment, infants were randomized in a 1:1 ratio using a computer-generated randomization sequence with variable block sizes of 2 and 4. Allocation was concealed using sequentially numbered, opaque sealed envelopes. The study was approved by the Siriraj Institutional Review Board (Si 300/2024, 12 Apr 2024) and registered with the Thai Clinical Trials Registry (TCTR no. 20240522005, 22 May 2024).

Study procedure

Prior to patient enrollment, neonatal fellows practiced CLT using mannequins for one month to ensure procedural consistency. Umbilical catheterization was performed by a pediatric resident or neonatal fellow under the supervision of a neonatal fellow or attending neonatologist. Catheter size was selected based on the infant's birth weight. Infants weighing less than 1,500 grams received a 3.5 Fr catheter for arterial and venous access. Infants weighing 1,500 grams and above received a 3.5 Fr catheter for arterial access and 5 Fr catheter for venous access. The insertion

depth was calculated using Shukla's birth weight-based formula for each catheter type.¹⁰ Following successful catheter placement, the securement method was assigned by opening a sequentially numbered, sealed opaque envelope. For all infants, initial catheter stabilization was achieved using a 3-0 silk suture tied around the catheter at the base of the umbilical stump with two to three knots to ensure secure anchoring. This step was performed consistently prior to applying the assigned securement technique. In the CLT group (Fig 1), a Tegaderm™ was used to affix the anchoring suture knot and the suture tail to the catheter. An additional suture was passed through the Wharton's jelly of the umbilical stump and tied to the dressing, providing added stability without the use of adhesive tape on the skin. In bridging technique group (Fig 2), the catheter was first stabilized with Micropore™ tape. A transparent film dressing (Tegaderm™) was placed over the infant's abdominal skin prior to final taping, so that the Micropore™ tape did not make direct contact with the skin. This was intended to reduce the risk of skin injury during tape removal.

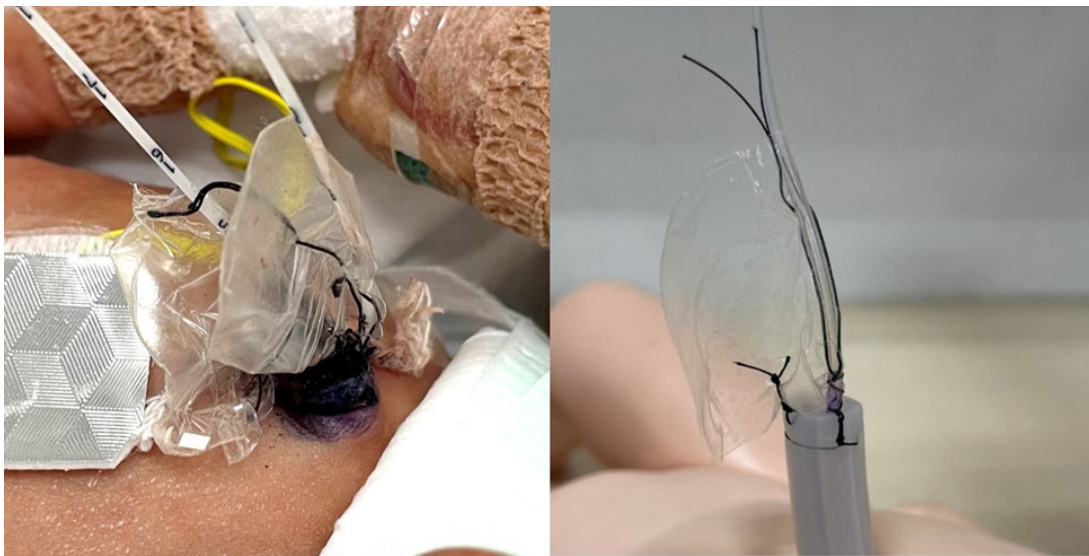


Fig 1. Contactless technique for umbilical catheter securement in a real patient (left panel) and a model (right panel).



Fig 2. Bridging technique for umbilical catheter securement.

Radiographic imaging was performed immediately after catheter securement to confirm tip position and was repeated as necessary to ensure continuously proper placement. The proper position of umbilical venous catheter (UVC) was defined as the tip located at the level of the T9-T10 vertebrae on chest X-ray¹¹, while the optimal position for the umbilical arterial catheter (UAC) was between T6-T10 vertebrae.¹² If malposition was detected, the catheter was repositioned accordingly.

Outcome measurements

Baseline characteristics of the enrolled infants were recorded at the time of enrollment. The primary outcome was the rate of catheter dislodgement, defined as displacement of the catheter by more than 0.5 cm from its originally secured position at the umbilical stump. This was assessed through daily visual inspection and documentation by bedside nurses. Secondary outcomes included total procedural duration, incidence of skin injury, omphalitis, catheter-related bloodstream infection (CRBSI), and changes in the infant's body temperature before and after the procedure. Skin injuries were classified based on criteria adapted from McNichol *et al.*¹³, which describe various levels of skin damage associated with adhesive use and tape removal. These included:

- Erythematous skin: redness without skin break, attributed to trauma from tape, adhesive removal, pressure, or contact dermatitis.
- Skin tear: separation of skin layers, categorized into:
 - *Grade 1*: partial-thickness tear with full flap closure (edges can be fully approximated),
 - *Grade 2*: partial-thickness tear with incomplete flap closure (edges cannot be fully approximated),
 - *Grade 3*: full-thickness skin loss with absent skin flap and open wound.

Statistical analysis

Data were analyzed using IBM SPSS Statistics version 22 (IBM Corp., Armonk, NY, USA). Continuous variables were summarized as mean \pm standard deviation (SD) for normally distributed data, or as median and interquartile range (IQR) for non-normally distributed data. Categorical variables were presented as frequencies and percentages. Between-group comparisons of outcomes that are continuous variables were performed using the student's *t*-test as they are normally distributed. Categorical variables, including rates of catheter dislodgement, skin injury and infection, were compared using the chi-square test or Fisher's exact test, as appropriate. A *p*-value $<$ 0.05 was considered statistically significant. As this was

a pilot study, the sample size was pragmatically set at 30 subjects without a formal power calculation.

RESULTS

A total of 68 preterm infants were assessed for eligibility. Thirty-eight patients were excluded, mostly because parents were not present to give informed consent. Thirty infants were enrolled in the study (Fig 3). Fifteen infants were allocated to the CLT group with 13 UVCs and 12 UACs placed, while the remaining 15 were assigned to the bridging group, with 14 UVCs and 10 UACs placed. Baseline demographic data are presented in Table 1. The mean gestational age was 30.2 ± 2.9 weeks in the CLT group and 30.9 ± 3.2 weeks in the bridging group ($p = 0.52$). Mean birth weight was $1,323 \pm 428$ g and $1,416 \pm 580$ g in the CLT and bridging groups, respectively ($p = 0.58$). Operator experience also did not differ between groups ($p = 0.22$). Forty-nine umbilical catheters were placed: 25 in the CLT group (13 UVCs and 12 UACs) and 24 in the bridging group (14 UVCs and 10 UACs), as shown in Table 2. The average duration of catheter placement ranged from 4.7 to 5.6 days across catheter types and groups.

One case of catheter dislodgement occurred in the CLT group (1 of 25 catheters, 4.0%), while no dislodgements occurred in the bridging group (0 of 24 catheters). This difference was not statistically significant ($p = 1.00$). The dislodged catheter was a UVC that migrated into the right atrium on day 3 due to umbilical stump shrinkage. Although the catheter appeared externally secure, internal displacement required repositioning. Due to umbilical stump dryness, re-suturing was not feasible, and the catheter was re-affixed to the prior suture tail using Tegaderm™. An additional suture through the Wharton's jelly (as described in materials and methods section) could not be placed due to umbilical stump dryness. The UVC was later dislodged during patient transfer.

Detailed procedural times and complications are shown in Table 3. The CLT group had longer mean suture time than the bridging group (10.9 ± 5.0 min vs 7.7 ± 4.2 min, $p = 0.08$), but a shorter total procedure time (28.5 ± 13.8 min vs 38.5 ± 14.5 min, $p = 0.06$), though these differences were not statistically significant. Bridging-specific taping added an average of 4.9 ± 1.9 minutes to the procedure. One infant (6.7%) in the bridging group developed a mild skin injury—localized erythema at the catheter site—while no skin injuries occurred in the CLT group ($p = 1.00$). The skin injury resolved spontaneously without intervention. All infants in the CLT group maintained normothermia (36.5 – 37.5°C) throughout the procedure. In the bridging group, one

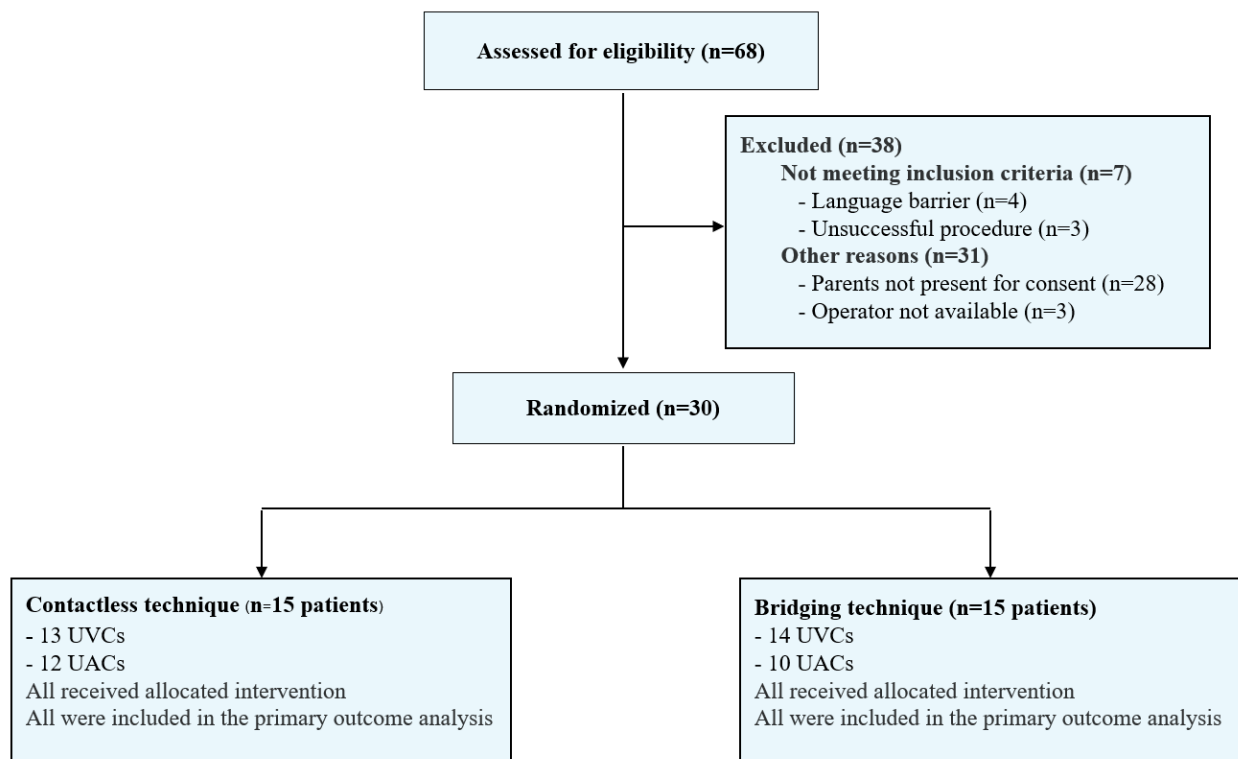


Fig 3. Study flow diagram.

TABLE 1. Demographic data and patient characteristics.

Demographic data and patient characteristics	CLT (n=15)	Bridging (n=15)	p-value
Gestational age (weeks)	30.2 ± 2.9	30.9 ± 3.2	0.52
Birth weight (grams)	1,323 ± 428	1,416 ± 580	0.58
Length (cm)	39.0 ± 4.0	39.1 ± 5.5	0.96
Male sex	7 (46.7)	4 (26.7)	0.45
Apgar score			
1-minute – median (IQR)	5 (2, 8)	7 (4, 8)	0.84
5-minute – median (IQR)	7 (6, 9)	9 (7, 9)	0.39
Operator			0.22
1 st year fellow	9 (60)	13 (86.7)	
2 nd year fellow	6 (40)	2 (13.3)	
Number of catheters			1
1 (UAC or UVC)	4 (26.7)	4 (26.7)	
2 (both UAC and UVC)	11 (73.3)	11 (73.3)	

Data are presented as mean ± standard deviation or number (%).

Abbreviations: CLT, contactless technique; UAC, umbilical arterial catheter; UVC, umbilical venous catheter

TABLE 2. Details of catheter placement.

Catheter placement data	Contactless (n=15)		Bridging (n=15)	
	UVC	UAC	UVC	UAC
Numbers and types of catheters in each group	13	12	14	10
Catheter duration (days)	4.8 ± 2.1	4.7 ± 2.0	5.6 ± 1.9	4.7 ± 2.0

Data are presented as mean ± standard deviation.

Abbreviations: UAC, umbilical arterial catheter; UVC, umbilical venous catheter

TABLE 3. Procedure time and complications.

Procedure time and other secondary outcomes	Contactless (n=15)	Bridging (n=15)	Mean Difference [95%CI]	p-value
Suture time (min)	10.9 ± 5.0	7.7 ± 4.2	3.1 [-0.3, 6.6]	0.08
Bridging time (min)	-	4.9 ± 1.9	-	-
Total securing time (min)	10.9 ± 5.0	12.7 ± 5.6	-1.8 [-5.8, 2.2]	0.36
Total procedure time (min)	28.5 ± 13.8	38.5 ± 14.5	-9.9 [-20.5, 0.6]	0.06
T before procedure				0.48
< 36.5 °C	0 (0)	0 (0)		
36.5 - 37.5 °C	15 (100)	13 (86.7)		
> 37.5 °C	0 (0)	2 (13.3)		
T after procedure				0.48
< 36.5 °C	0 (0)	1 (6.7)		
36.5 - 37.5 °C	15 (100)	13 (86.7)		
> 37.5 °C	0 (0)	1 (6.7)		
T change (°C)	-0.1 ± 0.3	0 ± 0.3	-0.1 [-0.4, 0.1]	0.17
Skin injury	0 (0)	1 (6.7)		1.00
Omphalitis	0 (0)	0 (0)		-
CRBSI	0 (0)	0 (0)		-

Data are presented as mean ± standard deviation or number (%).

Abbreviations: CI, confidence interval; CRBSI, catheter-related bloodstream infection; T, temperature

infant experienced mild hypothermia (temperature drop from 36.5°C to 36.0°C) and one developed low-grade hyperthermia (>37.5°C). Mean temperature change was $-0.1 \pm 0.3^\circ\text{C}$ in the CLT group versus $0 \pm 0.3^\circ\text{C}$ in the bridging group ($p = 0.17$). No omphalitis or catheter-related bloodstream infection (CRBSI) occurred in either group.

DISCUSSION

This pilot randomized controlled trial evaluated a contactless technique for umbilical catheter securement against the conventional bridging method in preterm infants. Both approaches demonstrate comparable safety and efficacy with respect to catheter dislodgement, skin complications and procedural duration. In our cohort, only one catheter dislodgement occurred in the CLT group, compared to none in the bridging group; a difference that was not statistically significant. Compared to emerging securement techniques, such as cyanoacrylate glue, the CLT offers a favorable profile. D'Andrea *et al.* reported a 7.7% dislodgement rate using glue combined with sutures, with greater benefit during the first 48 hours of catheter use.⁹ Similarly, the LifeBubble umbilical catheter securement device demonstrated superior performance in reducing catheter migration and malposition¹⁴, but required a specialized device and may not be cost-effective for widespread use, especially in resource-limited settings. Another advantage of the CLT is procedural simplicity and low cost. The method uses materials commonly available in neonatal units, with a total securing time comparable to the bridging technique (10.9 ± 5.0 vs 12.7 ± 5.6 minutes; $p = 0.36$).

In adults, prolonged use of strong adhesive tape is associated with skin complications such as increased rates of phlebitis.¹⁵ This highlights the potential risks that the adhesive tape pose, which are even more concerning in preterm infants whose fragile skin, is highly susceptible to medical adhesive-related skin injury.⁷ In our study, no skin injury was observed in the CLT group, supporting its potential as a securement method that is safe for the skin.

An important caution of the CLT method is the difficulty in readjusting catheter position and resecuring the catheter after several days, because the umbilical stump has shrunk and dried. This precludes re-suturing through the umbilical stump. As described above in the patient who had catheter dislodgement, we recommend against performing the CLT method on the dried umbilical stump as it probably increases the risk of catheter dislodgement. In this situation, bridging technique should be performed instead. Additionally, to avoid the need for catheter

repositioning, verifying catheter tip position in real time (such as with ultrasound) before securement may be beneficial, as ultrasound has been shown to improve placement accuracy in infants.^{16,17}

There are some limitations in this study. Small sample size may limit the ability to detect differences in outcomes (both umbilical catheter securement and CRBSI). The single-center design may limit generalizability, and the short follow-up period may not capture late-onset complications or long-term securement effectiveness.

CONCLUSION

The CLT demonstrated comparable catheter stability to the bridging technique and posed no risk for skin injury. It is easy to implement and may be especially advantageous for extremely preterm infants vulnerable to skin injury. Further larger studies with longer follow-up and additional survival analysis are warranted to confirm these findings.

Data Availability Statement

The research data in this study are available from the corresponding author upon reasonable request.

ACKNOWLEDGEMENTS

The authors thank neonatal fellows for patient recruitment and procedure performance, and NICU nurses for their support in data recording. We thank Assoc. Prof. Buranee Yangthara for her help with statistical analysis. We thank Ms. Juthatip Suwannatrai for the support in patient coordination and data collection.

DECLARATIONS

Grants and Funding Information

This study received no funding from any source.

Conflict of Interest

All authors declare that they have no conflict of interest.

Registration Number of Clinical Trial

Thai Clinical Trial Registry, TCTR20240522005

Authors Contributions

Conceptualization, ST, PW and WB; Data curation, ST and WB; Formal analysis, ST, PW and WB; Investigation, ST, CS and WB; Methodology, ST, PW and WB; Project administration, ST and WB; Supervision, WB; Visualization, ST, CS and WB; Writing – original draft, ST; Writing – review & editing, PW, CS and WB. All authors have read and agreed to the final version of the manuscript.

Use of Artificial Intelligence

The authors did not use artificial intelligence in the conduct and writing of this study.

REFERENCES

- Nash P. Umbilical catheters, placement, and complication management. *J Infus Nurs.* 2006;29(6):346-52.
- Elser HE. Options for securing umbilical catheters. *Adv Neonatal Care.* 2013;13(6):426-9.
- South M, Magnay A. Simple method for securing umbilical catheters. *Arch Dis Child.* 1988;63(7 Spec No):750-1.
- Stewart DL, Wilkerson S, Fortunato SJ. New technique for stabilizing umbilical artery catheters in very low birthweight infants. *J Perinatol.* 1989;9(4):458-9.
- Grauaug AA, Tompkins JR. The KEMH method for securing umbilical catheters. *J Paediatr Child Health.* 1992;28(6):436-7.
- Hindley DT, Lewis MA, Robinson MJ. Method for securing umbilical lines. *Arch Dis Child Fetal Neonatal Ed.* 1994;70(1):F79-80.
- de Oliveira Marcatto J, Santos AS, Oliveira AJF, Costa ACL, Regne GRS, da Trindade RE, et al. Medical adhesive-related skin injuries in the neonatology department of a teaching hospital. *Nurs Crit Care.* 2022;27(4):583-8.
- Visscher MO, McKeown K, Nurre M, Strange R, Mahan T, Kinnett M, et al. Skin Care for the Extremely Low-Birthweight Infant. *Neoreviews.* 2023;24(4):e229-e42.
- D'Andrea V, Prontera G, Pinna G, Cota F, Fattore S, Costa S, et al. Securement of Umbilical Venous Catheter Using Cyanoacrylate Glue: A Randomized Controlled Trial. *J Pediatr.* 2023;260:113517.
- Shukla H, Ferrara A. Rapid estimation of insertional length of umbilical catheters in newborns. *Am J Dis Child.* 1986;140(8):786-8.
- Akar S, Dincer E, Topcuoğlu S, Yavuz T, Akay H, Gokmen T, et al. Determination of Accurate Position of Umbilical Venous Catheters in Premature Infants. *Am J Perinatol.* 2022;39(4):369-72.
- Lean WL, Dawson JA, Davis PG, Theda C, Thio M. Accuracy of 11 formulae to guide umbilical arterial catheter tip placement in newborn infants. *Arch Dis Child Fetal Neonatal Ed.* 2018;103(4):F364-f9.
- McNichol L, Lund C, Rosen T, Gray M. Medical adhesives and patient safety: state of the science: consensus statements for the assessment, prevention, and treatment of adhesive-related skin injuries. *Orthop Nurs.* 2013;32(5):267-81.
- Perl JR, Crabtree-Beach T, Olyaei A, Hedges M, Jordan BK, Scottoline B. Reducing umbilical catheter migration rates by using a novel securement device. *J Perinatol.* 2024;44(9):1359-64.
- Thangkratok P, Pongpirul K, Sriratanaban J. Transpore Tape and Transparent Film Dressing on the Incidence of Early-Stage Phlebitis: A Comparative Randomized Trial. *Siriraj Medical Journal.* 2025;77(6):411-8.
- Mohamed A, Mohsen N, Solis-Garcia G, Nasef N, Shah P. Comparing Malposition and Complications Associated with Ultrasound-Guided versus Radiography-Guided Central Catheter Tip-Position in Neonates: A Systematic Review and Meta-Analysis. *Neonatology.* 2025:1-11.
- D'Andrea V, Prontera G, Rubortone SA, Pezza L, Pinna G, Barone G, et al. Umbilical Venous Catheter Update: A Narrative Review Including Ultrasound and Training. *Front Pediatr.* 2021;9:774705.

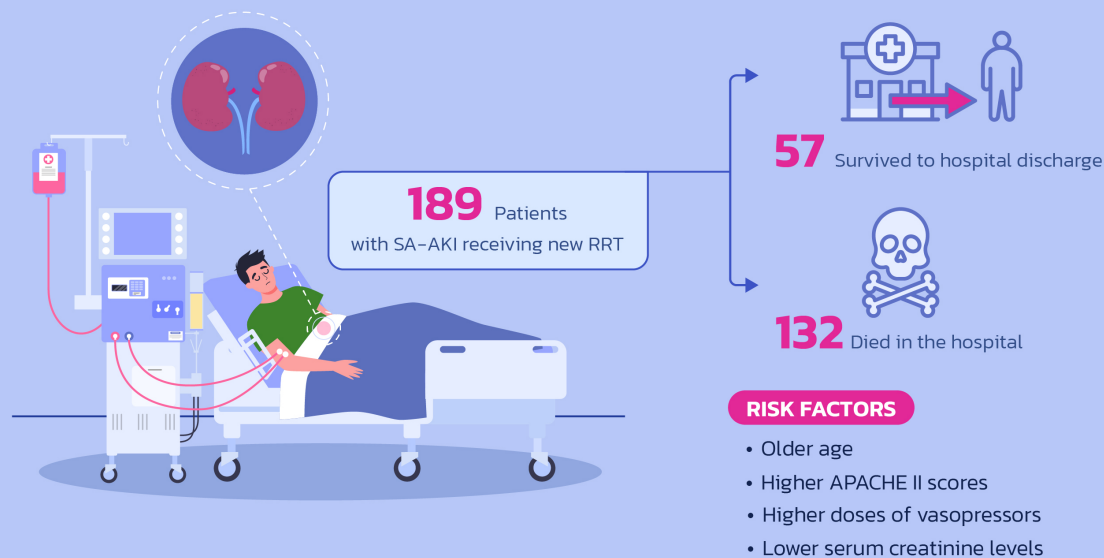
Hospital Mortality and Predicting Factors in Patients with Sepsis-associated Acute Kidney Injury Requiring Renal Replacement Therapy

Chairat Permpikul¹, Nattapat Wongtirawit^{1*}, Surat Tongyoo¹, Methawoot Khemmongkon¹, M.D.², Thummaporn Naorungroj¹, M.D.¹

¹Division of Critical Care, Department of Internal Medicine, Faculty of Medicine Siriraj Hospital, Mahidol University, Bangkok, Thailand, ²Division of Nephrology, Department of Internal Medicine, Faculty of Medicine Siriraj Hospital, Mahidol University, Bangkok, Thailand.

Outcome and Predictors of Hospital Death in Patients with Sepsis-associated AKI receiving RRT

- ▶ Hospital death was common in patients with sepsis-associated AKI (SA-AKI) receiving RRT.
- ▶ Multiple risk factors, mostly related to illness severity, were associated with higher hospital mortality



SIRIRAJ
MEDICAL
JOURNAL

Permpikul, et al. *Siriraj Med J* 2026;78(1):59-67.

©Siriraj Medical Journal. All rights reserved. Graphical abstract by T Vorwatanakul.



*Corresponding author: Nattapat Wongtirawit

E-mail: n.wongtirawit@gmail.com

Received 2 June 2025 Revised 4 August 2025 Accepted 5 August 2025

ORCID ID: <http://orcid.org/0000-0003-2502-2217>

<https://doi.org/10.33192/smj.v78i1.275788>



All material is licensed under terms of the Creative Commons Attribution 4.0 International (CC-BY-NC-ND 4.0) license unless otherwise stated.

ABSTRACT

Objective: To investigate the clinical predictors for hospital mortality in patients with sepsis-associated acute kidney injury who required renal replacement therapy.

Materials and Methods: A retrospective cohort study enrolling adult patients hospitalized in medical wards at Siriraj Hospital between 2018-2021, who were concurrently diagnosed with sepsis and acute kidney injury. Patients who previously received long-term renal replacement therapy were excluded. We compared clinical characteristics and treatment strategies, then analyzed the predictors of mortality according to hospital mortality.

Results: Among 189 patients with acute kidney injury requiring renal replacement therapy, 132 (69.8%) died during hospitalization. A receiver operating characteristic curve analysis for predictors of hospital mortality revealed cutoff values for age > 60 years, SOFA score > 10, APACHE II score > 20, total colloid in 72 hr > 1,500 mL, maximum vasopressor > 0.3 mcg/kg/min, white blood cell count < 12 cells/ μ L, serum creatinine < 4 mg/dL, and serum albumin < 2.5 g/dL. Multivariate analysis identified age > 60 (OR 2.8, 1.27-6.38), APACHE II score > 20 (OR 2.57, 1.23-5.42), and maximum vasopressor dose > 0.3 μ g/kg/min (OR 4.26, 1.94-9.86) as independent mortality predictors, while creatinine > 4 mg/dL was protective (OR 0.36, 0.17-0.75).

Conclusion: Patients with sepsis-associated acute kidney injury who underwent renal replacement therapy had high hospital mortality. Age > 60 years, APACHE II score > 20, maximum vasopressor dose > 0.3 mcg/kg/min, and serum creatinine \leq 4 mg/dL were predictors for hospital mortality.

Keywords: Acute kidney injury; sepsis; septic shock; renal replacement therapy; mortality (Siriraj Med J 2026;78(1): 59-67)

INTRODUCTION

Sepsis and septic shock are among the most common causes of admission to intensive care units worldwide.¹⁻⁵ They are associated with multiple organ dysfunction, including the kidney, resulting in acute kidney injury (AKI). The complication develops in up to 50% of patients with sepsis⁶⁻⁹, leading to worse outcomes like longer ICU stay and higher short-term mortality.^{1,6,7,10} In clinical practice, sepsis-associated AKI (SA-AKI) is defined as AKI in the presence of sepsis without other significant contributing factors explaining AKI.¹¹

Although most cases of SA-AKI could be conservatively managed with medications while allowing time for renal recovery, initiation of renal replacement therapy (RRT) was warranted in 45-72% of these patients.^{5,6,12} Few clinical studies have focused on the presentation, patient profile, and outcome of SA-AKI^{5,12,13}, particularly those undergoing RRT. A prospective cohort study of sepsis and septic shock patients who developed AKI across intensive care units (ICU) in European countries reported an overall mortality rate of 41%.¹⁴ Whereas for the subgroup of patients who received RRT, the mortality was reported to be as high as 69%.¹² Because of the scarcity of data, clinical predictors for death in patients with SA-AKI who required RRT are not fully elucidated.

To address this knowledge gap, the aim of this study was twofold. The primary objective was to determine the prognoses of the subgroup of patients with sepsis-associated

acute kidney injury who received renal replacement therapy in terms of hospital death. The secondary objective was to determine clinical and biochemical predictors for hospital mortality in this subgroup of patients.

MATERIALS AND METHODS

Design and setting

This was a single-center, retrospective observational cohort study. It was conducted at the Faculty of Medicine Siriraj Hospital, Mahidol University – a tertiary referral center in Thailand, consisting of 10 general medical units. Anonymized charts of patients admitted in these wards from January 1st, 2018 to December 31st, 2021 were reviewed for retrieval of the data.

The study protocol was approved by the Institutional Review Board of Siriraj Hospital (approval number COA no. Si 119/2022). The IRB allowed the study to waive the requirement to obtain informed consent. This study received no external funding.

Participants

The following inclusion criteria were used to identify eligible patients.

1. Adult patients 18 years or older
2. Patients were diagnosed with either sepsis or septic shock according to either the 2012 Surviving Sepsis Campaign guidelines¹⁵
3. Patients were diagnosed with acute kidney injury

according to the Kidney Disease Improving Global Outcomes 2012 guideline, using serum creatinine and urine output criteria¹⁶

4. Patients were treated with renal replacement therapy

Patients who satisfied the following exclusion criteria were excluded from the study.

1. Patients who had do-not-resuscitate orders
2. Patients who received surgical intervention in this hospital visit prior to ICU admission
3. Patients who were pregnant
4. Patients with end-stage malignancy
5. Patients with renal diseases who were previously receiving RRT
6. Patients with the following concurrent illnesses: acute stroke, acute coronary syndrome, acute pulmonary edema, status asthmaticus, active gastrointestinal bleeding, status epilepticus, severe trauma, fatal drug overdose

All participants were resuscitated according to current international guidelines for septic shock¹⁵, which included fluid resuscitation, vasopressor therapy, antimicrobial therapy, appropriate source control, and organ support.

The decisions to initiate RRT in each patient were made by consulting nephrologists together with attending intensivists. Standard indications for RRT initiation included uremic symptoms, fluid overload, metabolic acidosis, and other electrolyte abnormalities. The initial modes of RRT utilized were also up to the discretion of the nephrologists. Either intermittent hemodialysis, sustained low-efficiency dialysis, or continuous renal replacement therapy was used.

Data collection

We performed an electronic medical records review from which we collected and recorded patient baseline characteristics at the time of AKI diagnosis: age, sex, underlying conditions, severity score, vital signs, body mass index, site of infection, and laboratory investigations. Treatment data were also recorded, specifically to the amount of fluid resuscitation in the following three days after the diagnosis, as well as vasopressor type and dosage, organ support requirements, modes of RRT, indications of RRT, and treatment outcomes of the index hospitalization. The primary outcome of this study was hospital mortality.

Statistical analysis

Participants were classified as survivors and non-survivors, according to their status upon hospital discharge. Baseline characteristics at the time of enrollment – i.e., at the time of initiation of renal replacement therapy – were compared between the two groups.

Baseline characteristics were reported as percentages, means and standard deviations, and median and interquartile ranges as appropriate. Comparisons of these parameters between survivors and non-survivors were performed using independent t-tests, Mann-Whitney U-tests, or chi-square tests where appropriate.

Receiver operating characteristic (ROC) curve analyses were performed to identify cutoff values for continuous variables that differed significantly between survivors and non-survivors. Each optimal cutoff value, along with its sensitivity and specificity, was determined using Youden's index. The largest area under the ROC curve (AUROC) was used to identify variables best predicting hospital mortality. Variables were reclassified into two groups using the ROC curve-identified cutoff values. A comparative analysis was performed between each group using univariate analyses. Risk is expressed as an unadjusted OR with a 95% CI. Factors with *p-value* ≤ 0.1 and other factors of interest were included in multivariate analyses. The results of the multivariate analysis with stepwise forward variable selection are shown as adjusted OR with the 95% CI and *p-value*. Independent predictive factors associated with hospital mortality are those with a *p-value* ≤ 0.05.

All statistical analyses were performed using SPSS ver. 18 (SPSS Inc., Chicago, IL, USA).

RESULTS

A total of 356 sepsis and septic shock patients were screened. 167 patients were excluded, resulting in a total of 189 patients enrolled (Fig 1). Among these, 57 patients (30.16%) survived to hospital discharge, and 132 patients (69.84%) died in hospital. In the survivor group: 35 patients were discharged with RRT-free status, and 22 patients needed RRT after discharge.

The patients' baseline characteristics are shown in Table 1. Compared to survivors, non-survivors had significantly higher SOFA and APACHE II scores, but lower white blood cell count, serum creatinine, and serum albumin.

Concurrent treatments and interventions used are shown in Table 2. Compared to survivors, non-survivors received a higher volume of intravenous colloids in 72 hours, including human albumin solutions, gelatins, and plasmas. They were treated with more vasopressors, especially epinephrine and dopamine. They received more mechanical ventilation, and were more likely treated with continuous renal replacement therapy as their first mode of RRT. These are likely reflective of more severe disease.

To identify the optimal cutoff values for continuous variables predicting hospital mortality, ROC curve analyses

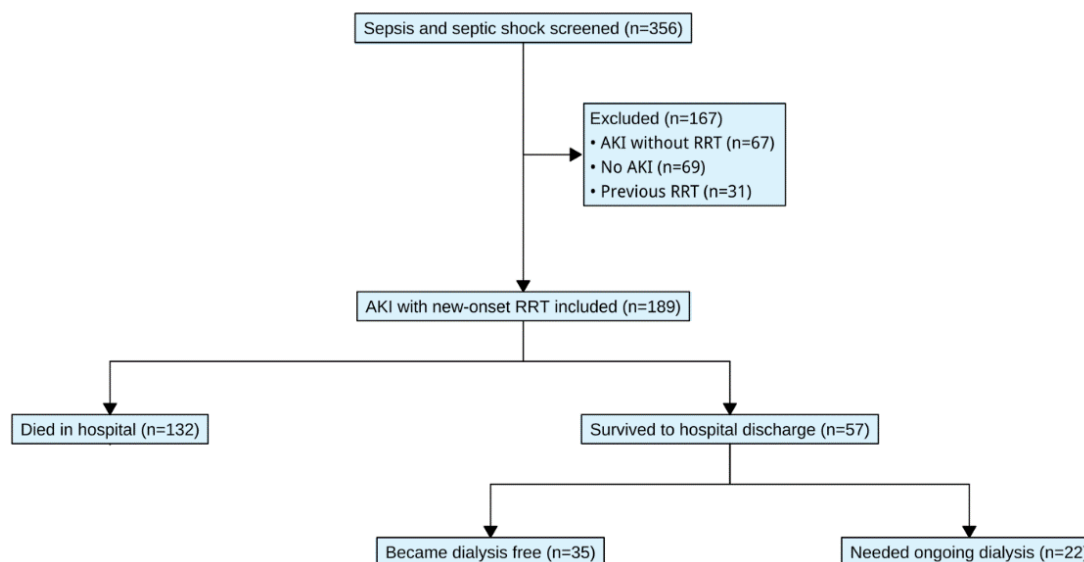


Fig 1. Flow diagram illustrating screening, inclusion, and outcome of patients.

were performed. The ROC curves and corresponding area under the curve are shown in Fig 2 and Table 3, respectively. Optimal cutoff values for each parameter are shown in Table 3, including SOFA score > 10, APACHE II score > 20, total colloid received in 72 hours > 1,500 mL, and maximum vasopressor dose > 0.3 mcg/kg/min were identified to be associated with hospital mortality. Conversely, WBC count > 12 cell/ μ L, serum creatinine > 4 mg/dL, and serum albumin > 2.5 g/dL were shown to be inversely associated with hospital mortality.

Table 4 shows the independent predictive factors for hospital mortality among septic-AKI patients requiring RRT. Variables with significant differences between survivors and non-survivors (identified from baseline characteristics and categorized using optimal AUC cutoffs) were included. Eight parameters were significant in univariate analyses. The multivariate model identified four independent predictors: age > 60 years, APACHE II score > 20, maximum vasopressor dose > 0.3 mcg/kg/min (all higher in non-survivors), and serum creatinine \leq 4 mg/dL (lower levels associated with higher mortality).

DISCUSSION

In this single-center, retrospective observational cohort study, we found that (1) in patients with sepsis-associated acute kidney injury, the need to receive RRT was associated with poor prognoses, with 69.84% hospital mortality rate, and (2) multiple clinical and biochemical factors were associated with higher hospital mortality in these patients, namely age > 60 years, APACHE II score > 20, maximum vasopressor dose > 0.3 mcg/kg/min, and serum creatinine \leq 4 mg/dL.

The impact of sepsis-associated acute kidney injury

on patients' prognoses was previously thought not to be substantial, as these patients usually have concurrent critical illnesses that are more directly linked to mortality, for instance, sepsis and circulatory shock. However, the receipt of renal replacement therapy is more strongly associated with worse outcomes, including mortality. Previous studies reported a mortality rate of 40-75% among patients with sepsis-associated AKI who were treated with RRT.^{6,12} These data were consistent with our cohort, which demonstrated 69.84% hospital mortality.

Various predictors have been reported to be associated with mortality in patients with sepsis-associated AKI receiving RRT. The most consistently reported are markers of severity of illness, such as the APACHE II and SOFA scores.^{6,13} As these tools reflect global organ failure in the patients, including renal function, they are more likely to be predictive of poor outcomes. Our study also concurred with these previous findings.

Similarly, higher vasopressor dose suggests more severe systemic complications. Vasopressor doses higher than that equivalent with 0.25 mcg/kg/min is generally considered as a threshold of severe shock, warranting the use of adjunct treatments¹⁵, while our cohort suggested similar cutoff value of 0.3. This aligned with previous reports showing that, in sepsis and septic shock, extra-renal organ failures are associated with increased mortality in patients who underwent RRT.^{18,19}

One interesting finding from our study was that having serum creatinine less than 4 mg/dL at the time of RRT initiation was associated with higher survival at hospital discharge. This finding could be explained in two ways. First, serum creatinine could also be falsely low, or only minimally elevated, in patients who are also fluid

TABLE 1. Baseline characteristics, compared between patients who survived to hospital discharge and patients who died in hospital.

Patient characteristic	Survivors (57) ¹	Non-survivors (132) ¹	P ²
Age, years	63 (49, 77)	68 (58, 77)	0.143
Sex	25 (44%)	57 (43%)	0.931
Body mass index, kg/m ²	23.6 (20.8, 26.2)	22.8 (20.0, 25.4)	0.293
SOFA score ³	10 (8, 13)	12 (9, 15)	0.005*
APACHE II score ⁴	20 (6)	26 (9)	<0.001*
Underlying conditions			
Hypertension	37 (65%)	84 (64%)	0.867
Diabetes mellitus	29 (51%)	58 (44%)	0.380
Chronic kidney disease	24 (43%)	53 (40%)	0.730
Ischemic heart disease	11 (19%)	20 (15%)	0.480
Cerebrovascular disease	6 (11%)	13 (9.8%)	0.887
Malignancy	4 (7.0%)	17 (13%)	0.239
Cirrhosis	3 (5.3%)	14 (11%)	0.239
Site of infection			
			0.372
Pneumonia	16 (28%)	56 (42%)	
Urinary tract infection	6 (11%)	9 (6.8%)	
Intra-abdominal infection	12 (21%)	25 (19%)	
Skin and soft tissue infection	4 (7.0%)	3 (2.3%)	
Catheter-related infection	4 (7.0%)	6 (4.5%)	
Primary bacteremia	12 (21%)	24 (18%)	
Other	3 (5.3%)	9 (6.8%)	
Vital signs			
Temperature, °C	38.1 (1.4)	37.9 (1.8)	0.315
Heart rate, beats/minute	110 (96, 125)	110 (90, 130)	0.611
Respiratory rate, times/minute	26 (24, 34)	28 (24, 32)	0.528
Mean arterial blood pressure, mmHg	62 (56, 68)	60 (55, 66)	0.274
Central venous pressure, mmHg	13 (10, 18)	12 (9, 17)	0.329
Laboratory investigations			
White blood cell, cells/ μ L	13.2 (10.2, 18.7)	12.2 (3.9, 17.0)	0.042*
Hemoglobin, g/dL	9.4 (7.8, 11.0)	9.0 (7.6, 10.9)	0.308
Platelet, cells/ μ L	133 (69, 235)	123 (45, 196)	0.289
Blood urea nitrogen, mg/dL	45 (32, 58)	42 (28, 71)	0.999
Creatinine, mg/dL	3.92 (2.30, 5.76)	2.86 (1.99, 4.71)	0.038*
Sodium, mmol/L	136 (134, 139)	137 (133, 141)	0.534
Potassium, mmol/L	4.2 (3.7, 4.7)	4.2 (3.7, 4.9)	0.541
Chloride, mmol/L	97 (94, 102)	98 (93, 103)	0.629
Bicarbonate, mmol/L	13 (11, 19)	14 (9, 19)	0.694
Serum lactate, mmol/L	4.4 (2.5, 9.2)	5.2 (2.8, 11.2)	0.333
Albumin, g/dL	2.9 (0.6)	2.6 (0.7)	0.002*
Serum pH	7.34 (7.25, 7.39)	7.30 (7.19, 7.40)	0.314
Partial pressure of carbon dioxide, mmHg	26 (22, 33)	27 (20, 35)	0.754
Partial pressure of oxygen, mmHg	127 (75, 197)	122 (84, 173)	0.786

¹Data are summarized in mean (SD), median (Q1, Q3), or n (%), as appropriate. For variables with missing data, summary data are based on available number

²Wilcoxon rank sum test; Pearson's Chi-squared test; Welch Two Sample t-test; Fisher's exact test

³Sequential Organ Failure Assessment (SOFA) score ranges from 0-24, with higher scores indicates greater organ failure and disease severity

⁴Acute Physiology and Chronic Health Evaluation II (APACHE II) score ranges from 0-71, with higher scores indicate greater organ failure and disease severity

* $p < 0.05$ when compared with survival to hospital discharge

TABLE 2. Detailed treatment strategies, compared between patients who survived to hospital discharge and patients who died in hospital.

Treatment	Survivors (57) ¹	Non-survivors (132) ¹	p ²
Fluid resuscitation			
Crystalloid volume on day 1, mL	2,800 (1,700, 4,400)	3,190 (1,850, 5,260)	0.333
Crystalloid volume on day 2, mL	750 (100, 1,770)	450 (0, 1,920)	0.437
Crystalloid volume on day 3, mL	3,850 (2,500, 7,100)	5,040 (2,150, 8,755)	0.428
Total crystalloid in 72 hours, mL	7,520 (4,400, 12,900)	9,605 (4,300, 15,960)	0.360
Colloid volume on day 1, mL	400 (0, 1,250)	745 (50, 1,500)	0.109
Colloid volume on day 2, mL	0 (0, 346)	0 (0, 992)	0.087
Colloid volume on day 3, mL	0 (0, 250)	0 (0, 632)	0.042*
Total colloid in 72 hours, mL	840 (0, 2,020)	1,534 (548, 3,064)	0.005*
Human albumin solutions use	23 (40%)	82 (62%)	0.006*
Gelofusine use	1 (1.8%)	18 (14%)	0.013*
Packed red cell use	22 (39%)	73 (55%)	0.035*
Fresh frozen plasma use	27 (47%)	66 (50%)	0.740
Vasopressors use			
Norepinephrine	50 (88%)	118 (89%)	0.737
Epinephrine	17 (30%)	87 (66%)	<0.001*
Dobutamine	2 (3.5%)	1 (0.8%)	0.217
Dopamine	5 (8.8%)	2 (1.5%)	0.028*
Maximum vasopressor dose, mcg/kg/min ³	0.12 (0.04, 0.36)	0.51 (0.14, 1.00)	<0.001*
Mechanical ventilator use	49 (86%)	128 (97%)	0.008*
Hydrocortisone use	41 (72%)	115 (87%)	0.012*
Indication for renal replacement therapy			0.255
Metabolic acidosis	30 (53%)	86 (65%)	
Volume overload	18 (32%)	25 (19%)	
Uremia	6 (11%)	12 (9.1%)	
Other	3 (5.3%)	9 (6.8%)	
Initial mode of renal replacement therapy			0.013*
Intermittent hemodialysis	10 (18%)	7 (5.3%)	
Sustained low-efficiency dialysis	9 (16%)	15 (11%)	
Continuous renal replacement therapy	38 (67%)	110 (83%)	

¹Data are summarized in mean (SD), median (Q1, Q3), or n (%), as appropriate. For variables with missing data, summary data are based on available number

²Wilcoxon rank sum test; Pearson's Chi-squared test; Welch Two Sample t-test; Fisher's exact test

³The maximum vasopressor dose was defined as the highest cumulative vasopressor exposure (in mcg/kg/min) within 72 hours after AKI diagnosis, calculated as:

(Norepinephrine + Epinephrine + [Dopamine ÷ 100] + [Dobutamine ÷ 100])

where all doses were converted to norepinephrine-equivalent units.

*p < 0.05 when compared with survival to hospital discharge

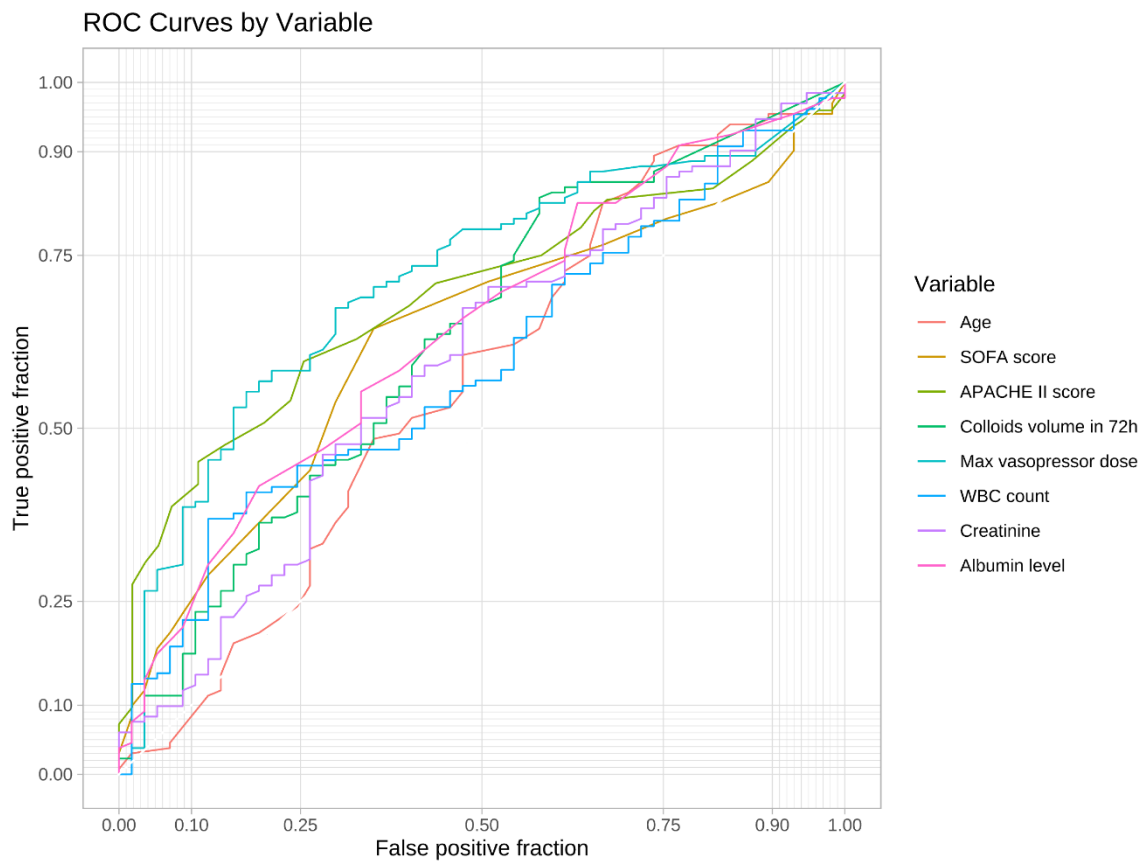


Fig 2. Receiver operating characteristic (ROC) curve analysis to identify the variable cutoff value predicting hospital mortality and table of area under the curve (AUC).

TABLE 3. Receiver operating characteristic (ROC) analysis to identify the cutoff values predicting hospital mortality and table of area under the curve (AUC). The p values are from tests comparing survivors and non-survivors.

Clinical Parameters	AUC (95% CI) ¹	Cutoff	p^2
Age	0.567 (0.474 - 0.661)	60 years	0.215
SOFA	0.628 (0.545 - 0.711)	10	<0.001*
APACHE II	0.69 (0.613 - 0.768)	20	<0.001*
Total colloid in 72 hours	0.63 (0.542 - 0.718)	1,500 mL	0.078
Maximum vasopressor dose	0.714 (0.637 - 0.791)	0.3 mcg/kg/min	<0.001*
White blood cell	0.594 (0.508 - 0.679)	12 cell/ μ L	0.262
Creatinine	0.595 (0.506 - 0.685)	4 mg/dL	0.018*
Albumin	0.641 (0.557 - 0.725)	2.5 g/dL	0.027*

¹Area Under the Receiver Operating Characteristic (ROC) Curve

²Pearson's Chi-squared test

TABLE 4. Univariate analyses and multivariate analyses to identify variables independently associated with hospital mortality in septic-acute kidney injury patients who required renal replacement therapy.

Clinical Parameters	Univariate analysis		Multivariate analysis	
	OR (95% CI)	p	OR (95% CI)	p
Age > 60 years	1.5 (0.78 - 2.86)	0.217	2.8 (1.27 - 6.38)	0.012*
SOFA score > 10	3.35 (1.76 - 6.5)	<0.001*	—	—
APACHE II score > 20	3.16 (1.64 - 6.16)	<0.001*	2.57 (1.23 - 5.42)	0.012*
Total colloid in 72 hours > 1,500 mL	1.77 (0.94 - 3.38)	0.08	—	—
Maximum vasopressor dose > 0.3 mcg/kg/min	4.07 (2.1 - 8.18)	<0.001*	4.26 (1.94 - 9.86)	<0.001*
WBC > 12 cell/ μ L	0.7 (0.37 - 1.31)	0.263	—	—
Creatinine > 4 mg/dL	0.47 (0.25 - 0.88)	0.019*	0.36 (0.17 - 0.75)	0.007*
Albumin > 2.5 g/dL	0.49 (0.25 - 0.92)	0.029*	—	—
Mechanical ventilator use	5.22 (1.57 - 20.31)	0.009*	—	—
Hydrocortisone use	2.64 (1.22 - 5.73)	0.013*	—	—
Continuous renal replacement therapy	1.97 (1.23 - 3.19)	0.005*	—	—

overloaded due to dilutional effect.²² Having markedly positive cumulative fluid balance has been consistently demonstrated to be associated with worse outcomes in the intensive care units.²³ Thus, patients with lower serum creatinine at the time of RRT initiation could have poorer outcomes if the low levels were caused by dilution. Secondly, the use of serum creatinine to determine the glomerular filtration rate generally assumes a steady state.²⁰ In patients with acute kidney injury, measured serum creatinine may not reflect the real-time decline in kidney function²¹; elevation of serum creatinine may lag behind the deterioration up to 48-72 hours. Therefore, lower serum creatinine level at the time of RRT initiation may suggest rapidly worsening kidney function such that the abnormalities in electrolytes and acid-base statuses preceded the elevation of serum creatinine.²⁰ These patients would predictably have worse outcomes than patients with a more gradual progression of AKI.

The strength of our study is that this is a large retrospective cohort study in a specific population, which is sepsis-associated AKI who require RRT. Previous studies in Thailand and other countries all focused on acute kidney injury in critical settings or overall causes of AKI. Therefore, the predictors of mortality in this study are more specific in severe groups in sepsis-associated AKI (need RRT). In addition, we enrolled patients for a long period of time (2018-2020). The data we collected contained various parameters based on real treatment

strategies for sepsis, which were more objective.

The limitations of this study should be mentioned. First, we did not collect and analyze the difference in timing of diagnosis of sepsis, AKI, and initiation of RRT, which could be predictors or confounding factors in mortality. Second, we did not follow long-term outcomes, such as 28-day or 90-day mortality, or incidence of long-term RRT. Future studies are needed to examine these outcomes. Third, the data from this study came from a single center which is a national tertiary referral center. As a result, the findings of this study might not be generalizable to other healthcare settings.

CONCLUSION

Among patients with sepsis, the mortality rate of patients who developed AKI requiring RRT is high. Older age, higher APACHE II scores, higher dose of vasopressor, and lower serum creatinine levels were also associated with higher hospital mortality.

Data Availability Statement

The datasets generated and/or analyzed during the current study are not publicly available due participant confidentiality, according to the REB, but are available from the corresponding author on reasonable request.

ACKNOWLEDGEMENT

Not applicable.

DECLARATIONS**Grants and Funding Information**

No external funding was received for this study.

Conflict of Interest

The authors declare no conflicts of interest related to this study.

Registration Number of Clinical Trial

Not applicable.

Author Contributions

C.P.: Conceptualization, Methodology, Writing – Review & Editing, Supervision, Project Administration

N.W.: Methodology, Investigation, Data Curation, Formal Analysis, Validation, Writing – Original Draft, Writing – Review & Editing, Visualization

S.T.: Conceptualization, Methodology, Data Curation, Formal Analysis, Validation, Writing – Review & Editing, Supervision, Project Administration

M.K.: Methodology, Resources, Investigation, Data Curation, Formal Analysis, Validation, Writing – Original Draft, Writing – Review & Editing

T.N.: Conceptualization, Methodology, Resources, Investigation, Writing – Review & Editing

Use of Artificial Intelligence

Not applicable.

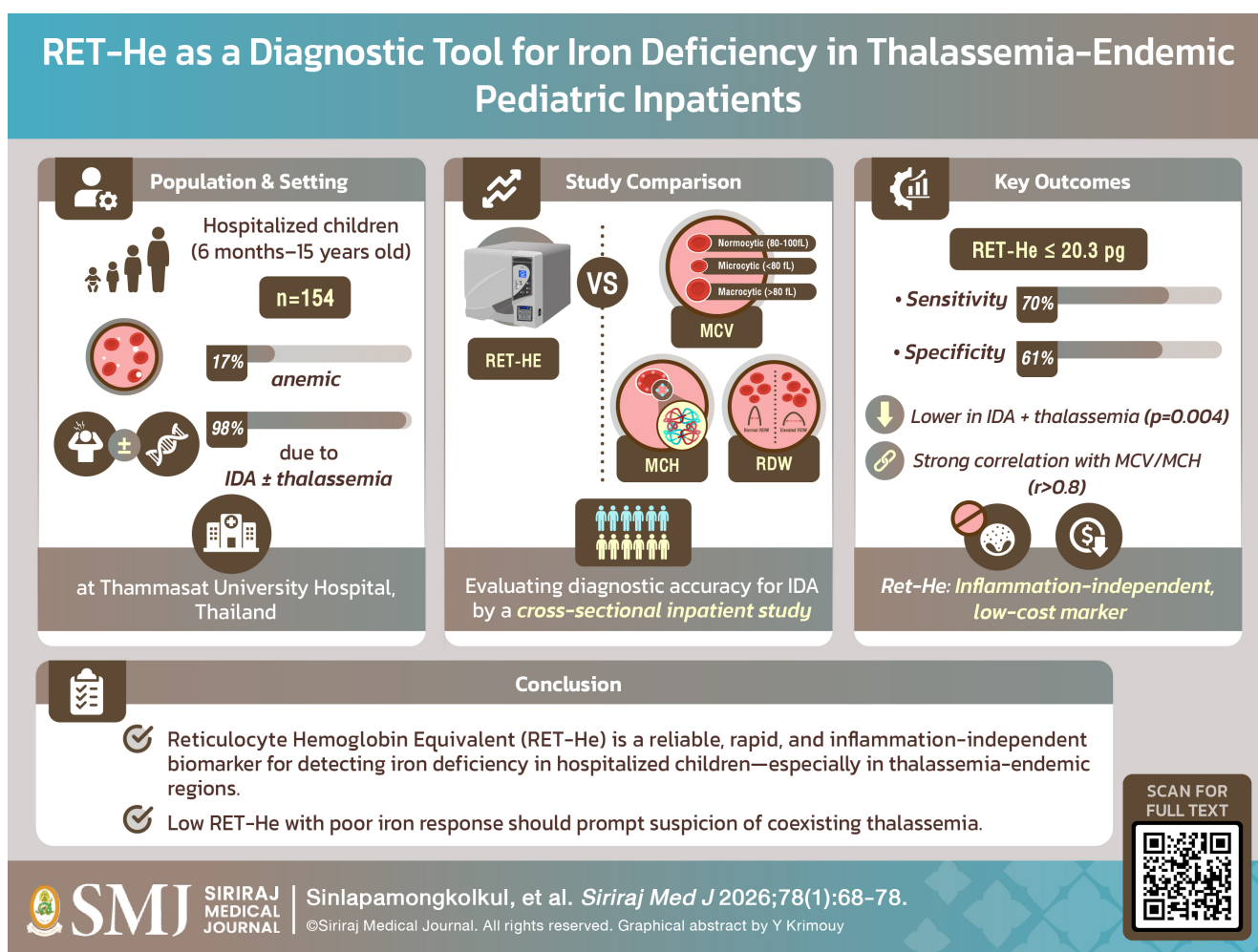
REFERENCES

- Uchino S, Kellum JA, Bellomo R, Doig GS, Morimatsu H, Morgera S, et al. Acute renal failure in critically ill patients: a multinational, multicenter study. *JAMA*. 2005;294(7):813-8.
- Angus DC, Linde-Zwirble WT, Lidicker J, Clermont G, Carcillo J, Pinsky MR. Epidemiology of severe sepsis in the United States: analysis of incidence, outcome, and associated costs of care. *Crit Care Med*. 2001;29(7):1303-10.
- Bagshaw SM, Laupland KB, Doig CJ, Mortis G, Fick GH, Mucenski M, et al. Prognosis for long-term survival and renal recovery in critically ill patients with severe acute renal failure: a population-based study. *Crit Care*. 2005;9(6):R700-9.
- Silvester W, Bellomo R, Cole L. Epidemiology, management, and outcome of severe acute renal failure of critical illness in Australia. *Crit Care Med*. 2001;29(10):1910-5.
- Neveu H, Kleinknecht D, Brivet F, Loirat P, Landais P. Prognostic factors in acute renal failure due to sepsis. Results of a prospective multicentre study. The French Study Group on Acute Renal Failure. *Nephrol Dial Transplant*. 1996;11(2):293-9.
- Bagshaw SM, Uchino S, Bellomo R, Morimatsu H, Morgera S, Schetz M, et al. Septic acute kidney injury in critically ill patients: clinical characteristics and outcomes. *Clin J Am Soc Nephrol*. 2007;2(3):431-9.
- Bouchard J, Acharya A, Cerda J, Maccariello ER, Madarasu RC, Tolwani AJ, et al. A Prospective International Multicenter Study of AKI in the Intensive Care Unit. *Clin J Am Soc Nephrol*. 2015;10(8):1324-31.
- Alobaidi R, Basu RK, Goldstein SL, Bagshaw SM. Sepsis-associated acute kidney injury. *Semin Nephrol*. 2015;35(1):2-11.
- Bagshaw SM, George C, Bellomo R, Committee ADM. Changes in the incidence and outcome for early acute kidney injury in a cohort of Australian intensive care units. *Crit Care*. 2007;11(3):R68.
- Hoste EA, Bagshaw SM, Bellomo R, Cely CM, Colman R, Cruz DN, et al. Epidemiology of acute kidney injury in critically ill patients: the multinational AKI-EPI study. *Intensive Care Med*. 2015;41(8):1411-23.
- Murugan R, Karajala-Subramanyam V, Lee M, Yende S, Kong L, Carter M, et al. Acute kidney injury in non-severe pneumonia is associated with an increased immune response and lower survival. *Kidney Int*. 2010;77(6):527-35.
- Yegenaga I, Hoste E, Van Biesen W, Vanholder R, Benoit D, Kantarci G, et al. Clinical characteristics of patients developing ARF due to sepsis/systemic inflammatory response syndrome: results of a prospective study. *Am J Kidney Dis*. 2004;43(5):817-24.
- Hoste EA, Lameire NH, Vanholder RC, Benoit DD, Decruyenaere JM, Colardyn FA. Acute renal failure in patients with sepsis in a surgical ICU: predictive factors, incidence, comorbidity, and outcome. *J Am Soc Nephrol*. 2003;14(4):1022-30.
- Vincent JL, Sakr Y, Sprung CL, Ranieri VM, Reinhart K, Gerlach H, et al. Sepsis in European intensive care units: results of the SOAP study. *Crit Care Med*. 2006;34(2):344-53.
- Dellinger RP, Levy MM, Rhodes A, Annane D, Gerlach H, Opal SM, et al. Surviving Sepsis Campaign: international guidelines for management of severe sepsis and septic shock, 2012. *Intensive Care Med*. 2013;39(2):165-228.
- Palevsky PM, Liu KD, Brophy PD, Chawla LS, Parikh CR, Thakar CV, et al. KDOQI US commentary on the 2012 KDIGO clinical practice guideline for acute kidney injury. *Am J Kidney Dis*. 2013;61(5):649-72.
- Tongyoo S, Tanyalakmara T, Naorungroj T, Promsin P, Permpikul C. The Association of High Dose Vasopressor and Delayed Vasopressor Titration with 28-Day Mortality in Adult Patients with Septic Shock. *J Health Sci Med Res*. 2023;41(1):e2022886.
- Chertow GM, Soroko SH, Paganini EP, Cho KC, Himmelfarb J, Ikizler TA, et al. Mortality after acute renal failure: models for prognostic stratification and risk adjustment. *Kidney Int*. 2006;70(6):1120-6.
- Chayakul MTS, Permpikul C. Incidence and Outcomes of Sepsis-Related Cardiomyopathy: A Prospective Cohort Study. *Journal of the Medical Association of Thailand*. 2021;104(3):497-505.
- Ronco C, Bellomo R, Kellum J. Understanding renal functional reserve. *Intensive Care Med*. 2017;43(6):917-20.
- Kadivarian S, Heydarpour F, Karimpour H, Shahbazi F. Measured versus estimated creatinine clearance in critically ill patients with acute kidney injury: an observational study. *Acute Crit Care*. 2022;37(2):185-92.
- Macedo E, Bouchard J, Soroko SH, Chertow GM, Himmelfarb J, Ikizler TA, et al. Fluid accumulation, recognition and staging of acute kidney injury in critically-ill patients. *Crit Care*. 2010;14(3):R82.
- Grams ME, Estrella MM, Coresh J, Brower RG, Liu KD, National Heart L, et al. Fluid balance, diuretic use, and mortality in acute kidney injury. *Clin J Am Soc Nephrol*. 2011;6(5):966-73.

Diagnostic Utility of Reticulocyte Hemoglobin Equivalent for Identifying Iron Deficiency in Hospitalized Children in a Thalassemia-endemic Region: A Single-center Cross-sectional Study

Phakatip Sinlapamongkolkul, M.D.¹, Tasama Pusongchai, M.D.¹, Jassada Buaboonnum, M.D.², Wallee Satayasai, M.D.¹, Pacharapan Surapolchai, M.D.^{1,*}

¹Division of Hematology and Oncology, Department of Pediatrics, Faculty of Medicine, Thammasat University, Pathumthani, Thailand, ²Division of Hematology and Oncology, Department of Pediatrics, Faculty of Medicine Siriraj Hospital, Mahidol University, Bangkok, Thailand.



*Corresponding author: Pacharapan Surapolchai

E-mail: doctorning@hotmail.com

Received 2 September 2025 Revised 18 October 2025 Accepted 18 October 2025

ORCID ID: <http://orcid.org/0000-0003-4180-8041>

<https://doi.org/10.33192/smj.v78i1.277456>



All material is licensed under terms of the Creative Commons Attribution 4.0 International (CC-BY-NC-ND 4.0) license unless otherwise stated.

ABSTRACT

Objective: Reticulocyte hemoglobin equivalent (RET-He) has been identified as a useful marker for diagnosing and monitoring iron deficiency anemia (IDA). This study evaluated anemia prevalence and assessed RET-He's effectiveness in detecting IDA in pediatric inpatients with high thalassemia burden.

Materials and Methods: A cross-sectional design was employed involving children aged 6 months to 15 years admitted with anemia. RET-He and red blood cell (RBC) indices were compared to explore diagnostic implications.

Results: Among the 881 pediatric inpatients included during the study period, 17% (154 patients) were identified as having anemia. IDA was the major cause of anemia (98%), including IDA (70.1%) and IDA coexisting with thalassemia (27.9%). Median RET-He (IQR) of all anemic patients was 21.05 (18.70, 24) pg. Notably, RET-He values were lower in patients with combined IDA and thalassemia than in those with IDA alone ($p = 0.004$). Significant correlations were observed between RET-He and RBC indices such as mean corpuscular volume (MCV) and mean corpuscular hemoglobin (MCH). With a cut-off of ≤ 20.3 pg, RET-He showed moderate sensitivity (70.3%) and specificity (60.5%) for diagnosing IDA.

Conclusion: These findings advocate for RET-He's use as an iron status marker in hospitalized children, especially in areas endemic for thalassemia. Low RET-He in non-responders to iron therapy should raise suspicion of underlying thalassemia.

Keywords: Anemia; children; diagnostic accuracy; hospitalization; iron deficiency; receiver operating characteristic; reticulocyte hemoglobin equivalent; thalassemia (Siriraj Med J 2026;78(1):68-78)

INTRODUCTION

Iron deficiency anemia (IDA) remains the leading cause of pediatric anemia worldwide, with the highest burden in resource-limited countries.¹ The incidence of IDA ranges from 20-40%, depending on age and socioeconomic status.² IDA can cause delayed growth and increased susceptibility to infection.³ Additionally, IDA can impair neurophysiological functioning, which in turn affects school performance and academic achievement.⁴ Diagnosing IDA relies on evaluating hemoglobin levels, serum ferritin, and iron studies.⁵ However, these diagnostic methods have notable limitations: ferritin measurements may yield misleadingly high values when infection or inflammatory processes are present, and iron studies are not universally accessible.⁶ Given the aforementioned disadvantages of such methods, further investigations are warranted. Reticulocytes are the immature form of erythroid cells, which subsequently differentiates into mature erythrocytes. Therefore, hemoglobin content in reticulocytes appears to reflect the availability of iron for heme production accurately. Furthermore, the reticulocyte hemoglobin equivalent (RET-He) is not affected by the inflammatory process and diurnal variations. Due to these advantages, RET-He is one of the diagnostic tools increasingly used in IDA.^{7,8}

Another crucial cause of microcytic anemia in Thailand and Southeast Asia is thalassemia and hemoglobinopathy, a group of genetic disorders affecting hemoglobin synthesis.^{9,10}

Differentiating between IDA, thalassemia, or the co-existence of both conditions is paramount for accurate diagnosis and appropriate management. Both IDA and thalassemia can manifest as microcytic hypochromic anemia, making their differential diagnosis challenging. Although Ret-He is valuable in diagnosing IDA, some studies indicate that Ret-He can also be reduced in thalassemia patients, particularly in those with thalassemia trait or combined IDA and thalassemia. However, RET-He tends to be reduced the most in subjects with concomitant IDA and thalassemia.^{11,12}

Hospitalized pediatric patients often present with complex health conditions, including co-existing inflammation, thereby complicating the assessment of iron status using traditional methods.^{13,14} The present study intends to evaluate the anemia prevalence and determine RET-He's utility in detecting IDA among hospitalized pediatric patients at Thammasat University Hospital, in the central region of Thailand. The benefits of our study include measuring the iron status of hospitalized pediatric patients and emphasizing the importance of IDA coexisting with thalassemia in this endemic area, which is applicable in inpatient settings. A thorough understanding of Ret-He values in hospitalized children with IDA, thalassemia, and combined conditions will enable clinicians to achieve more rapid and accurate diagnoses, leading to appropriate treatment and minimizing long-term health consequences for the pediatric population.

MATERIALS AND METHODS

Demography

This descriptive cross-sectional study complied with ethical standards and was approved by the Human Research Ethics Committee of Thammasat University (Medicine), Thailand (MTU-EC-PE-1-344/64). Patients aged above 7 years, as well as their parents or authorized guardians, provided the necessary assent and/or informed consent. The clinical characteristics of participants who were diagnosed with anemia and received treatment at the inpatient pediatric department of our institute, aged 6 months to 15 years old, were obtained through direct interviews and inpatient records of the electronic hospital database at Thammasat University Hospital, Thailand between January and December 2022, utilizing Research Electronic Data Capture (REDCap)¹⁵, a secure, web-based electronic data capture system managed by the Faculty of Medicine at Thammasat University, Thailand. Patients who were excluded: pediatric patients with incomplete records, known hematological problems, or bone marrow diseases. We obtained clinical and laboratory data using direct patient interviews combined with data extracted from medical files.

Anthropometric measurements

Weight, height and body mass index (BMI) were measured. Body mass index (BMI)-for-age Z-scores or standard deviation (SD) scores were computed using the WHO Anthro and AnthroPlus software programs.^{16,17} In this study, BMI Z-scores (BMIZ) less than -2 SD, greater than 1 SD, and greater than 2 SD were classified as underweight, overweight, and obese, respectively.

Laboratory investigations

EDTA blood samples were tested for a complete blood count, including RET-He, using automated hematology analyzers (DxH 900, Beckman Coulter, Brea, USA, for CBC and XN-1000, Sysmex, Kobe, Japan, for RET-He). Hemoglobin typing was performed on EDTA-anticoagulated blood samples using capillary electrophoresis with the Capillarys 2 Flex Piercing system (Sebia, Lisses, France). Serum ferritin was analyzed using clot blood samples by DxI 800, Beckman Coulter, Brea, USA. Genomic DNA was isolated from leukocytes present in peripheral blood by employing a conventional phenol-chloroform extraction method. For alpha-globin gene analysis, a single-tube multiplex gap-PCR was utilized to identify four prevalent deletions ($--SEA$, $--THAI$, $-\alpha^{3.7}$, $-\alpha^{4.2}$). Additionally, a single-tube multiplex amplification refractory mutation system (ARMS-PCR) was conducted to screen for two common non-deletion alpha-globin mutations in the

Thai population: the termination codon mutations leading to Hb Constant Spring (TAA \rightarrow CAA) and Hb Paksé (TAA \rightarrow TAT).¹⁸ Beta-globin genotyping involved ARMS-PCR targeting 16 frequent mutations including -28, CD8/9, CD17, CD19, CD26 (Hb E), CD26 G \rightarrow T (stop codon), CD27/28, IVSI-I, IVSI-5, CD35, CD41, CD41/42, CD43, CD71/72, CD95 and IVSII-654.¹⁹

Definition of anemia, iron deficiency, and thalassemia

In this investigation, anemia was defined based on WHO guidelines for age-specific hemoglobin thresholds regardless of gender: children aged 6 to 59 months were considered anemic if their hemoglobin (Hb) was below 11.0 g/dL; those aged 5 to 11 years if Hb was under 11.5 g/dL; and children aged 12 to 14 years if Hb was less than 12.0 g/dL. For individuals aged 15 years and older, anemia was classified as Hb below 12.0 g/dL in females and below 13.0 g/dL in males.²⁰ Iron deficiency (ID) was determined by either a RET-He less than 28 pg or serum ferritin levels below 30 ng/mL.²¹⁻²³ IDA was diagnosed based on either meeting laboratory criteria or showing a positive therapeutic response (either RET-He or serum ferritin) to iron supplementation administered at 3–6 mg/kg/day for a duration of 8 to 12 weeks, with follow-up by hematology specialists. Thalassemia genotypes were determined through hemoglobin analysis and molecular DNA testing. Diagnosis of beta-thalassemia trait was established when Hb A2 levels exceeded 3.5%. Children presenting with fetal hemoglobin (Hb F) levels above 10% underwent further screening for common beta-globin gene deletions to identify beta-thalassemia traits and hereditary persistence of fetal hemoglobin (HPFH).^{24,25}

Statistical data analysis

The sample size was calculated using Cochran's formula: $N = Z^2pq/d^2$, $Z = 1.96$, $p = 0.18$, $q = 0.82$, $d = 0.065$; based on an expected anemia prevalence of approximately 18% in hospitalized pediatric patients to estimate prevalence with adequate precision. A minimum of 150 participants was required, accounting for a 10% dropout rate. While the primary aim included assessing RET-He diagnostic performance for ID, formal sample size calculation for diagnostic accuracy parameters was not conducted. Diagnostic metrics were evaluated exploratively and internally validated using Receiver operating characteristic (ROC) curve analysis, Cohen's d effect size, and confidence intervals. This limitation is acknowledged, and diagnostic findings should be interpreted as preliminary. Continuous clinical and laboratory data were summarized as medians with interquartile ranges

(IQR), while categorical data were presented as counts and percentages. Differences between groups were assessed using appropriate tests according to data type and distribution: t-tests, Mann-Whitney U tests, ANOVA, or Kruskal-Wallis tests for continuous variables, and Chi-square or Fisher's exact tests for categorical variables. The strength of correlations was evaluated using Pearson's or Spearman's rank correlation coefficients, depending on data characteristics. ROC curve analysis was performed to determine the diagnostic accuracy of variables related to ID. Internal validation of the cut-off value was performed using multiple statistical approaches to assess threshold stability and discriminatory performance. Descriptive statistics, including mean, SD, 95% confidence interval (CI), and coefficient of variation (CV) were calculated for the entire dataset and stratified by threshold groups. The threshold validation was considered satisfactory if Cohen's $d \geq 0.8$, $CV \leq 30\%$, and minimal overlap existed in the critical threshold zone. Statistical analyses were carried out using Microsoft Excel 2019 and STATA version 14 (StataCorp, College Station, Texas, USA). A p -value less than 0.05 was considered statistically significant in two-tailed tests.

RESULTS

Clinical characteristics

A total of 881 pediatric inpatients were included during the study period. Of these, 154 patients (17%) were diagnosed with anemia, including 72 males (46.8%) with a mean age of 2.40 years (IQR 1–5.88). Of these 154 patients, 151 patients (98%) had IDA (with or without coexisting thalassemia), and three patients had other causes of anemia, including two with autoimmune hemolytic anemia, and one with anemia of inflammation. Besides gender, other clinical characteristics (age, nutritional status, and underlying diseases/conditions), including treatment of anemia, did not show significant differences (Table 1). Interestingly, 43 patients (27.9%) were diagnosed with IDA alongside some form of thalassemia or hemoglobinopathy. Among them, 18 individuals (11.7% of the total cohort) had alpha-thalassemia, 21 (13.6%) carried beta-globin mutations—primarily Hb E accounting for 11%—and 4 patients (2.6%) exhibited combined alpha- and beta-globin abnormalities. None of the patients with IDA who also had thalassemia exhibited clinical features typical of transfusion-dependent thalassemia, and none had ever received red blood cell transfusions. Therefore, all were categorized as non-transfusion-dependent and included in further analyses.

Laboratory characteristics

Comprehensive hematological data are detailed in Table 1. No significant differences were observed in hemoglobin (Hb), hematocrit (Hct), or mean corpuscular hemoglobin concentration (MCHC) between patients with IDA alone and those with IDA coexisting with thalassemia. However, patients presenting with both conditions showed significantly lower mean corpuscular volume (MCV) and mean corpuscular hemoglobin (MCH) values ($p < 0.001$ for both) compared to other groups. Conversely, RBC count and red cell distribution width (RDW) were markedly elevated in the combined IDA and thalassemia group ($p = 0.014$ and 0.030 , respectively). Notably, patients diagnosed with both IDA and thalassemia exhibited the greatest reduction in RET-He values ($p = 0.004$) (Fig 1).

Correlation analysis

As shown in Fig 2, RET-He exhibited strong positive correlations with MCV, MCH, and MCHC, all with p -values less than 0.001 and correlation coefficients (r) of 0.825, 0.853, and 0.713 respectively. Conversely, RET-He demonstrated moderate negative correlations with RBC count and RDW, with both p -values below 0.001 and correlation coefficients of -0.439 and -0.491 respectively.

Receiver operating characteristic curve and internal validation analysis

All the parameters examined exhibited an area under the curve (AUC) exceeding 0.4 in the ROC analysis, including RET-He, Hb, MCV, MCH, MCHC, and RDW. Among the parameters studied, RET-He exhibited a moderate diagnostic performance for detecting IDA in patients with concurrent thalassemia. At a diagnostic cut-off of ≤ 20.3 pg, the AUC was 0.649 (95% CI: 0.550–0.748), with a sensitivity of 70.3% and specificity of 60.5%. The mean RET-He value was 21.45 pg with an SD of 4.40 pg, 95% CI of 20.63 – 22.27 pg, resulting in a CV of 20.5% and a Cohen's d effect size of 1.55. Of the RBC parameters, MCV and MCH had higher AUCs of 0.708 and 0.680, respectively, at cut-off values ≤ 66.1 fL and ≤ 20.9 pg, but lower sensitivity and higher specificity. Lower AUCs of 0.543, 0.539, and 0.610, respectively, were observed for Hb, MCHC, and RDW. (Fig 3, Table 2)

DISCUSSION

Anemia remains a major public health concern among pediatric populations, especially in regions burdened by nutritional deficiencies and a high frequency

TABLE 1. Clinical and laboratory characteristics of study participants.

Characteristics	All patients (n=154)	IDA patients (n=108)	IDA coexisting with thalassemia patients (n=43)	p-values
Clinical characteristics				
Median age (IQR), years	2.40 (1, 5.88)	2.10 (1, 6.90)	2.90 (1.30, 5.40)	0.221
Male [n, (%)]	72 (46.8)	43 (39.8)	26 (60.5)	0.029*
BMI z-score (IQR)	-0.36 (-1.44, 0.81)	-0.39 (-1.55, 0.84)	-0.28 (-0.86, 0.66)	0.554
Nutritional status				0.432
Underweight [n, (%)]	22 (14.3)	18 (16.7)	4 (9.3)	
Normal [n, (%)]	100 (64.9)	66 (61.1)	32 (74.4)	
Overweight [n, (%)]	16 (10.4)	13 (12.0)	3 (7.0)	
Obese [n, (%)]	16 (10.4)	11 (10.2)	4 (9.3)	
Underlying diseases/conditions [n, (%)]	46 (30)	34 (31.5)	13 (30.2)	0.881
Treatment of anemia				0.555
Oral iron therapy [n, (%)]	135 (87.7)	95 (88.0)	40 (93.0)	
RBC transfusion [n, (%)]	2 (1.3)	2 (1.9)	0 (0)	
Oral iron therapy + RBC transfusion [n, (%)]	11 (7.1)	8 (7.4)	3 (7.0)	
Laboratory characteristics				
Hb (IQR), g/dL	9.90 (8.93, 10.68)	10.10 (9.10, 10.70)	9.80 (8.85, 10.55)	0.407
Hct, (IQR), %	31.20 (28.60, 33.05)	31.65 (29.13, 33.10)	30.90 (28.30, 32.90)	0.667
RBC count (IQR), x10 ⁶ /cu.mm.	4.80 (4.21, 5.32)	4.63 (4.20, 5.25)	5.07 (4.55, 5.38)	0.014*
MCV (IQR), fL	65.20 (59.23, 72.38)	67.55 (60.4, 73.4)	60.40 (54.55, 65.25)	< 0.001*
MCH (IQR), pg	20.7 (18.33, 23.6)	21.6 (18.9, 23.8)	18.9 (17.8, 20.75)	< 0.001*
MCHC (IQR), g/dL	31.90 (31.03, 32.60)	31.90 (31.03, 31.10)	31.80 (30.70, 32.45)	0.452
RDW (IQR), %	16.25 (14.63, 19.55)	15.95 (14.38, 19.30)	16.70 (15.75, 21.70)	0.030*
Platelet (IQR), x10 ³ /cu.mm.	360.50 (273.25, 474.50)	364.00 (282.50, 454)	351.00 (256, 530)	0.998
RET-He (IQR), pg	21.05 (18.70, 24)	21.80 (19.30, 24.30)	19.20 (17.50, 22.85)	0.004*

Data is expressed as median and IQR or N (%), according to the nature of the variables. Statistical method used: Mann-Whitney U or Student's t test, as appropriate.

* $p < 0.05$ was considered statistically significant.

Abbreviations: Hb, hemoglobin; Hct, hematocrit; IDA, iron deficiency anemia; IQR, interquartile range; MCV, mean corpuscular volume; MCH, mean corpuscular hemoglobin; MCHC, mean corpuscular hemoglobin concentration; RBC, red blood cells; RDW, red blood cell distribution width; RET-He, reticulocyte hemoglobin equivalent

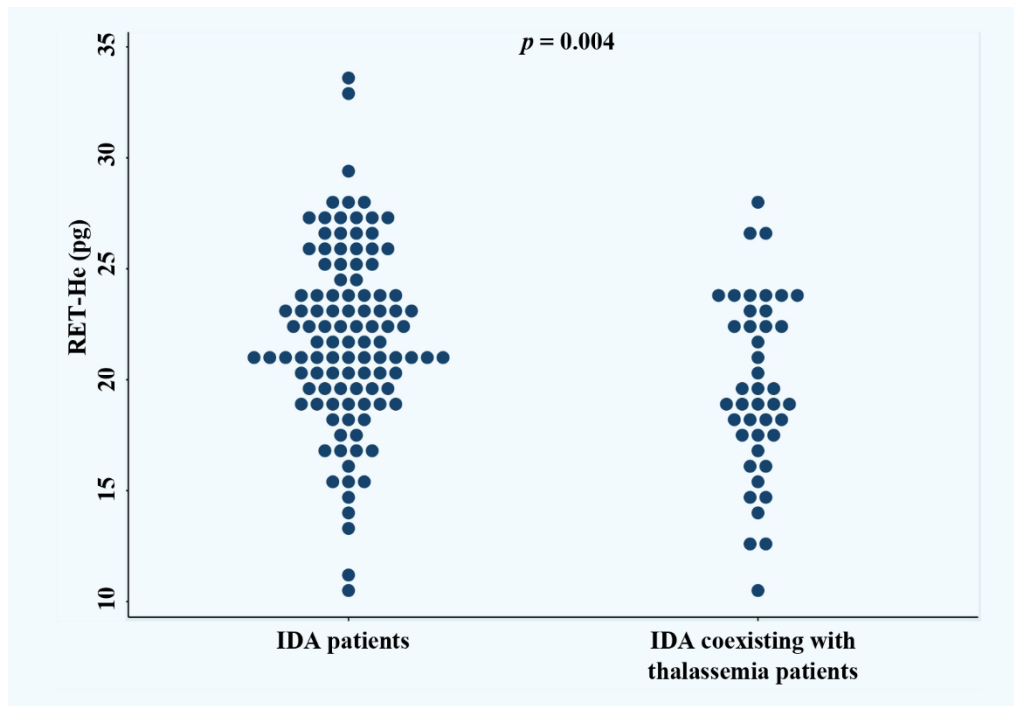


Fig 1. Differences in the RET-He among patients with IDA and IDA coexisting with thalassemia.

Statistical method used: Mann-Whitney U or Student's t test, as appropriate.

* $p < 0.05$ was considered statistically significant.

Abbreviations: IDA, iron deficiency anemia; RET-He, reticulocyte hemoglobin equivalent

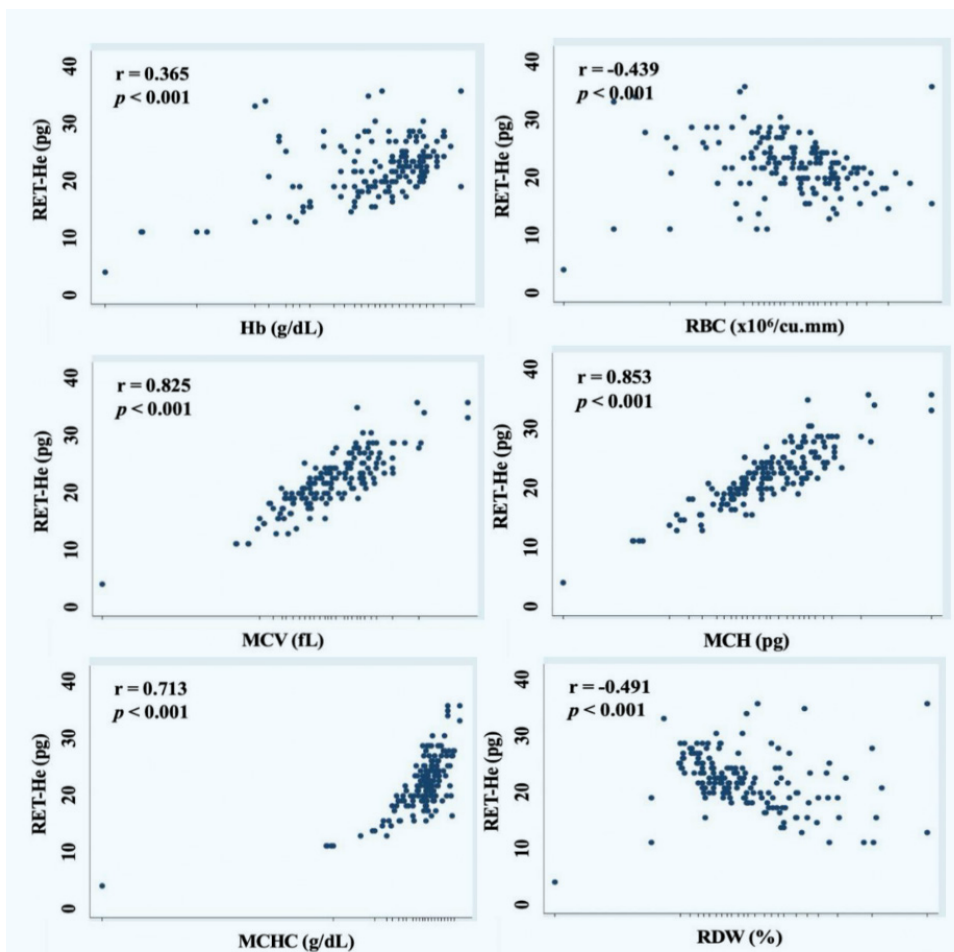


Fig 2. Relationship of RET-He and Hb, MCV, MCH, MCHC, and RDW. Data is expressed as a correlation coefficient (r).

Statistical method used: Pearson or Spearman rank correlation, as appropriate.

* $p < 0.05$ was considered statistically significant.

Abbreviations: Hb, hemoglobin; MCV, mean corpuscular volume; MCH, mean corpuscular hemoglobin; MCHC, mean corpuscular hemoglobin concentration; RBC, red blood cells; RDW, red blood cell distribution width; RET-He, reticulocyte hemoglobin equivalent

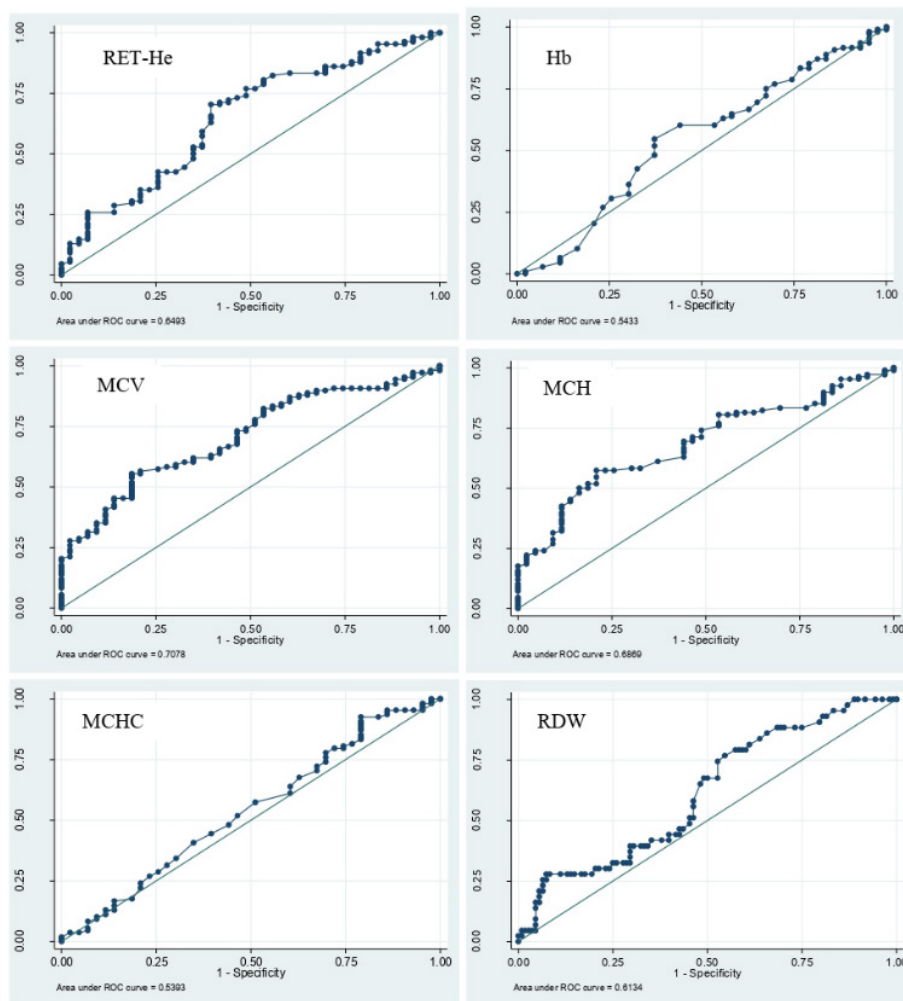


Fig 3. Receiver operating characteristic curve analysis of RET-He and Hb, MCV, MCH, MCHC, and RDW.

Data is expressed as AUC, sensitivity, and specificity.

Statistical method used: receiver operating characteristic (ROC) curves for diagnostic performance of RET-He and RBC parameters.

Abbreviations: AUC, area under the curve; Hb, hemoglobin; MCV, mean corpuscular volume; MCH, mean corpuscular hemoglobin; MCHC, mean corpuscular hemoglobin concentration; RET-He, reticulocyte hemoglobin equivalent

TABLE 2. Sensitivity and specificity of RET-He and RBC parameters for diagnosis of iron deficiency anemia.

Parameters	AUC	Cut-off	Sensitivity (%)	Specificity (%)
RET-He, pg	0.649	20.3	70.3	60.5
Hb, g/dL	0.543	9.9	54.6	62.8
MCV, fL	0.708	66.1	55.6	81.4
MCH, pg	0.680	20.9	57.4	79.1
MCHC, g/dL	0.539	31.8	57.4	48.4
RDW, %	0.610	15.8	74.2	47.2

Data is expressed as AUC, cut-off, sensitivity, and specificity.

Statistical method used: receiver operating characteristic (ROC) curves for diagnostic performance of RET-He and RBC parameters.

Abbreviations: AUC, area under the curve; Hb, hemoglobin; MCV, mean corpuscular volume; MCH, mean corpuscular hemoglobin; MCHC, mean corpuscular hemoglobin concentration; RDW, red blood cell distribution width; RET-He, reticulocyte hemoglobin equivalent

of thalassemia. This study provides new insights into the prevalence, etiology, and diagnostic approach to anemia in hospitalized children at Thammasat University Hospital, with particular emphasis on the utility of RET-He as a marker for IDA, especially in the context of coexisting thalassemia. Among pediatric inpatients in this study, anemia prevalence was 17%, aligning with previous reports from similar settings in Southeast Asia. The overwhelming majority (98%) of anemic cases were attributable to IDA, either alone or in combination with thalassemia, underscoring the dominance of nutritional and genetic causes in this population. Notably, 27.9% of anemic children had coexisting thalassemia, a figure that reflects the widespread occurrence of thalassemia traits in Thailand and neighboring countries. This dual pathology complicates both diagnosis and management, as clinical and laboratory features of IDA and thalassemia often overlap.

RET-He has emerged as a promising biomarker for assessing iron status, given its ability to reflect the hemoglobin content of newly produced reticulocytes and, by extension, the immediate availability of iron for erythropoiesis. In the context of hospitalized pediatric patients, RET-He is particularly advantageous. Traditional iron studies are not always feasible in acutely ill children, especially in those with infections or chronic inflammatory states. RET-He, being part of the automated CBC panel in modern hematology analyzers, offers a rapid, low-cost, and accessible alternative with the potential for point-of-care screening. Despite its promise, RET-He is not without limitations. Sedick *et al.* emphasized that while RET-He could reliably distinguish between IDA and thalassemia, its performance varied by patient age, analyzer platform, and the presence of coexisting disorders.¹¹ In our study, although RET-He showed a moderate diagnostic accuracy, other parameters like MCV and MCH had higher AUC values (0.708 and 0.680, respectively). However, the higher sensitivity of RET-He highlights its utility as an initial screening tool in clinical practice. In this study, the median RET-He among all anemic patients was 21.05 pg, with significantly lower values observed in those with both IDA and thalassemia compared to those with IDA alone ($p = 0.004$). Our observations align with the report by Kadegasem *et al.*, showing that RET-He decreases in ID and thalassemia, with the most marked reduction when both disorders are present.¹² This additive effect of ID on hemoglobin production in thalassemic patients can exacerbate anemia and complicate diagnosis.

There were strong positive associations observed between RET-He and MCV, MCH, and MCHC ($r = 0.825$,

0.853, and 0.713, respectively; all $p < 0.001$) reinforce the close relationship between iron supply and erythrocyte indices. Conversely, the moderate negative correlations with RBC count and RDW ($r = -0.439$ and -0.491 , respectively; both $p < 0.001$) reflect the compensatory erythropoietic response and anisocytosis characteristic of iron-restricted erythropoiesis and thalassemia. The diagnostic utility of RET-He was further supported by ROC analysis, which demonstrated that using a cut-off value of ≤ 20.3 pg yielded a sensitivity of 70.3% and a specificity of 60.5% for diagnosing IDA with coexisting thalassemia. The mean (range) RET-He value was 21.45 pg (10.6 to 34.3 pg), resulting in a CV of 20.5%, which indicates moderate variability of RET-He measurements around the mean. The internal validation of the RET-He threshold included calculation of Cohen's d effect size, which was 1.55, indicating a large standardized difference between groups defined by the 20.3 pg cut-off. This large effect size demonstrates that the threshold reliably separates patients with lower RET-He levels from those with higher levels, supporting its stability and clinical utility. These metrics support the stability and precision of the chosen cut-off value of 20.3 pg for the diagnosis within the study population. While these values indicate moderate diagnostic accuracy, they suggest that RET-He can serve as a useful screening tool, particularly when used in conjunction with other RBC indices such as MCV, MCH, and RDW. Lian *et al.* demonstrated that combining RET-He with RDW enhances diagnostic accuracy, particularly in identifying coexisting cases.²⁶ In our study, the combination of RET-He with MCV and RDW did show significant correlations, suggesting that a multiparametric approach could enhance the diagnostic utility beyond RET-He alone. Although not highly specific, this sensitivity makes RET-He a valuable tool for ruling out IDA in our hospitalized pediatric patients. RET-He can be considered a useful adjunct marker, but should be interpreted alongside other hematological indices for accurate diagnosis. This aligns with the findings from Jamnok *et al.*, who demonstrated that RET-He can be an effective early screening tool for ID in areas with high thalassemia prevalence, supporting its integration into diagnostic algorithms.²⁷ Complete blood count (CBC) parameters, including MCV, MCH, and RDW, offer some discriminatory value but lack specificity when thalassemia traits are prevalent. In this study, MCV and MCH also demonstrated reasonable diagnostic performance (AUCs of 0.708 and 0.680, respectively), but RET-He provided a more direct assessment of functional iron availability. Khorwanichakij *et al.* proposed a novel thalassemia-iron deficiency discrimination predictive score derived from

routine red blood cell indices, including MCH, RDW, RBC, and platelet count.²⁸ This score demonstrated high sensitivity (90.4%) and specificity (78.7%) for differentiating all thalassemia subtypes from IDA in a Thai cohort. Integrating such predictive formulas with RET-He values may enhance early and accurate discrimination between IDA and thalassemia, thereby guiding targeted management in settings with limited access to specialized confirmatory testing.

The commonness of thalassemia traits in Thailand and Southeast Asia necessitates careful interpretation of anemia workups. Both IDA and thalassemia present as microcytic, hypochromic anemia, and their coexistence can exacerbate anemia severity and complicate treatment decisions. The significantly lower RET-He values in patients with combined IDA and thalassemia highlight the need for clinicians to consider thalassemia in children who fail to respond to iron therapy despite low RET-He. This is critical to avoid unnecessary and potentially harmful iron supplementation in children with underlying thalassemia traits. Interestingly, reticulocyte parameters have also been proposed for therapeutic monitoring. Almashjary et al. showed that increases in RET-He following iron supplementation precede changes in hemoglobin, suggesting that RET-He can also be used to assess response to iron therapy within days.²⁹ Although our study did not longitudinally assess RET-He post-treatment, this represents an important future direction, especially in hospitalized patients requiring close monitoring. Genetic testing for alpha- and beta-thalassemia mutations, as performed in this study, remains the gold standard for definitive diagnosis. However, such testing may not be universally available, making RET-He and other hematological indices valuable adjuncts in the diagnostic algorithm. This supports earlier recommendations by Yuan *et al.* and Saboor *et al.*, who advocated for integrating RET-He, HbA2, and RDW to guide further genotyping and targeted management.^{30,31}

The high prevalence of thalassemia necessitates the proposed diagnostic protocols that address dual pathology: an initial assessment for children with microcytic anemia (MCV < 75 fL) and the measurement of RET-He and RBC indices. RET-He interpretation with clinically relevant thresholds is as follows: 1) a higher cut-off of >28 pg can be used to rule out IDA and prompt investigation of alternative etiologies; 2) values between 20 and 28 pg are ambiguous, warranting serum ferritin measurement if inflammation is absent; 3) a lower cut-off of ≤20 pg indicates high suspicion for IDA with or without coexisting thalassemia. For thalassemia risk stratification, a low RET-He combined with a high RBC count ($>5 \times 10^{12}/L$)

or a Mentzer index (MCV/RBC ratio) less than 13 should trigger further Hb electrophoresis and genetic testing. Therapeutic trials of iron supplementation at 3–6 mg/kg/day for 8–12 weeks, followed by subsequent RET-He reassessment, are recommended. Non-responders may require additional genetic evaluation. This approach mitigates the risks of inappropriate iron therapy in thalassemia carriers, which can accelerate oxidative organ damage.

Several limitations of this study should be acknowledged. First, the cross-sectional design limits the ability to assess changes in RET-He over time or evaluate treatment response longitudinally. Second, as a single-center study in a tertiary care hospital, the findings may not be generalizable to other settings or broader populations, particularly given the complexity of hospitalized pediatric patients. Third, although RET-He demonstrated moderate diagnostic accuracy and was internally validated using multiple statistical methods, the sample size was initially calculated based on anemia prevalence (using Cochran's formula) rather than formal sample size estimation for diagnostic accuracy measures such as sensitivity, specificity, or AUC. This may limit the precision and generalizability of the diagnostic performance estimates. Fourth, inflammatory markers like C-reactive protein (CRP) were not assessed, which could have helped clarify confounding effects of inflammation on iron status biomarkers. Fifth, while molecular genotyping for common alpha- and beta-thalassemia mutations was performed, rarer variants may have been missed. Finally, incorporation bias may be present, as RET-He was part of the composite reference standard for ID diagnosis, potentially inflating diagnostic accuracy estimates. Future studies should include prospective designs with sample size calculations specifically tailored for diagnostic accuracy endpoints to validate and build upon these preliminary findings. Nonetheless, this study underscores the need for practical and accessible tools for evaluating anemia in children, particularly in regions with high thalassemia prevalence. RET-He fulfills many of these criteria and should be considered a frontline screening tool alongside traditional red cell indices. It provides a rapid and cost-effective means of differentiating types of microcytic anemia and identifying patients who warrant further diagnostic evaluation, such as hemoglobin electrophoresis or genetic testing. Future research should focus on prospective studies evaluating the utility of RET-He as a screening tool for ID and for monitoring treatment response after iron therapy, and in differentiating between IDA, thalassemia, and other causes of anemia in diverse pediatric populations.

Integration of RET-He into standardized anemia workups, particularly in resource-limited and thalassemia-endemic areas, may improve early detection and management of ID and reduce the burden of anemia-related morbidity.

CONCLUSION

This study highlights RET-He as an effective and sensitive biomarker for detecting IDA among hospitalized pediatric participants, particularly in regions where thalassemia is prevalent. RET-He provides a rapid, reliable, and inflammation-independent assessment of iron status, and its use in combination with other hematological indices can facilitate more accurate diagnosis and appropriate management. Because of the frequent coexistence of thalassemia, physicians should be vigilant in interpreting low RET-He values and consider genetic testing or alternative diagnoses in children who do not respond to iron therapy. Broader implementation of RET-He in clinical practice may help to address the persistent challenge of anemia in pediatric populations and improve long-term health outcomes.

Data Availability Statement

De-identified data were available from the corresponding author upon reasonable request.

ACKNOWLEDGMENTS

We sincerely thank all patients and their parents or guardians for participating in this study. Our gratitude also goes to Professor Dr. Paskorn Sritipsukho and Associate Professor Dr. Sariya Prachukthum for their valuable guidance on statistical analysis. We appreciate the English editorial assistance provided by Ms. Sam Ormond, international instructor at the Clinical Research Center, Faculty of Medicine, Thammasat University.

DECLARATIONS

Grants and Funding Information

We gratefully acknowledge the financial support from the Faculty of Medicine, Thammasat University (contract: K.1-06/2565) and the Research Group in Pediatrics of the Faculty of Medicine, Thammasat University.

Conflict of Interest

The authors declare no conflict of Interest.

Author Contributions

Conceptualization and methodology, P.Si., P.Su. ; Investigation, P.Si., T.P., P.Su. ; Formal analysis, P.Si., T.P., P.Su. ; Visualization and writing – original draft, P.Su. ; Writing – review and editing, P.Si., J.B., P.Su. ; Funding

acquisition, P.Su. ; Supervision, W.S. All authors have read and agreed to the final version of the manuscript.

Use of Artificial Intelligence

AI-based tools (ChatGPT, Perplexity AI) were used for language editing under author supervision.

REFERENCES

1. Bathla S, Arora S. Prevalence and approaches to manage iron deficiency anemia (IDA). *Crit Rev Food Sci Nutr.* 2022;62(32): 8815-28.
2. Moscheo C, Licciardello M, Samperi P, La Spina M, Di Cataldo A, Russo G. New Insights into Iron Deficiency Anemia in Children: A Practical Review. *Metabolites.* 2022;12(4):289.
3. Angeles IT, Schultink WJ, Matulessi P, Gross R, Sastroamidjojo S. Decreased rate of stunting among anemic Indonesian preschool children through iron supplementation. *Am J Clin Nutr.* 1993; 58(3):339-42.
4. Lozoff B, Beard J, Connor J, Barbara F, Georgieff M, Schallert T. Long-lasting neural and behavioral effects of iron deficiency in infancy. *Nutr Rev.* 2006;64(5 Pt 2):S34-43; discussion S72-91.
5. Mei Z, Addo OY, Jefferds MED, Sharma AJ, Flores-Ayala RC, Pfeiffer CM, Brittenham GM. Comparison of Current World Health Organization Guidelines with Physiologically Based Serum Ferritin Thresholds for Iron Deficiency in Healthy Young Children and Nonpregnant Women Using Data from the Third National Health and Nutrition Examination Survey. *J Nutr.* 2023;153(3): 771-80.
6. Johnson-Wimbley TD, Graham DY. Diagnosis and management of iron deficiency anemia in the 21st century. *Therap Adv Gastroenterol.* 2011;4(3):177-84.
7. Mateos ME, De-la-Cruz J, López-Laso E, Valdés MD, Nogales A. Reticulocyte hemoglobin content for the diagnosis of iron deficiency. *J Pediatr Hematol Oncol.* 2008;30(7):539-42.
8. Ogawa C, Tsuchiya K, Maeda K. Reticulocyte hemoglobin content. *Clin Chim Acta.* 2020;504:138-45.
9. Fucharoen S, Winichagoon P. Haemoglobinopathies in southeast Asia. *Indian J Med Res.* 2011;134(4):498-506.
10. Leckngam, P. Thalassemia and Hemoglobinopathies in Thailand: A Systematic Review. *J Health Sci Altern Med.* 2023;5(3):104-13.
11. Sedick Q, Elyamany G, Hawsawi H, Alotaibi S, Alabbas F, Almohammadi M, et al. Diagnostic accuracy of reticulocyte parameters on the Sysmex XN 1000 for discriminating iron deficiency anaemia and thalassaemia in Saudi Arabia. *Am J Blood Res.* 2021;11(2):172-9.
12. Kadegasem P, Songdej D, Lertthammakiat S, Chuansumrit A, Paisooksantivatana K, Mahaklan L, et al. Reticulocyte hemoglobin equivalent in a thalassemia-prevalent area. *Pediatr Int.* 2019; 61(3):240-5.
13. Rohr M, Brandenburg V, Brunner-La Rocca HP. How to diagnose iron deficiency in chronic disease: A review of current methods and potential marker for the outcome. *Eur J Med Res.* 2023;28:15.
14. Lee NH. Iron deficiency in children with a focus on inflammatory conditions. *Clin Exp Pediatr.* 2024;67(6):283-93.
15. Harris PA, Taylor R, Thielke R, Payne J, Gonzalez N, Conde

-
- JG. Research electronic data capture (REDCap—a metadata-driven methodology and workflow process for providing translational research informatics support. *J Biomed Inform.* 2009;42:377-81.
16. World Health Organization. WHO Anthro for personal computers, version 3.2.2, 2011: Software for assessing growth and development of the world's children. Geneva: WHO, 2010. [cited 2024 Apr 30]. Available from: <https://www.who.int/childgrowth/software/en/>
 17. World Health Organization. WHO AnthroPlus for personal computers manual: software for assessing growth of the world's children and adolescents. Geneva: WHO; 2009. [cited 2024 Apr 30]. Available from: <https://www.who.int/growthref/tools/en/>
 18. Eng B PM, Walker L, Chui DHK, Waye JS. Detection of severe nondeletional α -thalassemia mutations using a single-tube multiplex ARMS assay. *Genet Test.* 2001;5:327-9.
 19. Newton CR, Graham A, Heptinstall LE, Powell SJ, Summers C, Kalsheker N, et al. Analysis of any point mutation in DNA. The amplification refractory mutation system (ARMS). *Nucleic Acids Research.* 1989;17(7):2503-16.
 20. World Health Organization. Iron deficiency anemia: assessment, prevention and control. A guide for programme managers. Geneva, World Health Organization; 2001.
 21. Tantawy AA, Ragab IA, Ismail EA, Ebeid FSE, Al-Bshkar RM. Reticulocyte Hemoglobin Content (Ret He): A Simple Tool for Evaluation of Iron Status in Childhood Cancer. *J Pediatr Hematol Oncol.* 2020;42(3):e147-51.
 22. Syed S, Kugathasan S, Kumar A, Prince J, Schoen BT, McCracken C, et al. Use of Reticulocyte Hemoglobin Content in the Assessment of Iron Deficiency in Children With Inflammatory Bowel Disease. *J Pediatr Gastroenterol Nutr.* 2017;64(5):713-20.
 23. Camaschella C. Iron deficiency: new insights into diagnosis and treatment. *Hematology Am Soc Hematol Educ Program.* 2015; 2015:8-13.
 24. Tritipsombut J, Phylipsen M, Viprakasit V, Chalaow N, Sanchaisuriya K, Giordano PC, et al. A single-tube multiplex gap-polymerase chain reaction for the detection of eight beta-globin gene cluster deletions common in Southeast Asia. *Hemoglobin.* 2012;3:571-80.
 25. Craig JE, Barnetson RA, Prior J, Raven JL, Thein SL. Rapid detection of deletions caused β -thalassemia and hereditary persistence of fetal hemoglobin by enzymatic amplification. *Blood.* 1994;83:1673-82.
 26. Lian Y, Shi J, Nie N, Huang Z, Shao Y, Zhang J, et al. Reticulocyte Hemoglobin Equivalent (Ret-He) Combined with Red Blood Cell Distribution Width Has a Differentially Diagnostic Value for Thalassemias. *Hemoglobin.* 2019;43(4-5):229-35.
 27. Jamnok J, Sanchaisuriya K, Chaitriphop C, Sanchaisuriya P, Fucharoen G, Fucharoen S. A New Indicator Derived From Reticulocyte Hemoglobin Content for Screening Iron Deficiency in an Area Prevalent for Thalassemia. *Lab Med.* 2020;51(5):498-506.
 28. Khorwanichakij N, Kungwankiattichai S, Owattanapanich W. Validation of Several Formulas to Differentiate Thalassemia from Iron Deficiency Anemia and Proposal of a Thalassemia–Iron Deficiency Discrimination (TID) Predictive Score. *Siriraj Med J.* 2022;74(4):256-65.
 29. Almashjary MN, Barefah AS, Bahashwan S, Ashankyty I, ElFayoumi R, Alzahrani M, et al. Reticulocyte Hemoglobin-Equivalent Potentially Detects, Diagnoses and Discriminates between Stages of Iron Deficiency with High Sensitivity and Specificity. *J Clin Med.* 2022;11(19):5675.
 30. Yuan QR, Niu SQ, Lin XP, Luo ZF. The Clinical Value of Combined Detection of RBC, Ret-He and HbA2 for Thalassemia. *Zhongguo Shi Yan Xue Ye Xue Za Zhi.* 2021;29(1):203-6.
 31. Saboor M. Discrimination of Iron Deficiency, Alpha and Beta Thalassemia on the Basis of Red Cell Distribution Width and Reticulocyte Indices. *Clin Lab.* 2021;67(6).

Dental Management in Natal and Neonatal Teeth

Narawan Chieowwit, D.D.S., M.P.H., Dip. Thai Board of Pediatric Dentistry

Department of Dentistry, Siriraj Hospital, Faculty of Medicine Siriraj Hospital, Mahidol University, Bangkok 10700, Thailand.

NATAL & NEONATAL TEETH CLASSIFICATION, DIAGNOSIS, AND MANAGEMENT

Natal teeth
(present at birth)

- Small, conical normal shape
- Often paired
- Usually lower central incisor
- Unclear exact causes

Neonatal teeth
(present within 1st month)

Retention is the first choice of treatment

Oral examination

- Tooth mobility
- Risk of aspiration
- Riga-fede disease
- Complications

Hebling et al.:
4 classification
types of natal and neonatal teeth

Type 1



Type 2



Type 3



Type 4



Intraoral X-ray

- 90-99% Normal Primary Teeth
- 1-10% Supernumerary Teeth

Extract

Supernumerary Teeth + Complications affect growth

- Receive Vit K prophylaxis after birth
- Curette the socket
- Apply a gauze pad with pressure
- Resume breastfeeding immediately
- Follow up

Retain

First Choice of Treatment

- Monitor
- Regular dental checkups
- Plaque control
- Plaque control

SCAN FOR FULL TEXT



*Corresponding Author: Narawan Chieowwit

E-mail: narawan10@yahoo.com

Received 16 April 2025 Revised 24 October 2025 Accepted 8 November 2025

ORCID ID: <http://orcid.org/0009-0003-8357-8456>

<https://doi.org/10.33192/smj.v78i1.274841>



All material is licensed under terms of the Creative Commons Attribution 4.0 International (CC-BY-NC-ND 4.0) license unless otherwise stated.

ABSTRACT

The premature eruption of teeth in newborns is categorized as natal teeth, which are present at birth, and neonatal teeth, which appear within the first month of life. Natal teeth are about three times more common, with 90-99% being normal primary teeth and 1-10% supernumerary. The exact causes are unclear. These teeth often appear small, conical, or similar to normal teeth. They are usually located in the lower central incisor region and often paired. This literature review aims to provide dental management for the accurate diagnosis and effective treatment of natal and neonatal teeth. Diagnosis relies on clinical examinations and may involve radiographic evaluation for supernumerary teeth. These teeth can lead to complications such as tooth mobility, raising concerns about aspiration, sublingual ulcerations (Riga-Fede disease), and nipple lacerations during breastfeeding. Since most of these teeth are normal primary teeth, they should be retained with periodic monitoring. Extraction is only indicated if a tooth is extremely mobile and poses a risk of aspiration, or if ulcerations affect the child's ability to suck effectively, particularly in conjunction with the use of a nasoalveolar molding appliance in children with cleft lip and palate.

Keywords: Newborn; premature eruption; natal teeth; neonatal teeth; retain; extract (Siriraj Med J 2026;78(1):79-86)

INTRODUCTION

Newborns typically receive an oral examination by a pediatrician immediately after birth. If any abnormalities are detected in the oral cavity, the pediatrician will refer the infant to a dentist for further diagnosis and appropriate management. Although the premature eruption of teeth in newborns is rare, it can lead to feeding difficulties and, in severe cases, pose life-threatening risks. Pediatricians may consult either general dentists or pediatric dentists for treatment. However, due to a shortage of pediatric dentists in Thailand, it is crucial for general dentists to have the knowledge and skills to accurately diagnose and manage these cases. This literature review, conducted between May and December 2024, gathered reliable information from PubMed and Google Scholar, along with insights from the author's experience with infant care. The study aims to provide a comprehensive overview of the literature and dental management techniques for dentists, ensuring accurate diagnosis and effective treatment for natal and neonatal teeth.

Premature tooth eruption in newborns includes natal and neonatal teeth. Natal teeth are present at birth, while neonatal teeth emerge within the first month.^{1,2} Primary teeth that erupt between one and three months of age are classified as early-erupting primary teeth.³ Natal teeth are more common than neonatal teeth,⁴⁻⁶ and three times more prevalent.^{1,2,7} The incidence of natal and neonatal teeth ranges from 1 in 2,000 to 1 in 3,500 births.^{1,4-6,8,9} The worldwide prevalence of natal teeth is about 34.55 per 10,000 births (95% CI, 20.12 to 59.26). In Asia, the prevalence rate is about 11.26 per 10,000 births (95% CI, 7.58 to 16.61), while in North America, it is higher at 75.32 per 10,000 births (95%

CI, 51.11 to 99.86). For neonatal teeth, the worldwide prevalence is around 4.52 per 10,000 (95% CI, 2.59 to 17.91). In Europe, the prevalence is estimated at 3.52 per 10,000 births (95% CI, 1.73 to 7.06). In South America, the prevalence is 6.01 per 10,000 births (95% CI, 2.25 to 16.60).¹⁰ No prevalence data have been reported in Thailand.

There is no significant difference in prevalence between males and females.^{1,11} However, some studies report a higher occurrence in females,^{4,12,13} with a ratio of 66% for females compared to 31% for males.^{4,12,14} Approximately 90-99% of natal and neonatal teeth are normal primary teeth, while 1-10% are supernumerary.^{3,11} A retrospective study by *Samuel et al.* involving 33 newborns found that all 52 teeth were normal primary teeth, with no supernumerary teeth noted.¹⁵ *Almeida and Gomide* highlighted a higher prevalence in infants with cleft lip and palate, with rates of 10.6% in the complete bilateral cleft group and 2.02% in the complete unilateral cleft group.¹⁶

Causes and factors

The exact causes of natal and neonatal teeth are still unknown.^{1,4,11} However, several factors have been proposed, with the most widely accepted theory suggesting that a superficial position of the tooth germ, possibly influenced by hereditary factors.¹¹ These factors include abnormalities in the position of tooth germs during alveolar development.^{4,17,18} For example, the tooth germ might be positioned too superficially.^{2,11} Another hypothesis proposes that excessive resorption of the overlying bone accelerates premature eruption.¹ For hereditary factors, no definitive evidence confirms a link between early

eruption of teeth and family history.¹¹ However, a study by *Zhu and King* reported familial association in 8% to 62% of cases,⁹ while *Bondenhoff and Gorlin* reported a 14.5% prevalence of family history.⁵ Similarly, *Kates et al.* identified a positive family history in 7 out of 38 cases of natal and neonatal teeth.¹² Some evidence suggests an autosomal dominant inheritance pattern.^{4,5,19,20} Natal and neonatal teeth have also been linked to various syndromes and developmental disturbances, including Ellis-Van Creveld syndrome, Hallerman-Streiff syndrome, Rubinstein-Taybi syndrome, Pierre-Robin syndrome, Sotos syndrome, Pallister-Hall syndrome, Pfeiffer syndrome, short rib-polydactyly type II, cleft lip and palate, craniofacial dysostosis, cyclopia, ectodermal dysplasia and epidermolysis bullosa simplex.^{1,4,11,13,20} Hormonal imbalances during pregnancy, such as excessive secretion from the pituitary gland, thyroid, or gonads, can influence premature eruption.^{1,2,4,6} Additionally, maternal illness during pregnancy such as fever and exanthemata may lead to premature eruption.⁴ Also, congenital syphilis has been associated with this condition.^{1,2,4} Maternal malnutrition or hypovitaminosis can adversely affect tooth development,^{1,2,4} while exposure to environmental toxins may also play a role in the eruption of neonatal teeth. There have also been reports that prenatal exposure to harmful substances such as polychlorinated biphenyls (PCBs), polychlorinated dibenzo-p-dioxins (PCDDs), and dibenzofurans (PCDFs) may contribute to neonatal tooth eruption.^{1,21,22} However, a study by *Alaluusua et al.* found no correlation between the presence of natal teeth and PCB or PCDF levels in breast milk.²³

Clinical characteristics

Natal and neonatal teeth vary in shape and size, often appearing conical or resembling normal teeth but typically smaller.^{3,4,11,13} These teeth frequently show enamel and dentin hypoplasia, with poor or absent root development. Due to their premature eruption and

lack of roots, they are typically mobile and attached only by soft tissue,^{9,13,24} posing a risk of swallowing or aspiration. In some cases, mobility leads to degeneration of Hertwig's epithelial root sheath, resulting in further root development and stability, and changes in the radicular structures.¹ The color of these teeth is often abnormal, ranging from white to yellow. Early eruption is associated with hypomineralization of enamel, known as dysplasia, which disrupts the calcium-rich enamel matrix, leading to smaller teeth with a yellowish-brown appearance. Furthermore, there is a decrease in the mineral content of the enamel layer, contributing to enamel hypoplasia, with the thinner enamel layer covering only about two-thirds of the crown.⁴

Natal and neonatal teeth most commonly occur in the mandibular central incisors,⁷ which are the first to erupt.^{5,15} Approximately 85% of natal teeth are mandibular incisors, 11% maxillary incisors, 3% mandibular canines and molars, and only 1% maxillary canines or molars.⁵ Natal teeth in the maxillary molar region are scarce.²⁴ However, *Varriano et al.* and *Roberts et al.* reported a rare case of two primary maxillary molars.^{18,25} In newborns with cleft conditions, teeth frequently erupt in the maxilla within the area of the cleft.²⁶ These natal and neonatal teeth usually present alone or in pairs,¹¹ while multiple natal or neonatal teeth are uncommon.⁴ Rare cases include 14 natal teeth reported by *Masatomi et al.*,²⁷ 12 natal teeth by *Gonçalves et al.*,²⁸ and 11 natal teeth by *Portela et al.*²⁹

Hebling et al. classified natal and neonatal teeth into four classification types.¹ (Fig 1)

Type 1: A shell-like crown structure loosely attached to the gum, with no root.

Type 2: A solid crown with little or no root, loosely attached to the gum.

Type 3: The cutting edge of the tooth has erupted through the gum.

Type 4: The gum appears swollen, with an unerupted tooth within the gum.



Fig 1. Hebling's classification of natal and neonatal teeth. (1A) Hebling's classification type 1 (1B) Hebling's classification type 2 (1C) Hebling's classification type 3 (1D) Hebling's classification type 4

Note: Fig 1A from "Management of an infant having natal teeth", by V. Khandelwal, U.A. Nayak, P.A. Nayak, and Y. Bafna, 2013, BMJ Case Report, p. 1. Copyright 2013 by BMJ Publishing Group Ltd. Adapted with permission of the author.

Histological characteristics

The crowns of natal and neonatal teeth are primarily covered with varying degrees of hypoplastic enamel.¹¹ Research by Jasmin and Clergeau-Guerithault, using scanning electron microscopy, showed that the enamel surface of these teeth exhibited hypoplasia, with no enamel layer present at the incisal edge.^{30,31} Masatomi et al. found that while some enamel exhibited a normal prism structure and mineralization, others lacked this prism structure in the cervical part of the enamel. They observed that cervical and apical dentin were tubular but changed into an irregular osteodentin containing enclosed cells.²⁹ Uzamis et al. reported that natal and neonatal teeth had an enamel thickness of about 280 µm, significantly less than the 1200 µm typical for primary teeth, indicating incomplete mineralization at birth.³¹ The dentino-enamel junction was irregular and not scalloped, with no predentin or odontoblast layers in the tubular dentin. Vascular inclusions were present in the osteodentin-like structure, but endothelial cells were absent. The cementum was hypertrophied, featuring numerous lacunae and a layer of acellular cementum.²⁷ Developing teeth showed thinner acellular cementum, wider pulp canals and chambers, and few inflammatory cells within the vascularized pulps.^{27,32}

Differential diagnosis

Inclusion cysts are often mistaken for natal and neonatal teeth. These benign oral mucosal lesions can be categorized into three types.⁴ Epstein's pearls are small, white, grayish nodules or papules that range from 0.5 to 3 mm in size. They can be found singly or in clusters along the mid-palatal raphe, particularly at the junction of the hard and soft palates. These nodules originate from remnants of ectodermal tissue that occur during palatal development.³³ Bohn's nodules are clusters of nodules located on the buccal and lingual aspects of the alveolar ridges.^{13,34} They arise from remnants of minor salivary glands.³⁵⁻³⁷ Dental lamina cysts appear

in white or cream-colored nodules, which can be found singularly or in multiples. They are typically located on the alveolar ridges of the lower incisors^{34,35} and jaws.^{34,38} They originate from remnants of the dental lamina after tooth formation.³⁹

Other differentiating conditions include eruption cysts and congenital epulis. An eruption cyst is a fluid-filled cyst around an erupting tooth, often appearing as clear, dome-shaped swellings, but may take on a blue or purple due to blood accumulation, known as an eruption hematoma.^{41,42} They originate from remnants of the dental lamina during the eruption,^{38,40} and can sometimes contain natal or neonatal teeth.⁴⁰ Congenital epulis is a rare benign tumor appearing as a smooth, raised mass on the upper or lower jaw or tongue, typically matching the color of the gum tissue.³⁵ It is most commonly found on the anterior alveolar ridge of the upper jaw^{33,43} and can vary in size from millimeters to centimeters.³⁵ About 10% of cases involve multiple lesions, making a thorough examination essential.⁴³ It is believed that estrogen and progesterone play a role in the development of this lesion.⁴⁴ (Fig 2)

Treatment planning

Treatment planning of natal and neonatal teeth relies on clinical examination and intraoral radiography. A thorough examination is essential for accurate diagnosis and appropriate treatment to prevent complications.³ Key factors to consider include the tooth's classification, appearance, position, degree of mobility, and risk of aspiration, which can lead to choking and asphyxia.⁴⁵ To assess tooth mobility, Miller's classification is commonly used. If mobility exceeds level 2 (i.e., movement from cheek to tongue greater than 2 mm.), there is a risk of aspiration during feeding.¹ The natal and neonatal teeth may cause lesions under the tongue, known as Riga-Fede disease. (Fig 3) This condition occurs in about 6-10% of cases,^{9,46} caused by repeated trauma from the sharp edges of the teeth as the tongue moves.¹ Severe lesions can



Fig. 2 The differential diagnosis of natal and neonatal teeth. (2A) Bohn's nodules. (2B) Dental lamina cysts. (2C) Eruption cyst. (2D) Congenital epulis.



Fig 3. Ulcer of Riga-Fede disease on the ventral surface of the tongue.

also lead to insufficient nutrient intake, affecting growth and development.⁴⁶ Additionally, some mothers also report pain or nipple lesions during breastfeeding. While *Moura et al.* found that 2 out of 23 mothers experienced nipple lesions due to natal teeth, leading to breastfeeding difficulties,⁴⁷ *Zhu and King* found no association between neonatal teeth and nipple lesions during breastfeeding. The tongue usually protects the nipple from the teeth.⁹ During breastfeeding, the nipple is positioned deep in the infant's mouth, with the tongue covering the lower gums and the lip contacting the maternal areola, reducing the likelihood of biting injuries.⁴⁸

Intraoral radiographs are essential for assessing whether the teeth are normal primary or supernumerary,^{11,13} as well as evaluating root development and surrounding tissues.⁴ An X-ray of a normal primary tooth shows a developing permanent tooth bud beneath an erupted natal or neonatal tooth. Conversely, an X-ray of a supernumerary tooth reveals the natal or neonatal tooth alongside the properly positioned permanent tooth bud, indicating an extra tooth beyond the typical 20 primary teeth. Since infants are more sensitive to radiation, dentists must weigh the benefits and risks before taking an X-ray. Extracting a very mobile tooth is crucial to prevent choking during breastfeeding. Radiographs may not change the treatment plan or be necessary before the extraction. When radiographs are necessary, appropriate radiation protection equipment should be used for infants, as their cells are more sensitive to radiation.

The decision to retain or extract an infant's tooth should be considered individually, based on the outlined treatment plan, and dentists must inform parents to weigh the benefits and risks. Parents must be involved in the decision-making process regarding treatment, with the primary goal being to ensure that an infant can continue breastfeeding and to prevent potential complications.

Typically, natal and neonatal teeth are usually normal primary teeth, so retention is the first choice of treatment.²⁰ Teeth with minimal mobility (less than Miller's classification level 2) pose a low aspiration risk

and can be retained, as root development and stabilization occur over time. If these teeth cause discomfort or lesions on the mother's nipple during breastfeeding, they may still be retained. Reports show that nipple lesions are not related to eruption of natal or neonatal teeth, and most lesions caused by these teeth typically occur only on the baby's tongue.^{9,11} Riga-Fede disease does not require tooth extraction. Instead, the sharp edges of the affected tooth can be smoothed using a finishing bur or sandpaper disk.⁴⁹ Alternatively, the tooth can be filled or covered with composite resin or glass ionomer cement.^{1,46,49,50}

Parents can adjust feeding methods to reduce tongue trauma by using bottles with larger nipple holes, sippy cups, or feeding with a spoon.⁵¹ The lesions can heal in 7 to 10 days once the source of trauma is eliminated, even without specific treatment. However, if a faster healing process and pain relief are needed, the dentist may recommend applying Solcoseryl dental adhesive paste to the lesion 3–5 times daily.⁵² This paste contains 5% protein-free haemodialysate, which increases tissue repair and regeneration and improves the healing of lesions, along with 1% polidocanol to relieve pain.⁵³

When the natal or neonatal teeth are Hebling's category type 4 and the teeth have some mobility, dentists need to follow up periodically. When these teeth emerge from the gum, they should reassess the level of tooth mobility to determine whether it poses a risk of aspiration. If the tooth is not very mobile, it may be retained, but if it is highly mobile and at risk of aspiration, extraction can be considered.

Additionally, tooth extraction should be considered in specific cases, such as supernumerary teeth confirmed through radiographs, if the tooth is extremely mobile, particularly in Hebling's type 1 and type 2 teeth, and Riga-Fede disease under the tongue if it impacts feeding, leading to failure to thrive. If the child has a cleft lip and palate with teeth positioned in a way that interferes with fitting a nasopalveolar molding (NAM) device, tooth extraction may be necessary. (Fig 4)

Treatment care approach for extraction

In the past, natal and neonatal tooth extractions were recommended only after 10 days of age to allow the infant's intestinal flora to produce enough vitamin K for proper blood clotting.^{7,11} If extraction cannot be delayed, a pediatrician should assess if vitamin K supplementation is needed, particularly if the infant did not receive vitamin K after birth. However, current guidelines have changed, and standard care now recommends a single intramuscular (IM) dose of 0.5 to 1.0 mg of vitamin K injection⁵⁴ or two oral doses of 2 mg vitamin K on day 1 and day 4.⁵⁵ If



Fig 4. Management of natal teeth in cleft lip and palate newborn. (4A) Natal tooth in the region of cleft area. (4B) Extracted natal tooth with no root development. (4C) Postoperative hemostasis achieved. (4D) Nasoalveolar molding appliance in the region of cleft area.

vitamin K is not given at birth, it should be administered before and possibly after extraction to prevent bleeding complications. *Shivpuri et al.* reported that 6 out of 12 infants below 10 days of age who were administered a vitamin K injection before extraction successfully controlled bleeding, as they had not been administered the same at birth.⁵⁴

Before tooth extraction, the dentist should securely swaddle the baby in a blanket to keep them calm. If the tooth is lightly attached, the dentist should dry the gums and apply a topical anesthetic while using a sterile gauze to prevent ingestion. For more firmly attached teeth, a few drops of local anesthetic with a vasoconstrictor, like 2% lidocaine with 1:100,000 epinephrine, should be injected around the gums to enhance the effect and to control bleeding. The amount of anesthetic should not exceed 4.4 mg/kg.⁵⁶ The tooth can be extracted with forceps. Post-extraction curettage of the socket is crucial to reduce the risk of ongoing development of the dental papilla cells.³ *Anton et al.* reported a case in which a residual tooth-like structure developed in place of the extracted lower left primary central incisor, likely due to ongoing dental papilla development.³ After the extraction, apply a gauze pad with pressure to the site for 5 to 10 minutes to control bleeding. Once the bleeding has stopped, the infant can resume breastfeeding immediately for comfort. The immunoglobulins present in breast milk can help promote wound healing.²

Complications after treatment

Long-term follow-up care is vital for individuals with retained or extracted natal and neonatal teeth. Follow-up is recommended throughout the eruption of permanent teeth.⁵⁷ For those who retain these teeth, consistent dental check-ups become essential. These visits help monitor stability and root development while preventing complications such as Riga-Fede disease. Retained teeth may have hypoplastic enamel and dentin, along with poor root formation, which increases their risk of early loss, fracture, or wear. The potential complications of retaining

these teeth include dental caries, pulp polyps, and early eruption of permanent teeth.¹ The poor development of enamel and rapid eruption can heighten the risk of caries, highlighting the importance of preventive dental care, including plaque control and regular fluoride application. If a supernumerary tooth is retained, it may interfere with the eruption of the underlying primary or permanent tooth. These teeth are often recommended for extraction, even if they are asymptomatic. However, if they remain, careful long-term radiographic and clinical monitoring is essential.

For those who have extracted these teeth, follow-up assessments confirm successful healing, resolution of any ulcers, and a return to normal feeding habits and weight gain. Complications that may arise from these extractions include loss of space in the jaw, tilting of adjacent primary teeth, and reduced bone growth at the extraction site.^{13,58} These issues can potentially lead to malocclusion and contribute to crowding in the permanent dentition.^{11,58} Early orthodontic intervention can prevent further complications.⁵⁷ However, no significant space loss was reported in 56 out of 72 natal teeth.⁵⁹ Other complications reported include the eruption of a residual natal tooth⁶⁰, accidental displacement of primary teeth⁶¹, neonatal osteomyelitis⁶², the development of gingival growth from a residual dental papilla, and peripheral ossifying fibroma, resulting from low-grade irritation.⁶³

CONCLUSION

Dental management of natal and neonatal teeth requires a case-by-case approach. Parents should be involved in the decision-making process. A radiographic examination is used to determine if the tooth is supernumerary or part of the normal primary dentition. Whether the tooth is supernumerary or primary dentition, if the mobility of the erupted teeth exceeds Miller's classification level 2, as in the case of Hebling's category type 1 and type 2, we recommend extraction due to the higher risk of aspiration. Before tooth extraction, a consultation with a pediatrician is recommended to ensure that the

infant has received vitamin K prophylaxis after birth. If the teeth are primary, they should be retained with close monitoring to prevent them from becoming an aspiration risk or affecting feeding. In case of discomfort during suckling or sublingual ulceration, the incisal edges can be smoothed or covered with composite resin. Parents should be informed of the need for adequate dental hygiene and the use of fluoride. Regular dental check-ups are important.

ACKNOWLEDGMENTS

The authors thank the Siriraj Medical Journal and the reviewers for providing a review article that made this more complete.

DECLARATIONS

Grants and Funding Information

None.

Conflicts of Interest

There are no conflicts of interest.

Registration Number of Clinical Trial

None.

Author Contributions

First author.

Use of Artificial Intelligence

Grammarly.

REFERENCES

- Mhaske S, Yuwanati MB, Mhaske A, Ragavendra R, Kamath K, Saawarn S. Natal and neonatal teeth: an overview of the literature. *ISRN Pediatr*. 2013;2013:956269.
- Chandler C, Silva Junior M, Solano M, Azevedo I. Management of Neonatal Teeth: Two Case Reports. *Inter Ped Dent Open Acc J*. 2020;4:283-7.
- Anton E, Doroftei B, Grab D, Fornä N, Tomida M, Nicolaiaciuc OS, et al. Natal and Neonatal Teeth: A Case Report and Mecanistical Perspective. *Healthcare (Basel)*. 2020;8(4):539.
- Markou I, Kana A, Arhakis A. Natal and Neonatal Teeth: A Review of the Literature. *Balk J Stom*. 2012;16:132-40.
- Seminario AL, Ivančáková R. Natal and neonatal teeth. *Acta Medica (Hradec Králové)*. 2004;47(4):229-33.
- Massler M, Savara BS. Natal and neonatal teeth; a review of 24 cases reported in the literature. *J Pediatr*. 1950;36(3):349-59.
- Khandelwal V, Nayak UA, Nayak PA, Bafna Y. Management of an infant having natal teeth. *BMJ Case Rep*. 2013;2013:bcr2013010049.
- Dymont H, Anderson R, Humphrey J, Chase I. Residual neonatal teeth: a case report. *J Can Dent Assoc*. 2005;71(6):394-7.
- Zhu J, King D. Natal and neonatal teeth. *ASDC J Dent Child*. 1995;62(2):123-8.
- Vitali FC, Santos PS, Massignan C, Cardoso M, Maia LC, Paiva SM, et al. Worldwide prevalence of natal and neonatal teeth: Systematic review and meta-analysis. *J Am Dent Assoc*. 2023;154(10):910-21.e4.
- Cunha RF, Boer FA, Torriani DD, Frossard WT. Natal and neonatal teeth: review of the literature. *Pediatr Dent*. 2001;23(2):158-62.
- Kates GA, Needleman HL, Holmes LB. Natal and neonatal teeth: a clinical study. *J Am Dent Assoc*. 1984;109(3):441-3.
- Leung AK, Robson WL. Natal teeth: a review. *J Natl Med Assoc*. 2006;98(2):226-8.
- Anegundi RT, Sudha R, Kaveri H, Sadanand K. Natal and neonatal teeth: a report of four cases. *J Indian Soc Pedod Prev Dent*. 2002;20(3):86-92.
- Samuel SS, Ross BJ, Rebekah G, Koshy S. Natal and Neonatal Teeth: A Tertiary Care Experience. *Contemp Clin Dent*. 2018;9(2):218-22.
- de Almeida CM, Gomide MR. Prevalence of natal/neonatal teeth in cleft lip and palate infants. *Cleft Palate Craniofac J*. 1996;33(4):297-9.
- Baghdadi ZD. Riga-Fede disease: report of a case and review. *J Clin Pediatr Dent*. 2001;25(3):209-13.
- Roberts MW, Vann WF, Jr., Jewson LG, Jacoway JR, Simon AR. Two natal maxillary molars. Report of a case. *Oral Surg Oral Med Oral Pathol*. 1992;73(5):543-5.
- Gautam U, Phuyal R, Sapkota A, Chikanbanjar VK. Multiple Neonatal Teeth in a Preterm Neonate: A Case Report. *JNMA J Nepal Med Assoc*. 2021;59(244):1323-5.
- Alvarez MP, Crespi PV, Shanske AL. Natal molars in Pfeiffer syndrome type 3: a case report. *J Clin Pediatr Dent*. 1993;18(1):21-4.
- Gladden BC, Taylor JS, Wu YC, Ragan NB, Rogan WJ, Hsu CC. Dermatological findings in children exposed transplacentally to heat-degraded polychlorinated biphenyls in Taiwan. *Br J Dermatol*. 1990;122(6):799-808.
- Miller RW. Congenital PCB poisoning: a reevaluation. *Environ Health Perspect*. 1985;60:211-4.
- Alaluusua S, Kiviranta H, Leppäniemi A, Hölttä P, Lukinmaa PL, Lope L, et al. Natal and neonatal teeth in relation to environmental toxicants. *Pediatr Res*. 2002;52(5):652-5.
- Galassi MS, Santos-Pinto L, Ramalho LT. Natal maxillary primary molars: case report. *J Clin Pediatr Dent*. 2004;29(1):41-4.
- Varriano BM, Ades L, Vaughan SR. Case Report: A rare case of bilateral molar natal teeth in a term newborn. *Front Dent Med*. 2024;5:1336865.
- Wongsirichat N, Mahardawi B, Manosudprasit M, Manosudprasit A, Wongsirichat N. The Prevalence of Cleft Lip and Palate and Their Effect on Growth and Development: A Narrative Review. *Siriraj Med J*. 2022;74(11):819-27.
- Masatomi Y, Abe K, Ooshima T. Unusual multiple natal teeth: case report. *Pediatr Dent*. 1991;13(3):170-2.
- Gonçalves FA, Birman EG, Sugaya NN, Melo AM. Natal teeth: review of the literature and report of an unusual case. *Braz Dent J*. 1998;9(1):53-6.
- Portela M, Damasceno L, Primo L. Unusual case of multiple natal teeth. *J Clin Pediatr Dent*. 2004;29(1):37-9.
- Jasmin JR, Clergeau-Guerithault S. A scanning electron microscopic study of the enamel of neonatal teeth. *J Biol Buccale*. 1991;19(4):309-14.
- Uzamis M, Olmez S, Ozturk H, Celik H. Clinical and ultrastructural

- study of natal and neonatal teeth. *J Clin Pediatr Dent.* 1999;23(3):173-7.
32. Friend GW, Mincer HH, Carruth KR, Jones JE. Natal primary molar: case report. *Pediatr Dent.* 1991;13(3):173-5.
 33. Merglova V, Hauer L, Broukal Z, Dort J, Koberova Ivancakova R. General and oral health status of preterm one-year-old very low and extremely low birthweight infants (a cross-sectional study). *Biomed Pap Med Fac Univ Palacky Olomouc Czech Repub.* 2021;165(2):209-15.
 34. van Heerden W, Van Zyl A. Diagnosis and management of oral lesions and conditions in the newborn. *SA Fam Pract.* 2010;52(6):489-91.
 35. Singh RK, Kumar R, Pandey RK, Singh K. Dental lamina cysts in a newborn infant. *BMJ Case Rep.* 2012;2012:bcr2012007061.
 36. Cohen RL. Clinical perspectives on premature tooth eruption and cyst formation in neonates. *Pediatr Dermatol.* 1984;1(4):301-6.
 37. Marini R, Chipaila N, Monaco A, Vitolo D, Sfasciotti GL. Unusual symptomatic inclusion cysts in a newborn: a case report. *J Med Case Rep.* 2014;8:314.
 38. Patil S, Rao RS, Majumdar B, Jafer M, Maralingannavar M, Sukumaran A. Oral Lesions in Neonates. *Int J Clin Pediatr Dent.* 2016;9(2):131-8.
 39. Kumar A, Grewal H, Verma M. Dental lamina cyst of newborn: a case report. *J Indian Soc Pedod Prev Dent.* 2008;26(4):175-6.
 40. de Oliveira AJ, Silveira ML, Duarte DA, Diniz MB. Eruption Cyst in the Neonate. *Int J Clin Pediatr Dent.* 2018;11(1):58-60.
 41. Dhawan P, Kochhar GK, Chachra S, Advani S. Eruption cysts: A series of two cases. *Dent Res J (Isfahan).* 2012;9(5):647-50.
 42. Mecarini F, Fanos V, Crisponi G. Anomalies of the oral cavity in newborns. *J Perinatol.* 2020;40(3):359-68.
 43. Merrett SJ, Crawford PJ. Congenital epulis of the newborn: a case report. *Int J Paediatr Dent.* 2003;13(2):127-9.
 44. Damm DD, Cibull ML, Geissler RH, Neville BW, Bowden CM, Lehmann JE. Investigation into the histogenesis of congenital epulis of the newborn. *Oral Surg Oral Med Oral Pathol.* 1993;76(2):205-12.
 45. Kim GY, Kim S, Chang JS, Pyo SW. Advancements in Methods of Classification and Measurement Used to Assess Tooth Mobility: A Narrative Review. *J Clin Med.* 2023;13(1):142.
 46. Jamani NA, Ardini YD, Harun NA. Neonatal tooth with Riga-Fide disease affecting breastfeeding: a case report. *Int Breastfeed J.* 2018;13:35.
 47. Moura LF, Moura MS, Lima MD, Lima CC, Dantas-Neta NB, Lopes TS. Natal and neonatal teeth: a review of 23 cases. *J Dent Child (Chic).* 2014;81(2):107-11.
 48. Jacobs L, Dickinson J, Hart P, Doherty D, Faulkner S. Normal Nipple Position in Term Infants Measured on Breastfeeding Ultrasound. *J Hum Lact.* 2007;23(1):52-9.
 49. Iandolo A, Amato A, Sangiovanni G, Argentino S, Pisano M. Riga-Fede disease: A systematic review and report of two cases. *Eur J Paediatr Dent.* 2021;22(4):323-31.
 50. Costacurta M, Maturo P, Docimo R. Riga-Fede disease and neonatal teeth. *Oral Implantol (Rome).* 2012;5(1):26-30.
 51. Slayton RL. Treatment alternatives for sublingual traumatic ulceration (Riga-Fede disease). *Pediatr Dent.* 2000;22(5):413-4.
 52. FDA Advisory No.2021-0352 || Product Recall of Specific Batches of Three (3) Dosage Forms of Deproteinized Calf Blood Extract (Solcoseryl). Available from: <https://www.fda.gov/ph/fda-advisory-no-2021-0352-product-recall-of-specific-batches-of-three-3-dosage-forms-of-deproteinized-calf-blood-extract-solcoseryl/>
 53. Yildirim A, Metzler P, Lanzer M, Lübbers HT, Yildirim V. Solcoseryl® Dental-Adhäsivpaste - Wirkmechanismus und Risiken. *Swiss Dent J.* 2015;125(5):612-3.
 54. Shivpuri A, Mitra R, Saxena V, Shivpuri A. Natal and neonatal teeth: Clinically relevant findings in a retrospective analysis. *Med J Armed Forces India.* 2021;77(2):154-7.
 55. Hand I, Noble L, Abrams SA. AAP Committee on Fetus and Newborn, Section on Breastfeeding, Committee on Nutrition, Vitamin K and the Newborn Infant. *Pediatrics.* 2022;149(3):e2021056036.
 56. American Academy of Pediatric Dentistry. Use of local anesthesia for pediatric dental patients. The Reference Manual of Pediatric Dentistry, Chicago, Ill. AAPD 2024;386-93. Available from: https://www.aapd.org/globalassets/media/policies_guidelines/bp_localanesthesia.pdf
 57. Awooda EM, Ali AY, Hassan MZ. Eight-year Follow-up after the Removal of a Maxillary Molar Natal Tooth. *J Clin Neonatol.* 2023;12(4):157-9.
 58. Rahul M, Kapur A, Goyal A. Management of prematurely erupted teeth in newborns. *BMJ Case Rep* 2018;2018:bcr2018225288.
 59. To EW. A study of natal teeth in Hong Kong Chinese. *Int J Paediatr Dent* 1991;1(2):73-6.
 60. Tsubone H, Onishi T, Hayashibara T, Sobue S, Ooshima T. Clinico-pathological aspects of a residual natal tooth: a case report. *J Oral Pathol Med.* 2002;31(4):239-41.
 61. Sridhar M, Sai Sankar AJ, Sankar KS, Kumar KK. Accidental displacement of primary anterior teeth following extraction of neonatal teeth. *J Indian Soc Pedod Prev Dent.* 2020;38(3):311-4.
 62. Vora E, Winnier J, Bhatia R. Neonatal osteomyelitis: An unusual complication of natal tooth extraction. *J Indian Soc Pedod Prev Dent.* 2018;36(1):97-100.
 63. Barreras CM, Alemán FM, Burgueño ER, Caldeira PC. Peripheral ossifying fibroma in a newborn: A potential complication after natal teeth extraction. *Odontoestomatologia.* 2022;24.

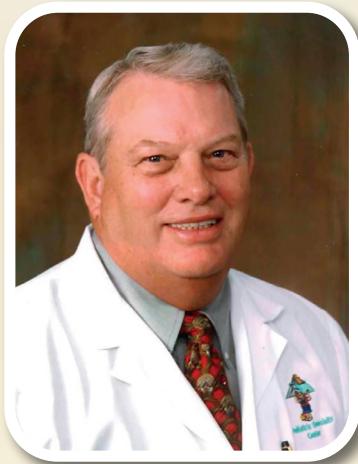


Congratulations to the 2025 Prince Mahidol Award Laureates

*We celebrate the visionary leadership and extraordinary contributions
of our distinguished lecturers:*



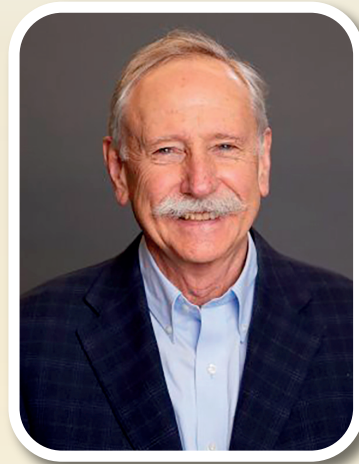
Dr. Terry Dean King



Lecture: “Challenging The Status Quo”

Recognized for his courage in redefining medical paradigms and advocating for transformative change in global healthcare.

Professor Dr. Walter C. Willett



**Lecture: “Finding a path to feed the
global population a diet that is healthy,
sustainable, and just”**

Recognized for his pioneering research at the intersection of human nutrition, environmental health, and social equity. In honor of your dedication to the health and well-being of humanity.